This document was produced by scanning the original publication.

Ce document est le produit d'une numérisation par balayage de la publication originale.

GEOLOGICAL SURVEY OF CANADA
PAPER 91-14

PHYSICAL VOLCANOLOGY, STRATIGRAPHY, AND DEPOSITIONAL SETTING OF THE MIDDLE PALEOZOIC VOLCANIC AND SEDIMENTARY ROCKS OF PASSAMAQUODDY BAY, SOUTHWESTERN NEW BRUNSWICK

N.A. Van Wagoner, K.A. Dadd, D.K. Baldwin, and W. McNeil

1994

Natural Resources Canada Ressources naturelles Canada

Canada

COOPERATION

COOPERATION AGREEMENT ON MINERAL DEVELOPMENT

ENTENTE DE COOPÉRATION SUR L'EXPLOITATION MINÉRALE

Contribution to Canada-New Brunswick Cooperation Agreement on Mineral Development (1990-1995), a subsidiary agreement under the Economic and Regional Development Agreement.

Contribution à l'Entente de coopération Canada - Nouveau-Brunswick sur l'exploitation minérale (1990-1995), entente auxiliaire négociée en vertu de l'Entente Canada / Nouveau-Brunswick de développement économique et régional.

Canada

New Nouveau Brunswick

GEOLOGICAL SURVEY OF CANADA
Paper 91-14

PHYSICAL VOLCANOLOGY, STRATIGRAPHY, AND DEPOSITIONAL SETTING OF THE MIDDLE PALEOZOIC VOLCANIC AND SEDIMENTARY ROCKS OF PASSAMOQUODDY BAY, SOUTHWESTERN NEW BRUNSWICK

N.A. Van Wagoner, K.A. Dadd, D.K. Baldwin, and W. McNeil

1994

© Minister of Energy, Mines and Resources Canada 1994

Available in Canada through
authorized bookstore agents and other bookstores

or by mail from

Canada Communication Group - Publishing
Ottawa, Canada K1A 0S9

and from

Geological Survey of Canada offices:

601 Booth Street
Ottawa, Canada K1A 0E8

3303-33rd Street N.W.,
Calgary, Alberta T2L 2A7

A deposit copy of this publication is also available for reference
in public libraries across Canada

Cat. No. M44-91/14E
ISBN 0-660-15523-0

Price subject to change without notice

Cover description

Columnar joints in rhyolite flow, MacDougalls Island. Photo taken by M. Thicke. (GSC 1993-324)

Authors' address

N.A. Van Wagoner
K.A. Dadd
D.K. Baldwin
W. McNeil
Department of Geology
Acadia University
Wolfville, Nova Scotia
B0P 1X0

Original manuscript received: 1990-02-21
Final version approved for publication: 1993-08-16

CONTENTS

1 Abstract/Résumé

2 Summary/Sommaire

3 Introduction

4 Regional setting

5 Lithology
- 5 Nonvolcaniclastic sedimentary rocks
- 12 Volcaniclastic rocks
- 16 Mafic lava flows
- 19 Mafic pyroclastic rocks
- 23 Felsic flows and domes
- 28 Felsic pyroclastic rocks

38 Stratigraphy

40 Metamorphism

41 Structure
- 42 Domain 1
- 43 Domain 2
- 43 Domain 3

44 Mafic dykes

44 Acknowledgments

44 References

Table

6 1. Summary of the stratigraphic sequence and evolution of the volcanic and sedimentary rocks in the Passamaquoddy Bay area, southwestern New Brunswick.

Figures

3 1. Location of the map area

4 2. Correlation of the volcanic and sedimentary sequence in the Passamaquoddy Bay area with the Eastport Succession in Maine

3. Lithostratigraphic map of the Middle Paleozoic volcanic and sedimentary rocks of the Passamaquoddy Bay area, southwestern New Brunswick *(in pocket)*

5 4. Explanation of rock unit names

5 5. Graphical log of a 5 m thick section in unit D4sl

9 6. Photomicrograph of a fine grained sandstone from unit D3s1

9 7. Photomicrograph of a fine grained sandstone from unit D2s1

9 8. Vertical section through interbedded fine grained sandstone, siltstone, and mudstone from unit D4s1

10 9. Sinuous crested, current ripples in medium grained sandstone from unit D4sl

10 10. Polygonal mudcracks in siltstone to mudstone from unit D2sl

10 11. Photomicrograph of an oblique cross-section through vertical burrows in siltstone in unit D1s1

10 12. Tabular low- and high-angle crossbedding in medium grained sandstone from unit D4sl

11 13. Lingulid type brachiopod in fine grained micaceous sandstone, unit D2sl

12 14. Interbedded sandstone and pebble conglomerate from unit D3s1

12 15. Photomicrograph of a coarse grained sandstone from unit D3s1
13 16. Matrix of basaltic boulder conglomerate from unit D1vc1
13 17. Thinly-bedded to laminated, basaltic, coarse- to fine-grained sandstone from unit D1vc1
13 18. Pumice-rich pebble conglomerate from unit D1vc1
14 19. Photomicrograph of the matrix of basaltic pebble conglomerate from unit D1vc3
14 20. Photomicrograph of a basaltic pebble conglomerate from unit D1vc3
15 21. Photomicrograph of a basaltic siltstone from unit D2vc2
16 22. Photomicrograph of basaltic lapilli-bearing sandstone from unit D4vc1
16 23. Pahoehoe toes with red iron-stained oxidized margins, unit D3mf1
16 24. Basaltic pahoehoe flow showing a flow contact (arrow) in unit D3mf1
17 25. Graphical log of a section of unit D2mf1
17 26. Graphical log of unit D4mf1 and of over- and underlying sedimentary rocks of unit D4s1
17 27. Photomicrograph of porphyritic basaltic lava from unit D3mf1
17 28. Photomicrograph of basaltic lava from unit D4mf1
18 29. Contact of basaltic flow unit D4mf1 and underlying sedimentary rocks of unit D4s1
18 30. Peperitic breccia from unit D1mf1
18 31. Photomicrograph of peperitic breccia from unit D2mf1
18 32. Peperitic breccia from unit D2mf1
19 33. Photomicrograph of peperitic breccia from unit D2mf1
20 34. Correlation of measured sections through units D2sl, D2vc2, D3ms1, D3tb1, D3mf1, D3lvt1, D3lvt2, D3tb2, and D3vt1 at Holt's Point
20 35. Basaltic bomb (arrow) in basaltic scoria deposit of unit D3ms1
20 36. Photomicrograph of a mafic tuff breccia unit from unit D3tb1
21 37. Gabbroic bomb with a rim of oxidized basalt in mafic tuff breccia unit D3tb1
21 38. Mafic heterolithic-vitric lapilli tuff from unit D4lvt1
22 39. Graphical log of a 7 m section through unit D4tb1
22 40. Photomicrograph of vitric tuff from unit D4tb1
22 41. Photomicrograph of heterolithic lapilli tuff to tuff breccia from unit D4tb1
22 42. Heterolithic lapilli tuff to tuff breccia from unit D4tb1
23 43. Photomicrograph of rhyolitic peperitic breccia from unit D2ff1
23 44. Contorted fluidal folds in a rhyolite lava dome of unit D4ff1
24 45. Photomicrograph of flow banding in a trachytic rhyolite flow from unit D1ff1
24 46. Monolithic autobreccia at the edge of a rhyolite flow unit, D2ff4
24 47. Fragmented segments of flow bands in rhyolite lava dome of unit D4ff1
24 48. Photomicrograph of an isolated segment of folded flow banding in a devitrified rhyolitic groundmass from unit D4ff1
25 49. Pseudobreccia in a rhyolite lava flow or dome, unit D3ff1
26 50. Graphical log of a 435 m section through unit D4ff1
26 51. Rhyolitic peperitic breccia with angular clasts of rhyolite in a grey siltstone matrix from unit D4ff1
26 52. Typical view of the central part of intrusive rhyolite dome, unit D4ff1
27 53. Photomicrograph of flow banding in an intrusive rhyolite dome from unit D4ff1
27 54. Clastic dyke in an intrusive rhyolite dome, unit D4ff1
27 55. Photomicrograph of felsic peperitic breccia from unit D4ff1
27 56. Photomicrograph of felsic peperitic breccia from unit D4ff1
28 57. Photomicrograph of a sample from an intrusive rhyolite dome, unit D4ff3
29 58. Photomicrograph of massive vitric tuff from unit D1xvt1
29 59. Photomicrograph of massive vitric tuff from unit D1xvt1
29 60. Photomicrograph of massive vitric tuff from unit D2vt1
29 61. Photomicrograph of massive vitric tuff from unit D4vt1
30 62. Photomicrograph of massive lithic-crystal-vitric tuff from unit D2xvt2
30 63. Photomicrograph of massive lithic-crystal-vitric tuff from unit D2lvt1
31 64. Tuff breccia at the base of a graded bed in unit D3vt1
32 65. Photomicrograph of bedded crystal-vitric tuff from unit D1xvt3
32 66. Photomicrograph of bedded crystal-vitric tuff from unit D1xvt3
32 67. Photomicrograph of bedded accretionary lapilli tuff from unit D2xvt1

32 68. Photomicrograph of bedded accretionary lapilli tuff from unit D2xvt1
34 69. Graphical log through a representative section of unit D2lxt1
35 70. Bedded lithic-crystal lapilli tuff from unit D2lxt1
35 71. Photomicrograph of bedded lithic-crystal lapilli tuff from unit D2lxt1
35 72. Lithic-crystal-vitric lapilli tuff from unit D2lxt1
35 73. Photomicrograph of bedded crystal tuff unit D2xlt1
36 74. Photomicrograph of bedded crystal tuff from unit D2xlt1
36 75. Outcrop of poorly sorted felsic heterolithic tuff breccia of unit D2tb1
37 76. Graphical log of unit D3lvt3
37 77. Thinly- to thickly-bedded sequence of lithic-lapilli tuff, crystal-lithic tuff, and crystal tuff of unit D3lvt3
37 78. Photomicrograph of bedded crystal-lithic tuff from unit D3lvt3
38 79. Bedded crystal-lithic lapilli tuff from unit D3lvt3
38 80. Photomicrograph of bedded lithic-vitric tuff from unit D4lvt2
39 81. Composite section of the stratigraphic sequence of the map area
40 82. Graphical log and interpretation of eruptive mode of units D2ff2, D2svt1, and D2vt1 at Cow Head
41 83. Photomicrograph of metamorphosed, laminated, nonvolcaniclastic siltstone from unit D1s1
41 84. Structural domains in the Passamaquoddy Bay map area, southwestern New Brunswick
41 85. Contour plot of poles to bedding in Domain 1
41 86. Contour plot of poles to cleavage in Domain 1
42 87. Contour plot of poles to flow foliation in Domain 1
42 88. Synoptic plot for Domain 1
42 89. Contour plot of poles to bedding in Domain 2
42 90. Contour plot of poles to cleavage in Domain 2
43 91. Synoptic plot for Domain 2
43 92. Contour plot of poles to bedding in Domain 3
43 93. Contour plot of poles to cleavage in Domain 3
44 94. Interbedded, red, fine grained sandstone and siltstone of unit D4s1 in structural Domain 3
44 95. Rose diagram showing the trend of mafic dykes from cycles 1-4

PHYSICAL VOLCANOLOGY, STRATIGRAPHY, AND DEPOSITIONAL SETTING OF THE MIDDLE PALEOZOIC VOLCANIC AND SEDIMENTARY ROCKS OF PASSAMAQUODDY BAY, SOUTHWESTERN NEW BRUNSWICK

Abstract

The Lower Paleozoic volcanic and sedimentary belt of Passamaquoddy Bay, southwestern New Brunswick comprises a 4 km thick sequence of intercalated bimodal volcanic and sedimentary rocks deposited in a tidal flat to subaerial environment. The belt preserves four cycles of volcanism. Basaltic volcanism accompanied rhyolitic volcanism in each of the four cycles, with rhyolitic units being the most voluminous in the first three. In the final cycle, sedimentary rocks predominate and mafic flows dominate over felsic rocks, suggesting waning volcanism.

Rhyolitic volcanic rocks are welded and unwelded pyroclastic deposits, domes, and lava flows. Basaltic volcanic rocks are predominantly lava flows with rare pyroclastic deposits. Proximal and distal vent facies are represented. Reworked volcanic rocks are rare.

A spectrum of eruptive styles is present. The basaltic scoria and flows are typical of Hawaiian and Strombolian volcanism. Bedded rhyolitic tuffs and densely welded tuffs indicate Plinian- or sub-Plinian volcanism. Rhyolitic and basaltic lapilli-tuffs and tuff breccias containing accretionary lapilli and blocky and bubble-wall shards, suggest phreatomagmatic (Vulcanian) volcanism.

Flow directions of rhyolitic pyroclastic and lava flows are complex, suggesting several small eruptive centres. Basaltic flows exhibit consistently southward flow directions, suggesting eruption from a localized vent system.

Sedimentary rocks typically have sedimentary structures and a faunal assemblage typical of peritidal conditions with a microtidal range. All sedimentary units contain well preserved shards indicating deposition in a low energy environment with rapid sedimentation rates. The sequence remained at or near sea level for its entire depositional history.

Résumé

La zone volcanique et sédimentaire du Paléozoïque inférieur dans la baie de Passamaquoddy, dans le sud-ouest du Nouveau-Brunswick, comporte une séquence de 4 km d'épaisseur de roches volcaniques et sédimentaires bimodales intercalées, déposées dans une zone allant d'un estran à un milieu subaérien. On y trouve quatre cycles de volcanisme. Le volcanisme basaltique a accompagné le volcanisme rhyolitique dans chacun des quatre cycles, les unités rhyolitiques étant le plus volumineuses dans les trois premiers cycles. Dans le dernier cycle, les roches sédimentaires prédominent et les coulées mafiques sont plus abondantes que les roches felsiques, indiquant un volcanisme en décroissance.

Les volcanites rhyolitiques comprennent des dépôts, des cônes et des coulées de laves pyroclastiques soudés et non soudés. Les volcanites basaltiques comportent surtout des coulées de laves avec de rares dépôts pyroclastiques. On trouve des faciès proximaux et distaux d'évents. Les volcanites remaniées sont rares.

Une gamme de styles éruptifs est observée. Les scories et coulées basaltiques sont représentatives du volcanisme hawaiien et strombolien. Les tufs rhyolitiques lités et les tufs densément soudés indiquent un volcanisme plinien ou subplinien. Les tufs à lapillis rhyolitiques et basaltiques et les brèches tufacées contenant des lapillis accrétionnés et des blocs et fragments vésiculaires indiquent un volcanisme phréatomagmatique (vulcanien).

La direction d'écoulement des coulées pyroclastiques rhyolitiques et des coulées de laves est complexe et laisse croire qu'il y a eu plusieurs petits centres éruptifs. La direction d'écoulement des coulées basaltiques est toujours vers le sud, ce qui indique une éruption à partir d'un système d'évents localisés.

En général, les roches sédimentaires présentent des structures sédimentaires et une association faunistique typiques de conditions péritidales à faible amplitude de marée. Toutes les unités sédimentaires contiennent des fragments bien conservés qui attestent un dépôt dans un milieu à faible énergie caractérisé par des taux de sédimentation élevés. La séquence est demeurée au niveau de la mer ou près de ce niveau tout au long de son évolution séquentielle.

SUMMARY

The Passamaquoddy Bay area comprises the eastern portion of the Coastal Volcanic Belt. Detailed mapping and measuring of sections have allowed us to determine the lithology, stratigraphy, and physical volcanology of the volcanic and sedimentary sequence of the Passamoquoddy Bay area, southwestern New Brunswick, and in doing so, reconstruct part of an ancient volcano.

The mapped area covers about 185 km^2 and is divided into 63 lithological units. The age of the volcanic and sedimentary sequence is controversial, but recent radiometric age determinations of the granitoid rocks that intrude the sequence, and a rhyolitic flow within the sequence, suggest Silurian age.

The stratigraphy of the sequence was interpreted based on correlations of the most laterally extensive units. The sequence has a minimum thickness of 4 km. The eruptive sequence is bimodal and there are four cycles of mafic-felsic volcanism. Rhyolitic rocks predominate over basaltic rocks in cycles 1-3 and there are no periods of volcanic quiescence which would be marked by continuous sedimentary horizons. In the final cycle, sedimentary rocks predominate and mafic flows dominate over felsic, suggesting waning volcanism.

Several eruptive systems are represented. The mafic scoria cone and mafic flows indicate Hawaiian and Strombolian volcanism. Some of the pyroclastic flows and bedded and banded tuff units indicate more explosive Plinian and sub-Plinian volcanism. Characteristics of some of the rhyolitic lapilli tuffs and mafic tuff breccias suggest phreatomagmatic (Vulcanian) volcanism.

Flow direction of the felsic rocks is varied and complex, providing evidence for several small eruptive centres. In contrast, the mafic flows probably originated from a single rift or vent area.

Volcanic rocks are interbedded with sedimentary rocks over almost the entire thickness of the sequence. The sedimentary rocks have primary structures and a faunal assemblage typical of peritidal conditions with a microtidal range. The excellent preservation of such features as unbraided cuspate and pumiceous shards in the sedimentary rocks indicates deposition in a low energy environment.

Regional metamorphic grade is lower greenschist to subgreenschist facies except in the vicinity of the Saint George Batholith where the grade reaches hornblende hornfels facies. The map area is divided into three

SOMMAIRE

La région de la baie de Passamaquoddy comprend la partie orientale de la zone volcanique côtière. Des travaux de cartographie détaillée et de mesure des coupes ont permis de déterminer la lithologie, la stratigraphie et la volcanologie de la séquence volcanique et sédimentaire de la région de la baie de Passamaquoddy dans le sud-ouest du Nouveau-Brunswick et, de ce fait, de reconstituer une partie d'un ancien volcan.

La région cartographiée couvre une superficie d'environ 185 km^2 et se divise en 63 unités lithologiques. L'âge de la séquence volcanique et sédimentaire est contesté, mais des datations radiométriques récentes de roches granitoïdes qui recoupent la séquence ainsi que d'une coulée rhyolitique au sein de la séquence portent à croire qu'elle remonte au Silurien.

L'interprétation de la stratigraphie de la séquence se fonde sur la corrélation des unités qui ont la plus grande étendue latérale. La séquence a une épaisseur minimale de 4 km. La séquence éruptive est bimodale, et l'on dénombre quatre cycles de volcanisme mafique-felsique. Les roches rhyolitiques sont plus abondantes que les roches basaltiques dans les cycles 1 à 3, et l'on n'observe aucune période de repos volcanique qui serait marquée par des horizons sédimentaires continus. Dans le dernier cycle, les roches sédimentaires prédominent et les coulées mafiques sont plus abondantes que les coulées felsiques, indiquant un volcanisme en décroissance.

Plusieurs systèmes éruptifs sont représentés. Le cône de scories mafiques et les coulées mafiques attestent un volcanisme hawaiien et strombolien. Certaines des coulées pyroclastiques et des unités de tufs lités et rubanés témoignent d'un volcanisme plinien et subplinien plus explosif. Les caractéristiques de certains tufs à lapillis rhyolitiques et de certaines brèches tufacées mafiques indiquent un volcanisme phréatomagmatique (vulcanien).

La direction d'écoulement des roches felsiques est variée et complexe et indique la présence de plusieurs petits centres éruptifs. Par contre, les coulées mafiques proviennent probablement d'une seule zone d'effondrement ou d'évents.

Les volcanites sont interstratifiées avec des roches sédimentaires dans presque toute l'épaisseur de la séquence. Les roches sédimentaires présentent des structures primaires et une association faunistique typiques de conditions péritidales à faible amplitude de marée. L'excellente conservation, entre autres, de fragments courbes et ponceux non anastomosés dans les roches sédimentaires atteste une sédimentation dans un milieu à faible énergie.

Le métamorphisme général varie du faciès des schistes verts inférieur aux faciès inférieurs aux schistes verts, sauf à proximité du Batholite de Saint George où le métamorphisme atteint le faciès des cornéennes à hornblende. On divise la région car-

structural domains based on bedding attitude and fold style. In general, the rocks are gently folded and cut by northeast- to northwest-trending faults. Mafic dykes intrude rocks of all four cycles. There are at least three ages of dykes. The oldest are feeder dykes for the mapped sequence. Younger dykes are related to later magmatic events.

tographiée en trois domaines structuraux d'après l'attitude de la stratification et le style de plissement. En général, les roches sont doucement plissées et sont fracturées par des failles à direction nord-est à nord-ouest. Les dykes mafiques recoupent des roches des quatre cycles. Les dykes représentent au moins trois âges différents. Les plus anciens sont des dykes qui ont alimenté la séquence cartographiée. Les dykes les plus récents sont associés à des événements magmatiques plus récents.

INTRODUCTION

The Coastal Volcanic Belt of the northeastern United States and New Brunswick, Canada (Boucot et al., 1974; Boucot, 1968) comprises marine to subaerial Silurian and Early Devonian volcanic and sedimentary rocks. The Mascarene lithostratigraphic terrane of New Brunswick (Fig. 1) (Fyffe and Fricker, 1987) probably forms the northeastern extension of the Coastal Volcanic Belt as it comprises similar rocks (McCutcheon and Ruitenberg, 1987). Dewey and Kidd (1974), Bird and Dewey (1970), and Wilson (1966) suggested that the Coastal Volcanic Belt was a volcanic arc related to the closing of the Iapetus Ocean, but Gates and Moench (1981) documented a bimodal volcanic sequence in the Coastal Volcanic Belt in the Machias-Eastport area in Maine and suggested an extensional tectonic setting. Interpretation of the Coastal Volcanic Belt has important implications for interpreting the nature of the Acadian orogeny and mineral potential of the volcanic belt.

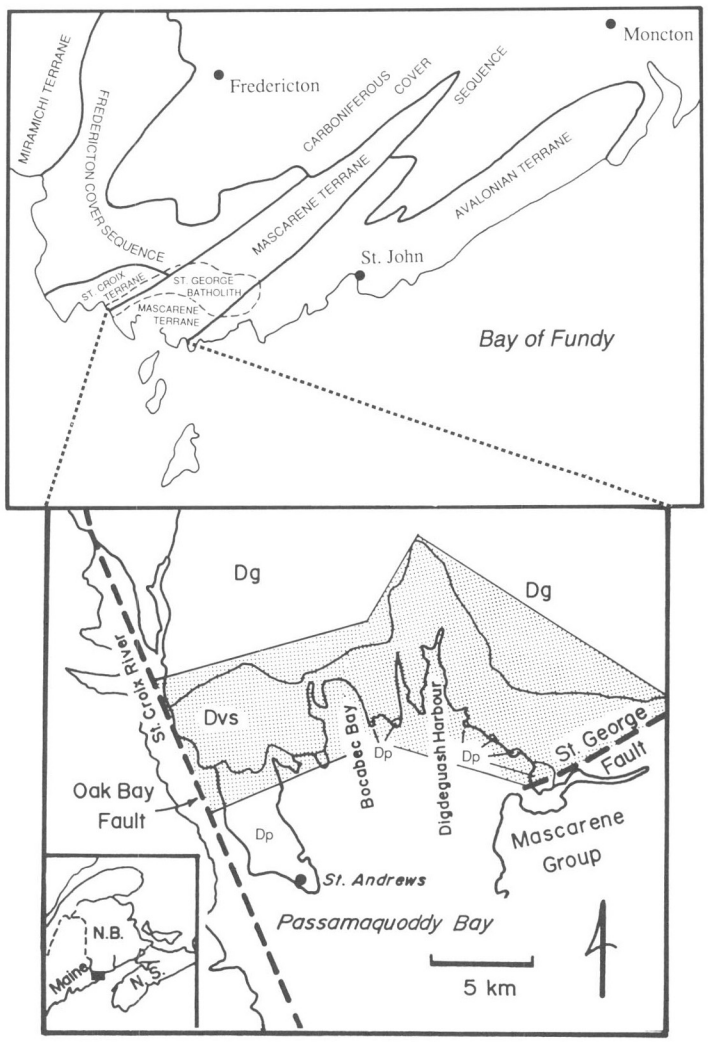

Figure 1. Location of the map area. Lithostratigraphic terranes are from Fyffe and Fricker (1987). Dvs = volcanic and sedimentary rocks of the map area; Dg = Saint George Batholith; Dp = Late Devonian Perry Formation.

This paper is a report on a detailed study of the lithology, stratigraphy, and physical volcanology of the Siluro-Devonian volcanic and sedimentary sequence of the Passamaquoddy Bay area of southwestern New Brunswick (Fig. 1). This type of study is important because the style of volcanism is indicative of tectonic setting. The Passamaquoddy Bay area of the Coastal Volcanic Belt was chosen for study because rocks are exposed in coastal outcrop, there is a lack of a major secondary tectonic fabric, the rocks are only weakly hydrothermally altered, the metamorphic grade is very low, and primary volcanic and sedimentary structures and textures are well preserved.

The most detailed maps of the study area are by Van Wagoner et al. (1988), Whaley (1981), and Hay (1967). Whaley (1981) examined the mineral potential of the area and concluded that there is potential for vein-stockwork tin and porphyry tungsten mineralization like the Mount Pleasant deposit, New Brunswick (Kirkham and Sinclair, 1984). Fay (1988) mapped the central portion of the area, concentrating on the sedimentology. Our geological investigations of the area commenced in 1984. Mapping was done on 1:10 000 scale aerial photographs with detailed stratigraphic sections measured bed by bed.

REGIONAL SETTING

The study area comprises the eastern portion of the Coastal Volcanic Belt (Boucot et al., 1974; Boucot, 1968) and covers an area of about 185 km^2 (Fig. 1). It is bound to the east by the St. George Fault, and by the Oak Bay Fault and St. Croix River on the west. The mapped sequence is overlain unconformably by the subaerial clastic rocks of the Late Devonian Perry Formation in the south and intruded in the north by the Saint George Batholith.

Ruitenberg (1968), Cumming (1967), and Hay (1967) correlated this sequence with volcanic formations in Maine ranging in age from Wenlockian to Gedinnian. Pickerill and Pajari (1976) correlated the rocks with the Early Devonian Eastport Formation of Maine on the basis of similar lithology and faunal assemblage, and proposed that the New Brunswick rocks also be included in the Eastport Formation. Faunal age control in the Eastport succession in Maine is considered good (Watkins and Boucot, 1975; Berdan, 1971; Berry and Boucot, 1970; Boucot et al., 1966) and fossils from the base and middle of the Passamaquoddy Bay sequence are similar to those in the Eastport Formation (M.J. McLeod, pers. comm., 1989; Pickerill and Pajari, 1976).

Recent radiometric age determinations make this correlation suspect. The Utopia Granite, a part of the Saint George Batholith, was given a U-Pb (zircon) age of 430 ± 3 Ma (Bevier, 1989) and a $^{40}Ar/^{39}Ar$ total gas age of 418 ± 5 Ma (McLeod, 1988). The Bocabec Complex of the Saint George Batholith intrudes rocks in the north and northwest of the study area. On the basis of contact relationships, the Bocabec Complex is thought to be of similar age to the Utopia Granite (M.J. McLeod, pers. comm., 1989). These radiometric dates suggest that the intruded volcanic rocks may be as old as Ludlovian to Llandoverian (Fig. 2).

As part of this study we collected a sample of zircon-bearing tuff for U-Pb (zircon) age determination. Our preliminary results indicate a Silurian age (work with M. Bevier, in progress).

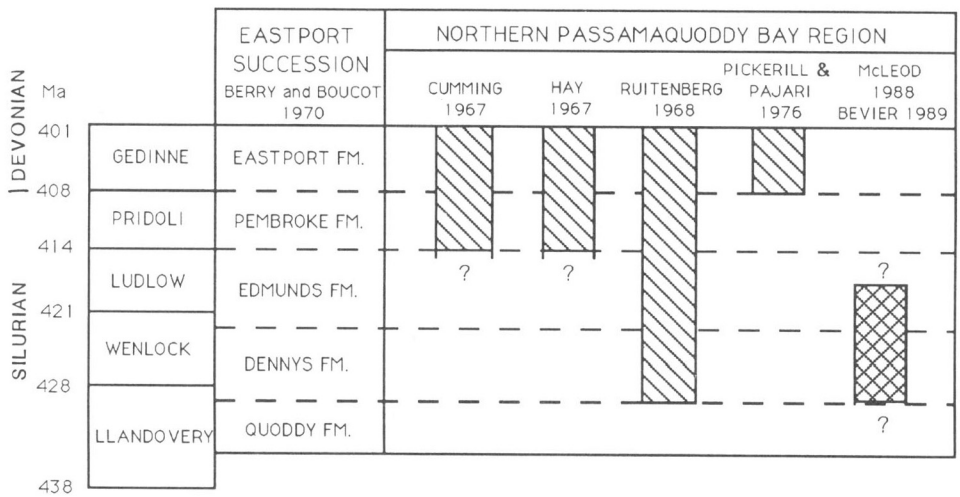

Figure 2. Correlation of the volcanic and sedimentary sequence in the Passamaquoddy Bay area with the Eastport Succession in Maine (modified after Pickerill and Pajari, 1976). Diagonal pattern indicates data taken from Pickerill and Pajari (1976). Cross-hatch pattern shows the range in radiometric ages for the Utopia Granite which intrudes the Passamaquoddy Bay sequence (McLeod, 1988; Bevier, 1989). This range indicates a minimum age for the sedimentary and volcanic sequence of the Passamaquoddy Bay area, but does not imply lithostratigraphic correlation with the lower formations in the Eastport succession.

The Saint George Fault separates rocks of the study area from the Silurian Mascarene Group (Fig. 1). Several workers (e.g., McLeod and Rast, 1988) included the volcanic and sedimentary sequence on the northern Mascarene shore with the rocks of the study area. Pickerill and Pajari (1976) however, excluded these rocks from their "Eastport Formation". Our preliminary examination of these rocks suggests that, although more tightly folded than the sequence in the study area, they are similar in lithology and faunal assemblage. They may be correlatives of either the Eastport Formation or the underlying Leighton Formation in Maine.

LITHOLOGY

The area mapped comprises 63 lithological units (see Fig. 3, in pocket). Rocks of the Saint George Batholith (Dsg) (Bevier, 1989; McLeod, 1988; Gardiner, 1987; Cherry, 1976), minor intrusions (Di), and rocks of the Late Devonian Perry Formation (Dpf) (Schluger, 1973) are beyond the scope of this study and are therefore not discussed. The remaining units are grouped into four cycles of mafic-felsic volcanism. The lithology, depositional style, and depositional environment has been interpreted for each unit (Table 1) (Van Wagoner et al. 1989, 1988, 1987; Van Wagoner and Fay, 1988; Van Wagoner, 1986, 1984). We have named the rocks according to the descriptive classifications of Schmid (1981) for the pyroclastic rocks, of Folk (1980) for the siliciclastic sedimentary rocks, and of Dunham (1962) for the carbonate rocks. The usage of "peperitic breccia" is from Cas and Wright (1987). Nomenclature for stratification thickness is after Ingram (1954). Pyroclastic ejecta are classified as juvenile, essential, cognate, or accidental after Fisher and Schmincke (1984).

Abbreviation	Meaning
D	Siluro-Devonian
1 to 4	volcanic cycle
s	sedimentary rock (mudstone, siltstone, sandstone)
c	conglomerate
vc	volcaniclastic rock
mf	mafic flow
ms	mafic scoria deposit
tb	tuff breccia
ff	felsic flow or dome
td	trachydacite dome
v	vitric
x	crystal
l	lithic
t	tuff
1 to 4	stratigraphic position

Figure 4. *Explanation of rock unit names.*

Hydrothermal alteration of the rocks is weak. Metamorphic grade is very low except adjacent to the Saint George Batholith where the sedimentary and mafic volcanic rocks contain quartz, biotite, cordierite, and rare garnet and belong to the hornblende hornfels facies.

Table 1 is a description of lithological units, grouped according to depositional style. The table outlines the thickness, lithology, and mineralogical composition of each group, as well as a facies analysis and evaluation of the environment of deposition. Each rock unit is named systematically according to geological age, volcanic cycle, stratigraphic position, and lithology (Fig. 4; Fig. 3, in pocket).

Nonvolcaniclastic sedimentary rocks

The dominant nonvolcaniclastic sedimentary rock types, in order of decreasing abundance, are red siltstone, fine- to medium-grained sandstone and grey-green mudstone, siltstone, and sandstone. Minor rock types include conglomerate, volcaniclastic sandstone, and rip-up clast breccia. Sedimentary units are up to 900 m thick but are mostly about 200 m

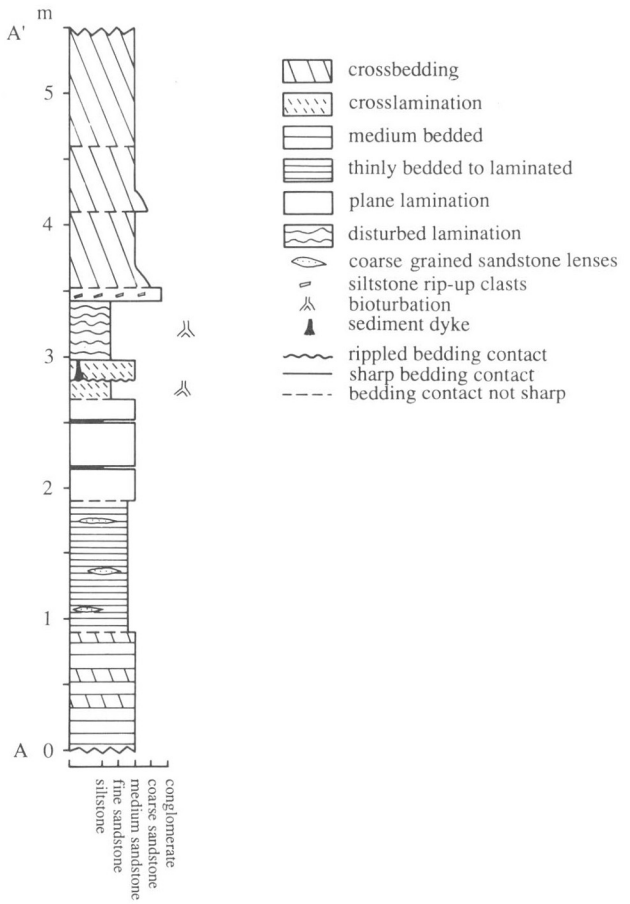

Figure 5. *Graphical log of a 5 m thick section in unit D4sl. The log illustrates a typical section in unit D4sl with interbedded fine- and medium-grained sandstone. Within this section there is no systematic change in grain size or bed thickness. Location of section A-A' shown on Figure 3 (in pocket).*

Table 1. Summary of the stratigraphic sequence and evolution of the volcanic and sedimentary rocks in the Passamaquoddy Bay area, southwestern New Brunswick.

Unit #	Thickness (metres)	Maximum Dominant rock types	Minor rock types	Minerals and texture*	Facies analysis and depositional environment	Environmental indicators	Comments
SEDIMENTARY ROCKS							
D4s2 D4s1 D3s1 D2s1 D1s1	165-900	Red siltstone, fine- to medium-grained sandstone and dark grey to green mudstone and sandstone.	D4s1: Rip-up clast breccia and volcaniclastic sandstone. D2s1, D3s1: Pebble conglomerate.	C: quartz, feldspar, muscovite, Fe-oxides, altered mafic shards, rare pyroxene, siltstone, vitric tuff, basalt. M: clay, sericite. T: immature, angular to subrounded grains, moderately well to poorly sorted. D4s1: Volcaniclastic: C: basalt, rare rhyolite, siltstone, quartz, plagioclase. D2s1: Conglomerate: C: rhyolite, plagioclase, basalt.	Shallow marine fossils (D2s1), lack of indication of reworking by waves, sedimentary structures and grain size indicate peritidal conditions. Coarser grained beds interpreted to be lower-mid intertidal and tidal channel deposits. Volcaniclastic beds (D4s1) indicate proximity to a mafic volcanic source.	Thinner beds: ripple crosslamination, herringbone crosslamination, interference ripples, mucracks; horizontal and vertical burrows. Thicker beds: lensshaped, low angle crosslamination, ripple crosslamination, rare basal lag gravel.	D2s1: Fossil assemblage: lingulid brachiopods, bivalves, ostracods, rare gastropods, possible plant impressions and vertical nonbranching tubular burrows (Pickerill and Pajari, 1976).
D4vc1	35	Grey volcaniclastic sandstone with mafic lapilli.		C: mafic lapilli, quartz, plagioclase, muscovite, altered mafic shards, alkali feldspar, rare pyroxene. M: clay, sericite T: immature, angular to subrounded grains, poorly sorted.	Littoral environment proximal to a mafic volcanic source.	Volcaniclastic sandstone is interbedded with littoral sedimentary rocks as in D4s1.	
D2vc2	40	Brownish-red siltstone.	Siltstone rich in volcanic fragments.	C: siltstone rip-up clasts, mafic volcanic fragments, bubble-wall and blocky mafic glass shards, rare armoured lapilli, rare rhyolitic fragments.	Tidal flat facies, proximal to an intermittently active mafic volcano. Volcanic fragments, except shards, are airfall due to large size.	Ripple to horizontally laminated red siltstone similar to D3s1.	Excellent preservation of glass shards indicates little reworking and rapid burial due to high sedimentation rates.
D2vc1 D1vc3 D1vc2	60 140 380	Basaltic boulder to pebble conglomerate.		D2vc1: C: basalt, rhyolite, mudstone to siltstone. M: dark grey-green siltstone. D1vc3: C: basaltic scoria, platy and pumiceous glass shards, rhyolite, siltstone, welded tuff and plagioclase. D1vc2: C: basalt, plagioclase microphyric basalt, quartz (rhyolitic fragments or shards), plagioclase, brown clay altered fragments. M: no separate matrix.	Fluvial reworking of mafic and felsic pyroclastic deposits. The magmatic component is both mafic and felsic. Sedimentary structures typical of a fluvial environment.	Lower sequence: beds are planar, commonly internally massive, with rare channels, ripple marks, and normal grading. Upper sequence: massive to vaguely normally graded.	Units are thickly laminated to medium bedded over the lower third of the unit and massive at the top.
D1vc1	344	Green-grey siltstone to fine-grained sandstone, basaltic boulder conglomerate to fine-grained basaltic sandstone pumice-rich pebble conglomerate.		Siltstone: C: quartz, alkali feldspar, plagioclase, zircon, rhyolite. M: secondary biotite, actinolite, zoesite, and calcite. Basaltic boulder conglomerate: C: basalt, basaltic scoria, siltstone, plagioclase. M: Green-grey siltstone and altered ash. Pumice-rich pebble conglomerate: C: pumice, altered volcanic rock, sandstone, feldspar. M: Green-grey siltstone, altered ash and silicic shards.	Volcaniclastic layers probably represents fluvial reworking of a nearby mafic tuff (basaltic conglomerate) and felsic tuff (pumice-rich conglomerate) erupted onto the tidal flat sediments. Beds are commonly lensshaped and discontinuous, with normal and reverse grading, cross-bedding, pebble trains and soft-sediment load structures and faults.		Volcaniclastic layers become more dominant upward in the section.
D4c1	40+	Coarse grained conglomerate.		C: lithic tuff, porphyritic andesite, grey sandstone M: red sandstone and smaller lithic clasts T: clast-supported, very poorly sorted, angular to subround clasts.	Debris flow; clast type reflects local lithologies; angular block sized clasts suggest a proximal source.		Clast types originated from topographically high local sources.
MAFIC LAVA FLOWS							
D4mf2	35 Flows: 1-12	Porphyritic basalt. Highly to sparsely amygdaloidal.	Fine grained grey sandstone, crystal vitric tuff.	P: olivine, clinopyroxene, rare plagioclase G: plagioclase, clinopyroxene, Fe-oxide, rare altered glass T: fine grained, intergranular to subophitic.	Subaerial to littoral pahoehoe sheet flows.	High vesicularity, lack of hyaloclastite.	
D4mf1 D3mf1 D2mf1 D1mf1	12-460 Flows: 1-12	Highly to sparsely amygdaloidal basalt.	Peperitic breccia, mudstone, siltstone.	P: rare plagioclase G: plagioclase and rare clinopyroxene microlites; chlorite, quartx, epidote, actinolite. T: tachylitic or pilotaxitic. D4mf1: T: intergranular to supophitic.	Extensive subaerial to littoral sheet, pahoehoe flows. peperitic breccia formed by the interaction of lava or magma with cold, wet sediment.	Pahoehoe toes associated with littoral sediments, high vesicularity, lack of hyaloclastite.	

Unit #	Thickness (metres)	Maximum Dominant rock types	Minor rock types	Minerals and texture*	Facies analysis and depositional environment	Environmental indicators	Comments
MAFIC PYROCLASTIC ROCKS							
D4lvt1	35	Basaltic heterolithic lapilli tuff.		C: rhyolite, basalt, sandstone, siltstone, mafic scoria XL: plagioclase, minor clinopyroxene M: altered mafic shards, ash, Fe-oxides.	Phreatomagmatic tuff. Both blocky nonvesicular shards and vesicular shards occur, indicating formation by a combination of vesiculating magma and quenching by steam.		
D3tb2 D3tbv1	35 15	Heterolithic basaltic tuff breccia.		C: siltstone, basalt, gabbro, rare lithic-cored bombs. M: nonwelded, basaltic vitric tuff.	Phreatomagmatic explosion breccias. Both blocky nonvesicular shards and vesicular shards occur, indicating formation by a combination of vesiculating magma and quenching by steam. Airfall depositional due to lack of internal structures. Most clasts are angular but some are bomb-shaped.	Nonwelded. AL of siltstone, gabbro, and volcanic rocks.	
D3ms1	82	Mafic scoria.		EL: basaltic AL: siltstone M: none CT: calcite and agglutination.	Large clasts indicate proximity to vent.	Accidental clasts of siltstone suggest eruption through tidal flat deposits.	
D4tb1	7	Mafic heterolithic lapilli tuff to tuff breccia.	Grey, vitric tuff.	Tuff breccia: EL: mafic flow banded bombs. V: mafic and felsic shares, pumice, and scoria CL: basalt, vesicular basalt AL: red siltstone, rhyolite M: fine to coarse ash Vitric tuff: V: felsic fiamme, bubble wall and blocky shards AL: sandstone, basalt M: recrystallized fine ash.	Tuff breccia: phreatomagmatic air-fall deposit. Large grain size and fluidal magmatic bombs suggests this is a proximal unit. Shards are both blocky and bubble-wall shapes. Vitric tuff: welded pyroclastic flow deposit, due to poor sorting, massive structure and fiamme.	Accidental siltstone clasts in tuff breccia indicate eruption through shallow water sediments. Welding in vitric tuff indicates subaerial deposition.	Tuff breccia: Clasts size increases upward until fluidal magmatic clasts dominate. Matrix-supported breccia lacking internal structure.
FELSIC TO INTERMEDIATE LAVA FLOWS AND DOMES							
D4ff2 D3ff1 D2ff4 D2ff3 D2ff2 D1ff4 D1ff3 D1ff2	60-350	Pink flow-banded and massive aphyric rhyolite.		P: plagioclase, rare sanidine. G: plagioclase microlites; quartzofeldspathic T: microgranophyric, rare felty.	Rhyolite lava flows and domes. Flow banding defined by variation in colour and grain size.		
D4ff1	435	Purple, flow-banded, sparsely porphyritic rhyolite.	Peperitic breccia.	P: plagioclase, altered biotite, pyroxene?, olivine? G: microcrystalline quatz and feldspar T: granophyric, perlitic cracks near contacts.	Intrusive dome. Peperitic breccia and quench textures at upper and lower contacts with surrounding sedimentary rocks.	Intrusion into water saturated tidal flat sedimentary rocks with mixing to form peperitic breccia.	Vesicles in the sedimentary component of peperite indicate that the pore spaces contained water.
D4ff3	?	Flow-banded rhyolite.		P: feldspar G: devitrified glass with plagioclase and clinopyroxene microlites. T: holocrystalline to hypocystalline.	Intrusive rhyolite dome. Intrudes littoral sedimentary rocks (D4s1).		
D4ff4	60	Porphyritic rhyolite.		P: sanidine ?, altered mafic mineral, Fe-oxides G: altered and recrystallized, quartzofeldspathic, altered mafic mineral T: holocrystalline.	Small domes that intrude littoral sedimentary rocks (D4s1).		
D2ff1	350	Pink, porphyritic rhyolite.		P: plagioclase, sanidine T: microgranophyric to felty or pilotaxitic. Rare mafic xenoliths.	Rhyolite lava flow. Flow banding poorly developed and defined by differential weathering.		
D1ff1	400	Rhyolite with trachytic-texture		G: feldspar microlites in a recrystallized silicic groundmass.	Felsic dome based on the limited lateral extent of the unit.		
D4td2	?	Flow-banded trachydacite.		P: plagioclase, clinopyroxene, hornblende AL: basalt G: devitrified glass to phaneritic T: holocrystalline to hypocystalline.	Lack of intrusive contacts and baked zones suggests an extrusive dome. A near vent facies.		
D4td1	90	Flow-banded trachydacite.	Mafic trachydacite.	Trachydacite dome: P: plagioclase, rare sanidine, rare altered mafic mineral, Fe-oxides G: fine grained, recrystallized/devitrified quartzofeldspathic, sericite T: holocrystalline. Mafic trachydacite dome: P: plagioclase, clinopyroxene, Fe-oxides, altered mafic mineral G: very fine grained feldspathic T: holocrystalline.	Intermediate and intermediate-mafic intrusive dome complex. Intrudes 'ittoral sedimentary rocks (D4s1).		Rare mafic lithics in felsic dome.

Table 1. (cont.)

Unit #	Thickness (metres)	Maximum Dominant rock types	Minor rock types	Minerals and texture*	Facies analysis and depositional environment	Environmental indicators	Comments
FELSIC PYROCLASTIC ROCKS							
D4lvt3	25	Felsic lithic vitric tuff to lapilli tuff.		XL: Sanidine, plagioclase, zircon, opaques V: wispy felsic pumice; felsic blocky and bubble-wall glass shards; mafic platy and blocky glass shards CL: basalt, rhyolite AL: siltstone, sandstone, crystal tuff M: fine to medium ash.	Phreatomagmatic air-fall deposit based on shard and bedding type. Poor sorting indicates proximity to vent. Nonwelded.		
D4lvt2 D4vt2 D4vt1	10-50	Lithic-vitric tuff, vitric tuff and flow-banded vitric tuff.	D4vt1: Rare peperitic breccia.	XL: feldspar V: pumice, felsic shards M: vitric D41vt2: XL: plagioclase, quartz EL: rhyolite AL: basalt, siltstone, vitric tuff T: recrystallized or pilotaxitic. D4vt1: devitrified glassy; perlitic cracks.	Pyroclastic flow deposits based on poor sorting, massive structure and aligned pumice and shards. Shard type indicates a magmatic source.	Poor to moderate welding indicating subaerial deposition.	Crystal alignment and pumice flattening define a bedding parallel foliation.
D3vt1 D3lvt2 D3lvt3	30-65	Lithic-vitric lapilli tuff, crystal lithic lapilli tuff and crystal-vitric tuff.		Lithic-vitric lapilli tuff: XL: feldspar CL: mafic volcanic AL: siltstone M: vitric Crystal lithic lapilli tuff: XL: alkali feldspar V: pumice CL: mafic and felsic volcanics M: vitric Crystal-vitric tuff: XL: alkali feldspar V: pumice.	Thicker beds: near vent welded ash flow tuff. Magmatic due to vesicularity of shards and pumice. Laminated tops: ash cloud deposits. Crossbedded layers: ground surge deposits. Thin, massive tuff beds: air-fall deposits.	Dense welding indicating subaerial deposition.	
D3vt1	500	Banded and welded tuff.	Densely welded heterolithic tuff breccia.	XL: minor feldspar, rare altered ferromagnesian minerals AL: basalt, rhyolite M: microcrystalline quartz and feldspar T: granophyric.	Ash flow tuff. Flow banding-typically folded, minor flow top brecciation. Dense welding and coarseness of tuff breccia suggest proximity to source.	Dense welding indicating subaerial deposition.	Flow banding defined by extremely stretched pumice. Folding of flow foliation possibly due to rheomorphism.
D2lvt2	50	Accretionary and lithic-vitric lapilli tuff.		V: pumice CL: accretionary lapilli M: fine-ash tuff.	Phreatomagmatic air-fall and surge deposits. Most bedding structures (massive bedding, normal and reverse grading) consistent with air-fall deposition. Crossbedding and climbing ripples are more typical of surge deposits.	Accretionary lapilli and juvenile pumice. Massive or crosslaminated bedding; normal to reverse grading.	
D2xlt1	534 Beds: 2	Red to buff crystal tuff, crystal lithic tuff and lapilli tuff.	Red siltstone.	XL: feldspar V: pumice CL: accretionary lapilli AL: rhyolite, basalt, rare mudstone M: fine to coarse ash.	Magmatic pyroclastic fall and flow deposits with local hydroclastic airfall activity. Increase in degree of welding and grain size indicates a southern source.	Welding. Beds are massive, laminated, normally reversely and multiply graded.	Convolute lamination in some tuffs may indicate rheomorphism.
D2tb1	115	Heterolithic tuff breccia.		V: pumice EL: rhyolite bombs CL: rhyolite AL: siltstone and basaltic lapilli.	Near vent pyroclastic airfall and rare ground surge deposits. The near vent equivalent of D2xlt1. Large grain size and welding of airfall deposits indicate proximity to vent.	Welding. Thin laminated and crosslaminated beds. Typically massive to vaguely bedded.	
D2xvt1 D1xvt3	75 200	Felsic crystal vitric tuff and accretionary lapilli tuff.		Crystal vitric tuffs: XL: placioclase V: pumice, platy, bubble-wall and blocky shards CL: coarse grained rhyolite AL: basalt M: fine ash tuff Accretionary lapilli tuff: V: pumice, platy shards CL: accretionary lapilli M: fine- to coarse-ash tuff.	Pyroclastic base surge deposits from a hydroclastic eruption. Units are internally vaguely thinly bedded or laminated, locally cross-laminated and reverse and normally graded. D1xvt3 has rare welded beds that are probably pyroclastic flow deposits.	Welding indicating subaerial deposition.	Abundance of steam in the eruption column would account for the accretionary lapilli.
D2lxt1	100	Lithic crystal and lithic crystal vitric tuff, and lapilli tuff.	Red and green siltstone and mudstone.	XL: feldspar V: pumice, platy and bubble-wall shards CL: rhyolite AL: basalt M: recrystallized and altered fine ash.	Ash flow and surge deposits with minor airfall deposits and siltstone. Lack of welding and thinness of units suggests distal deposits.	Some beds welded indicating subaerial deposition.	Some beds have extreme crystal enrichment with up to 80% broken feldspar crystals.
D1xvt2 D1xvt1 D1xvt1a D2xvt2 D2lvt1 D2vt1 D1vt2 D1vt1	40-700	Massive vitric tuff, and crystal vitric tuff.		V: pumice and glass CL: mafic and felsic volcanics AL: minor sedimentary rocks M: vitric.	Pyroclastic flows, poorly sorted, massive, flow alignment of pumice, and broken crystals.	Welding indicating subaerial deposition.	D1xvt1a is an alteration zone within D1xvt1.

* C = clast type; M = matrix; CT = cement; V = vitric, XL = crystal; EL = essential lithic; CL = cognate lithic; AL = accidental lithic; P = phenocryst; G = groundmass; T = texture.
# Lithology codes: D = Siluro-Devonian; 1,2,3,4 = Cycle of volcanic activity; s = sedimentary rock; vc = volcaniclastic rock; c = conglomerate; mf = mafic flow; t = tuff; tb = tuff breccia; ms = mafic scoria; ff = felsic flow or dome; td = trachydacite dome; x = crystal; v = vitric; l = lithic; 1-4 = stratigraphic order within cycle. See also Figure 4.

thick. Bed thickness ranges from lamination in the finer grained siltstone and sandstone to beds up to several metres thick in the coarser grained sandstone and conglomerate (Fig. 5). Many of the siltstone and sandstone units are similar in composition, texture, and structure throughout the study area and are discussed together. They are divided into separate map units largely on the basis of stratigraphic position. Units D3s1, D4c1, and carbonate breccia beds in D4s1, are markedly different and are discussed separately.

Units D1s1, D2s1, D4s1, and D4s2

The sandstone and siltstone consist predominantly of grains of quartz (40-55%), feldspar (5-15%), primary muscovite (1-5%), are rare pyroxene, detrital zircon, chloritized mafic shards and lithic clasts (0-15%), in an altered clay matrix (typically <15%) (Fig. 6, 7). The clay is typically altered to sericite and chlorite. Most monocrystalline and polycrystalline quartz grains are elongate, have moderate undulose extinction, sutured grain boundaries, and mica inclusions that indicate derivation from a predominantly metamorphic source (Folk, 1980). Minor common, vein, and volcanic quartz clasts also occur. Most rhyolitic rocks in the study area are quartz-free or rarely quartz-poor, suggesting that the volcanic quartz was not locally derived.

Lithic clasts are siltstone (Fig. 6), mudstone, felsic and mafic lava and pyroclastic rocks, a variety of foliated, low-grade pelites, and sutured quartz aggregates. The framework grains are typically angular to subrounded and elongate to subspherical. The siltstone and sandstone are moderately well sorted to poorly sorted. The rock composition and shape of the grains indicate that these rocks are immature.

Secondary minerals include chlorite, sericite, and epidote. At some locations adjacent to the Saint George Batholith, there is abundant metamorphic biotite and rare cordierite.

Primary sedimentary structures in the thinner beds (1 cm-2 m) include plane lamination, ripple crosslamination, herringbone crosslamination, mud drapes on ripples (Fig. 8), dewatering structures, interference ripples, current ripples (Fig. 9), mudcracks (Fig. 8, 10), and rare raindrop imprints. Ripples are typically 0.5-1 cm high, but up to 5 cm in amplitude, and have a wavelength of 4-10 cm. These thinner beds are commonly bioturbated, with horizontal and vertical burrows (Fig. 11) and traces. In the thicker beds (up to 2 m), the structures include low- and high-angle cross-stratification

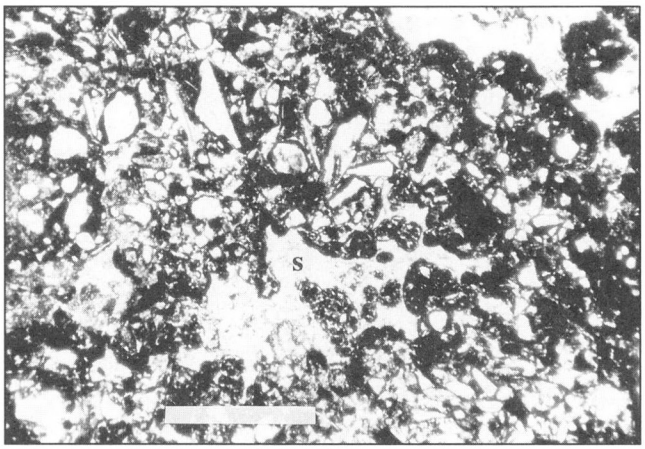

Figure 7. Photomicrograph of a fine grained sandstone from unit D2s1 showing an unabraded, chloritized mafic scoria fragment (s) and shards, as well as mineral grains as in Figure 6. The black areas are hematite-stained lithic grains and matrix. Hematite also occurs as cement. Bar scale represents 0.3 mm (plane polarized light). (GSC 1993-217B)

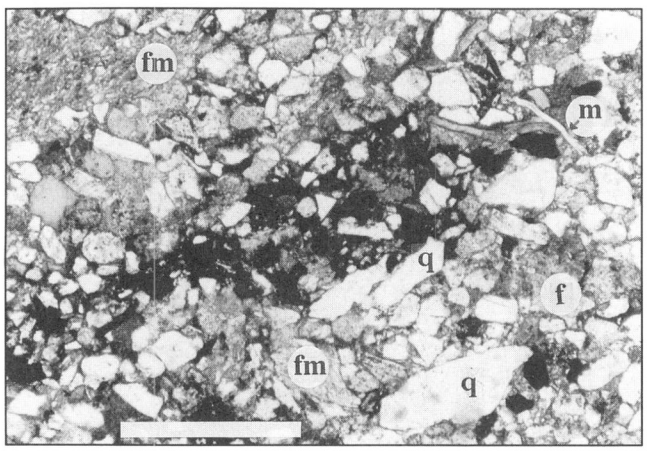

Figure 6. Photomicrograph of a fine grained sandstone from unit D3s1, showing quartz (q), feldspar, muscovite, and lithic grains. The lithic grains are siltstone and foliated mudstone (fm). The black areas are hematite-stained lithic grains and hematite cement. The sandstone is texturally and compositionally immature. Bar scale represents 0.5 mm (plane polarized light). (GSC 1993-217A)

Figure 8. Vertical section through interbedded fine grained sandstone, siltstone, and mudstone from unit D4s1. Primary sedimentary structures include plane bedding and lamination, mud curls (lamina above base of pen) and mud drapes on cross laminations (arrow). (GSC 1993-212FF)

(Fig. 12), ripple crosslamination, planar and trough crossbedding, channels and rare basal lag gravel. Rare channels (D4s1) have a width of about 2 m and are up to 1 m deep. Channel fill is typically crossbedded, medium grained sandstone.

The fossils (upper part of unit D2s1 on Holt's Point) include lingulid brachiopods (Fig. 13), bivalves, ostracods, and rare gastropods. The fossil assemblage is indicative of a shallow marine (tidal facies) environment (Pickerill and Pajari, 1976).

Carbonate rip-up clast breccia in unit D4s1

Unit D4s1 contains two beds of carbonate rip-up clasts in a sandstone matrix. The upper bed is massive and up to 15 cm thick. The lower bed is crossbedded and from 0.5 m to 0.75 m thick.

Figure 9. *Sinuous crested, current ripples in medium grained sandstone from unit D4sl. (GSC 1993-212EE)*

Figure 10. *Polygonal mudcracks in siltstone to mudstone from unit D2sl. (GSC 1993-212DD)*

Figure 11. *Photomicrograph of an oblique cross-section through vertical burrows in siltstone in unit D1s1. Bar scale represents 1.5 mm (plane polarized light). (GSC 1993-217C)*

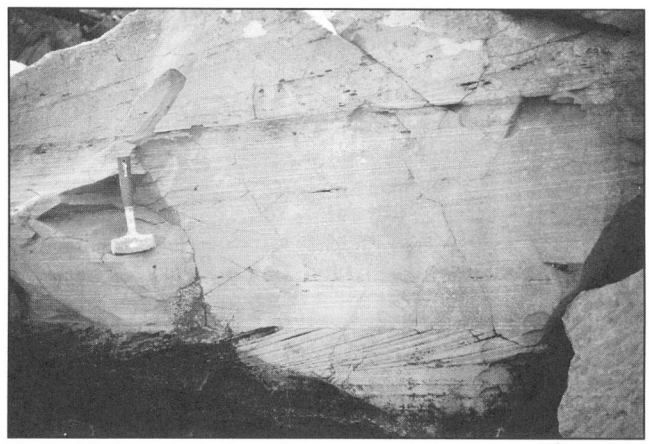

Figure 12. *Tabular low- and high-angle crossbedding in medium grained sandstone from unit D4sl. (GSC 1993-212A)*

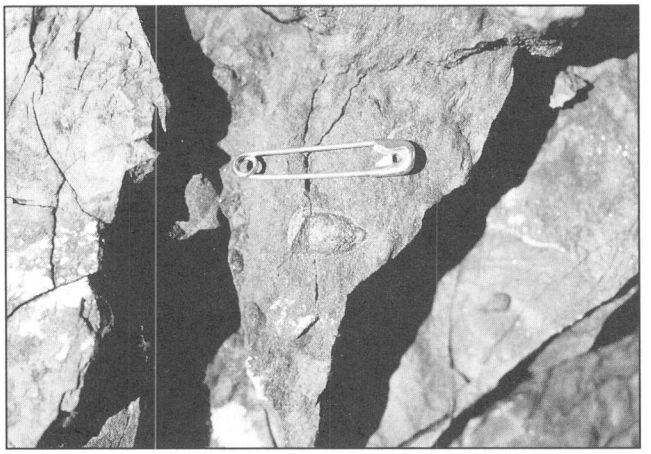

Figure 13. Lingulid type brachiopod in fine grained micaceous sandstone, unit D2sl. Safety pin is approximately 2 cm long. (GSC 1993-212C)

Carbonate clasts in the upper bed (up to 40% of the bed) are subangular to rounded, elongate to irregular, and up to 7 cm long. Clasts vary in composition from 100% carbonate grains to a mixture of carbonate and silicic grains. The carbonate is both micritic and sparry. Noncarbonate grains in the clasts are similar to those in the sandstone described previously. Some carbonate clasts are thinly bedded with bedding defined by a change in grain size from sparry calcite to micrite, or by a change in the amount of silicic grains.

The matrix of the carbonate breccia is wackestone with silicic grains in a sparry calcite matrix. Matrix grains include volcanic and metamorphic, angular to subrounded quartz (20%), rock fragments (5%), muscovite (2%), grains altered to chlorite (2%), and plagioclase (<1%). Sparry calcite makes up 70% of the matrix.

The lower bed of rip-up clasts is heterolithic and contains thin lenses of medium grained sandstone. The breccia is a poorly-sorted packstone. The clasts are up to 15 mm in size, irregular in shape, have irregular grain contacts, and include carbonate wackestone with quartz and muscovite grains in a matrix/cement of sparry calcite (40%), vaguely bedded hematite-stained siltstone (20%), and massive and amygdaloidal, porphyritic basalt (10%). The matrix of the breccia (30%) consists of quartz, metamorphic rock fragments, and mafic volcanic rock fragments. These grains are up to 1 mm in size. The cement is sparry calcite or chlorite.

Interpretation of units D1s1, D2s1, D4s1, and D4s2

The combination of sedimentary structures, fossil assemblage, and fine grain size of the rocks indicates a low-energy, peritidal depositional environment (Evans, 1975; Reineck, 1975). The preservation of unabraded mafic shards within the sedimentary rocks indicates minor reworking. Near the base of the mapped sequence (D1s1, lower part of D2s1) mudstone and siltstone are more abundant than sandstone. Beds lack abundant rippled tops and reworked shell debris. These features suggest deposition in a zone not influenced by wave action (Weimer et al., 1982), possibly the upper intertidal zone. Mudcracks indicate periodic exposure.

Higher in the sequence (upper parts of D2s1, D3s1) the units comprise siltstone to sandstone as well as coarser grained sandstone beds and conglomerate. The thinner beds in unit D2s1 on Holt's Point, contain up to 50% fossils (listed above). These features, as well as an increase in the abundance of rippled tops on fine grained beds, and the extent of bioturbation, may indicate a slight increase in water depth.

This deepening trend continues into the final cycle (D4s1, D4s2) where sandstone dominates over siltstone. Sedimentary structures in units D4s1 and D4s2 include crosslamination, current ripples, planar crossbedding, and channels. Evidence of exposure such as mudcracks is rare although bedding surfaces are covered by tracks and trails. The crossbedded channel sandstone may represent tidal channels (Carter, 1975). Channels are typically up to 1 m in thickness and may also be referred to as tidal creeks (Weimer et al., 1982).

The sequence from D1s1 to D4s1 suggests an increasing water depth or transgression and a change from the upper to the lower intertidal zone. Channel-fill deposits are rare in the sequence but are typical of the proposed environment. Herringbone cross-stratification is common only in cycles 2 and 3. The most convincing evidence for a tidal flat origin for this sequence includes the marine nature of the sedimentary rocks, which is based on the fossil assemblage (upper part of D2s1), mud drapes on crosslaminations in fine grained sandstone, indicating alternating slack and running water periods, and structures such as mudcracks and raindrop imprints indicative of exposure (Ginsburg, 1975).

The beds of carbonate rip-up clasts in unit D4s1 are interpreted to be storm-generated rip-up beds with clasts derived from a bedded carbonate sequence in the supratidal zone. Carbonate deposits in the supratidal environment are typically laminated, have rare fossils or burrows, and commonly have mudcracks (Laporte, 1975), consistent with the characteristics of the clasts in the breccia.

From the lack of tidal channels necessary to carry off the outgoing water, and the paucity of herringbone cross-stratification (Walker and Harms, 1975), a microtidal environment is postulated for the sedimentary sequence (D1s1-D4s2). Preservation of mafic glass shards, leading to a thick succession of relatively immature sedimentary rocks indicates that the sedimentation and subsidence rates were probably rapid.

Unit D3s1

Unit D3s1 comprises interbedded red conglomerate, sandstone, siltstone, and mudstone (Fig. 14). This unit has a maximum thickness of 165 m. Pebbles and cobbles of amygdaloidal basalt, diabase, rhyolite, mudstone, siltstone, and minor carbonate are up to 5 cm in length. Most clasts are subangular. The sand-sized particles are quartz, plagioclase, mica, and rhyolitic volcanic and sedimentary rock fragments (Fig. 15). The matrix is clay-sized material.

Figure 14. Interbedded sandstone and pebble conglomerate from unit D3s1. Clasts in the conglomerate include mudstone, siltstone, and rare carbonate. Section is oriented north (hammer)-south. (GSC 1993-212D)

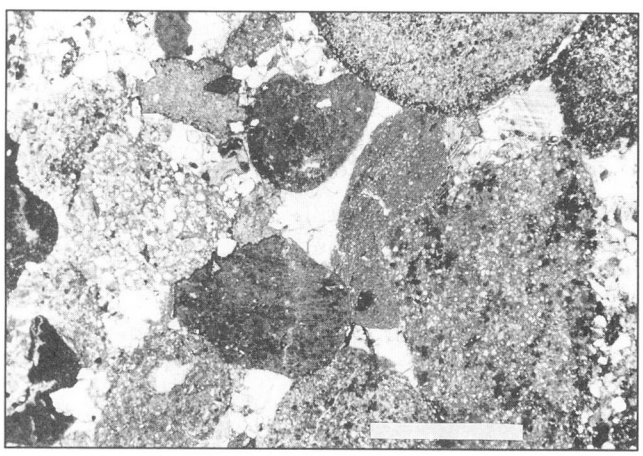

Figure 15. Photomicrograph of a coarse grained sandstone from unit D3s1 showing rounded to subrounded sedimentary and volcanic rock fragments with a sparry calcite cement. Bar scale represents 1.5 mm (plane polarized light). (GSC 1993-217D)

Beds are 0.5 cm to 1 m thick. The thickest beds tend to be the coarsest, but finer grained beds form the largest percentage of the unit. The entire sequence coarsens upward and the abundance of volcanic clasts increases upward. Beds are massive, normally graded, current-ripple and ripple-drift crosslaminated, and parallel laminated. There is rare pebble imbrication in the conglomerate beds. Other sedimentary structures are current ripple marks, oscillation ripple marks, cut and fill-forming conglomerate channels, mudcracks, shrinkage polygons, concretions up to 3 cm in diameter, and raindrop impressions.

Interpretation of unit D3s1

The rock type and structures in this unit are consistent with deposition in an alluvial fan (Reineck and Singh, 1975) on the slope of a volcanic edifice. The scour and fill, current-ripple crossbedding and cross-lamination, and gravel-lag deposits are characteristic of braided channels on an alluvial fan. The massive conglomerates and those with imbricated clasts are probably mud-flow deposits. Upward coarsening of the sequence represents either progradation of the fan or migration of channels across the fan.

Unit D4c1

Unit D4c1 is red, clast-supported conglomerate. The unit is a minimum of 1 m thick. Clasts in the conglomerate (70%) are angular to subrounded, up to 60 cm in size, and include lithic tuff (80%), aphanitic and porphyritic trachydacite (5%), and sandstone (5%). The matrix (30%) is sand- to silt-sized and comprises quartz, feldspar, and lithic fragments with the same range in composition as the framework clasts.

Interpretation of unit D4c1

The unit is interpreted as a debris flow deposit on the basis of poor sorting, the angularity of clasts, the clast-supported and massive structure, and the immature lithic-rich composition of the matrix. The trachydacite clasts were derived locally from the trachydacite dome to the south (D4td2). The lithic tuff clasts are also interpreted to be locally derived due to their large size and angular shape.

Volcaniclastic rocks

Volcaniclastic rocks are rare and dominantly from mafic sources. Volcaniclastic rocks vary in composition but most comprise basaltic scoria, massive basaltic clasts, altered mafic shards, rare rhyolitic shards, and sedimentary rock fragments as well as silicic grains, as in the nonvolcaniclastic sedimentary rocks described above.

Unit D1vc1

Unit D1vc1 comprises interbedded grey-green siltstone, buff to grey sandstone, basaltic boulder conglomerate to fine grained basaltic sandstone, and pumice-rich pebble conglomerate. The siltstone and sandstone are identical to those previously described.

The basaltic boulder conglomerate to fine grained, basaltic sandstone beds contain 20-80% fragments of vesicular basalt, basaltic scoria, laminated siltstone to fine grained sandstone, and plagioclase crystals in a silt- to sand-sized green-grey matrix. Volcanic clasts are usually 15-20% but up to 80% of individual volcaniclastic beds. Volcanic clasts are up to 15 cm in size, angular and irregularly shaped. Siltstone and sandstone clasts are up to 5%, 4 cm to 1 m in size, and angular to subangular. Larger siltstone and sandstone clasts are irregular in shape (Fig. 16) and may have been deposited while still wet. The matrix is clay- to sand-sized and contains volcanic ash and clastic grains as in the previously described nonvolcaniclastic sandstone. The ash is altered to clay and chlorite and contains metamorphic biotite. Beds are poorly sorted, thickly- to thinly-bedded and are planar to lens shaped. Primary structures include normal and reverse grading, cross-bedding, pebble lags, and load structures (Fig. 17).

The pumice-rich pebble conglomerate beds comprise feldspar crystals (<1% and up to 2 mm), lithic clasts (3-7%), and light grey pumice (30-50%). The pumice is equant to elongate, has very irregular, commonly wispy edges (Fig. 18), and contains 5-10% plagioclase phenocrysts. The lithic clasts include: (1) white, altered mafic volcanic clasts (1-2%), that are equant to irregular, up to 5 cm in size, surrounded by alteration haloes, and commonly contain sulphide minerals altered to hematite, (2) fine grained plagioclase-phyric, grey volcanic clasts (2-5%), up to 1.5 cm in size and rounded to irregular, and (3) rare fine grained sandstone clasts, up to 20 cm and elongate to irregular. Sandstone clasts are also found in the basaltic boulder conglomerate beds. The matrix is similar to that of the basaltic beds but contains rare platy rhyolitic glass shards.

The pumice-rich pebble conglomerate beds are poorly sorted and massive to vaguely bedded with bedding defined by flattening of some pumice. The thickness of pumice-rich pebble conglomerate beds could not be determined due to poor outcrop.

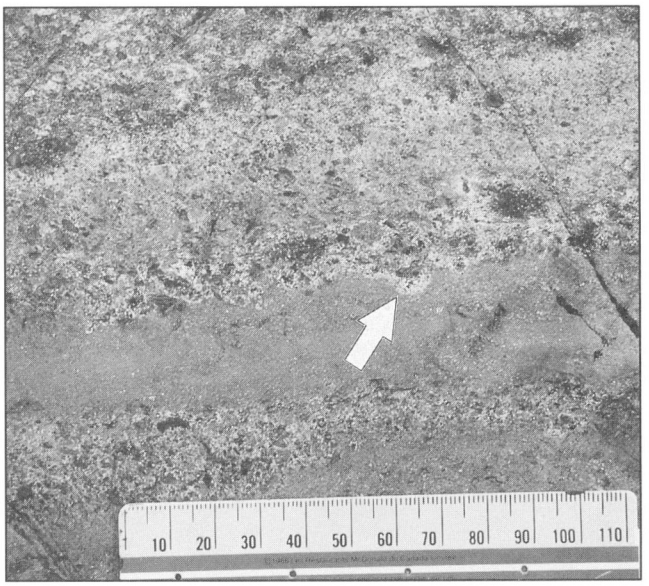

Figure 17. Thinly-bedded to laminated, basaltic, coarse- to fine-grained sandstone from unit D1vc1 showing bedding defined by grain size. The bed in the centre of the field of view has load casts (arrow) at the contact with the underlying bed. (GSC 1993-212B)

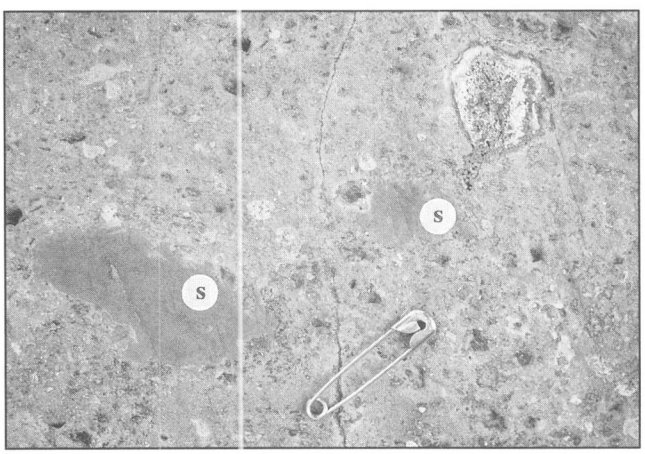

Figure 16. Matrix of basaltic boulder conglomerate from unit D1vc1 showing irregular siltstone clasts (s) with fragile-looking edges. Other clasts include vesicular basalt and basaltic scoria. Safety pin is approximately 2 cm long. (GSC 1993-212CC)

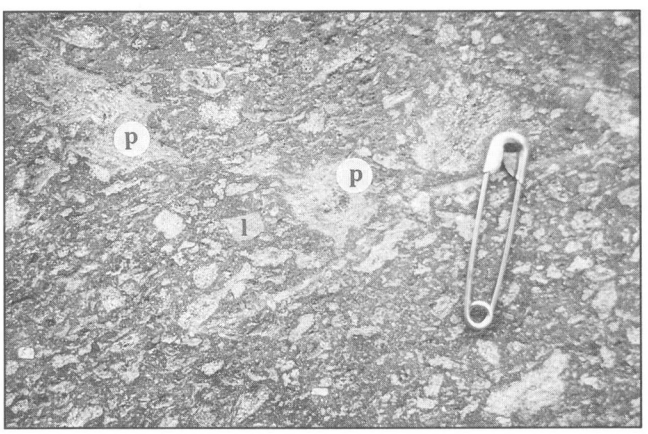

Figure 18. Pumice-rich pebble conglomerate from unit D1vc1 showing irregular and unabraded light-coloured pumice (p) and rounded to angular lithic clasts (l). Safety pin is approximately 2 cm long. (GSC 1993-212BB)

Interbedded with the pumice-rich pebble conglomerate beds, are beds of red, fine grained, laminated sandstone similar to unit D1s1. These sandstone beds are the same composition as the irregular sandstone clasts in the basaltic boulder conglomerate and pumice-rich pebble conglomerate beds. Contacts between the pumice-rich pebble conglomerate and sandstone units are sharp. Lamination in the sandstone drapes irregularities in the underlying pebble conglomerate. The sandstone grades locally into a coarse-grained sandstone with pumice (5-10%) and rare lithic clasts.

Units D1vc2 and D1vc3

Units D1vc2 and D1vc3 are up to 380 m and 140 m thick, respectively. They comprise basaltic boulder to pebble conglomerate beds interbedded with minor grey siltstone. The conglomerate beds contain basaltic scoria (commonly 10-30%, rarely 60%; Fig. 19), banded rhyolite (5%), microphyric basalt (30%), plagioclase (2-5%), and rare rhyolitic tuff and siltstone. The basaltic scoria clasts are 1 mm to 1 cm in size, subrounded to rounded, and have unabraded scalloped edges. Coarser rhyolitic fragments (up to 30 cm), generally occur near the base of units D1vc2 and D1vc3. Relict siliceous, platy, and bubble-wall (Fig. 20) glass shards are locally abundant. The matrix (0-40%) is clay-sized and comprises an assemblage of crystals, lithic fragments, and clay minerals. Alteration minerals include chlorite and epidote. Locally, clasts are cemented with calcite.

Unit D1vc2 is generally massive, although crude bedding is locally defined by concentrations of coarser volcanic clasts. Unit D1vc3 is divided into two sections; a lower bedded section and an upper massive, poorly sorted section. Beds in the lower section are up to 30 cm thick, generally planar and internally massive. Bedding structures include rare channels, ripple marks, and normal grading.

Unit D2vc1

Unit D2vc1 is a 60 m thick basaltic cobble conglomerate unit. It comprises clasts of vesicular to dense basalt, banded and porphyritic rhyolite, and siltstone. Basalt clasts (70%) are 1-15 cm in size and subrounded. Flow banded and porphyritic rhyolite clasts (2-3%) are 0.3-1 cm in size, and subrounded to rounded. Siltstone and mudstone clasts are 1-5 cm in size, rounded, and rare. The unit is massive, very poorly sorted, and clast supported.

Interpretation of units D1vc1, D1vc2, D1vc3, and D2vc1

Volcaniclastic units D1vc1, D1vc2, D1vc3, and D2vc1 are reworked mafic and felsic pyroclastic deposits. Reworking is indicated by the roundness of basaltic scoria grains, sedimentary matrix, interbedded sedimentary rocks, and sedimentary structures such as channelized bedding, crossbedding, ripple marks, pebble trails, and lens shaped beds. The basaltic scoria and rhyolitic pumice were probably derived from poorly consolidated scoria or tuff cones. Eruption, deposition, and subsequent reworking of the volcanic material likely occurred in a tidal flat environment, based on temporal and spatial association with nonvolcaniclastic tidal flat sedimentary rocks. Many sedimentary clasts incorporated in the volcaniclastic rocks are irregular in shape and were probably derived from unconsolidated tidal flat material. Siliceous glass shards, found in abundance in some units (D1vc1, D1vc2, D1vc3), record either earlier or contemporaneous proximal silicic pyroclastic activity. The degree of reworking varies from strong (D1vc2, D1vc3, D2vc1) to poor (D1vc1, D2vc1), based on the ratio of volcaniclastic to nonvolcaniclastic sedimentary rocks, abundance of volcanic clasts, and preservation of siliceous glass shards and unabraded clasts of basaltic scoria. The preservation of siliceous glass shards and unabraded scoria grains suggests relatively rapid deposition in a low energy environment.

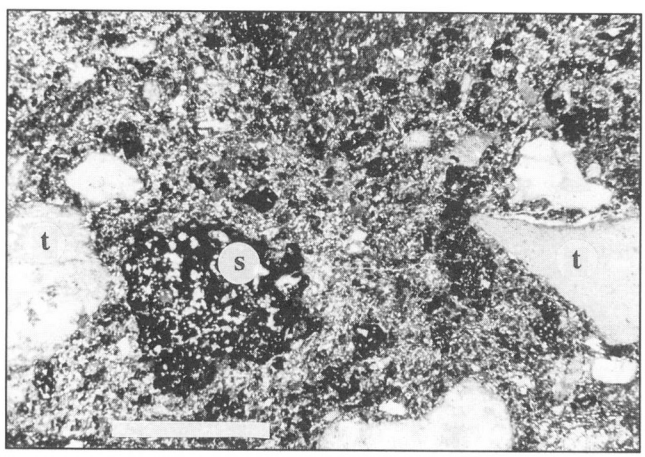

Figure 19. Photomicrograph of the matrix of basaltic pebble conglomerate from unit D1vc3 comprising angular to subangular basaltic scoria (s), plagioclase, felsic tuff (t), and siltstone in a clay-sized matrix. Bar scale represents 3 mm, (plane polarized light). (GSC 1993-217E)

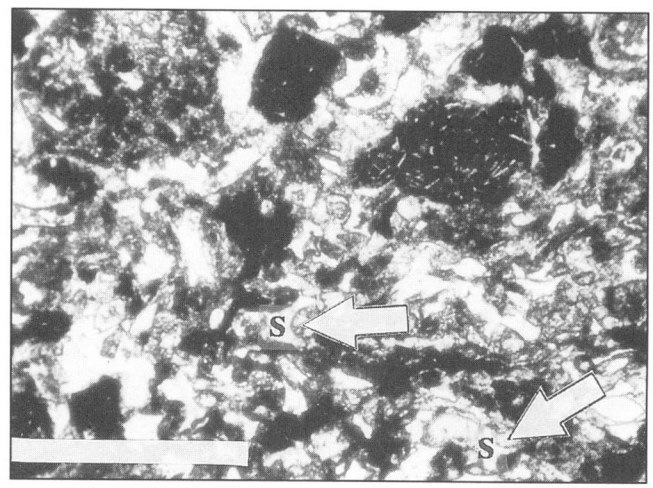

Figure 20. Photomicrograph of a basaltic pebble conglomerate from unit D1vc3 showing relict siliceous bubble-wall (arrow) shards (s). Bar scale represents 0.5 mm (plane polarized light). (GSC 1993-217F)

Unit D2vc2

Unit D2vc2 is thinly bedded, brownish-red siltstone similar to the upper parts of unit D2s1, with lenses and beds of green basaltic volcanic fragments. Maximum unit thickness is about 40 m. The abundance of volcaniclastic layers increases upward to 90%, the unit coarsens upward, and bed thickness increases upward from 2 mm-3 cm to 10-30 cm. Most layers are lenticular but irregular due to soft sediment deformation.

Red siltstone layers contain about 1-25% volcanic fragments, and are horizontally laminated, massive, or very rarely ripple laminated. Coarse grained volcaniclastic layers are massive or rarely normally graded.

The lithic clasts of the siltstone and volcaniclastic layers are up to pebble sized, mostly subrounded, and heterolithic. The clasts include siltstone rip-up clasts, amygdaloidal and nonamygdaloidal mafic volcanic fragments, rare armoured lapilli consisting of siltstone fragments mantled by volcanic glass, and rare rhyolitic fragments. As in unit D2s1, the matrix contains bubble-wall and blocky mafic glass shards as well as nonvolcanic grains (Fig. 21).

Interpretation of unit D2vc2

Unit D2vc2 was deposited in a tidal flat environment proximal to an intermittently active mafic volcano(es). The volcanic fragments in the volcaniclastic beds are air-fall deposits because most (except the glass shards) are too large to have been transported by weak tidal currents. The rare volcanic fragments within the siltstone beds are scoriaceous fragments which were light enough to be transported by tidal currents. The excellent preservation of the glass shards and glass surrounding armoured fragments indicates little reworking and rapid burial due to high sedimentation rates in a low energy environment.

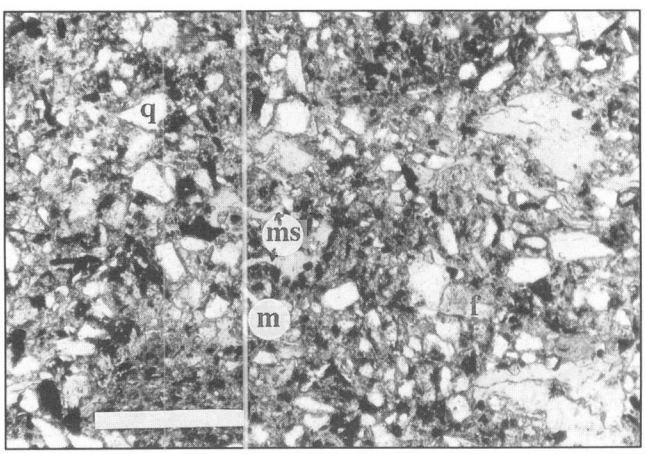

Figure 21. Photomicrograph of a basaltic siltstone from unit D2vc2 comprising bubble-wall and blocky mafic shards (ms), quartz (q), feldspar (f), primary muscovite (m), and lithic clasts in clay-rich matrix. Bar scale represents 0.3 mm, (plane polarized light). (GSC 1993-217G)

Volcaniclastic beds in unit D4s1

Unit D4s1 contains a 2 m thick sequence of bedded granule conglomerate and medium- to fine-grained sandstone, which occurs near the upper contact of a mafic flow unit. Beds range from generally massive granule conglomerate to laminated, fine grained sandstone.

Clasts in the massive granule conglomerate beds comprise scoriaceous porphyritic basalt that is unabraded with irregularly shaped, bubble-controlled walls (90%); porphyritic, sparsely amygdaloidal basalt (1%); and siltstone and mudstone (1%). The matrix and cement make up to 8% of beds. The matrix consists of sand- and silt-sized grains of the same composition as the framework clasts, quartz, and minor feldspar. The cement is hematite, calcite, or both.

The rock is clast supported with varied, and in some cases, very close packing. Beds are 3-30 cm thick. Bedding and lamination are defined by changes in the size of framework clasts from very coarse to coarse sand-sized, and in the percentage of carbonate cement. Primary sedimentary structures are plane lamination and plane bedding.

The laminated, fine grained sandstone beds contain more abundant nonvolcanic grains than the granule conglomerate beds. The grains include metamorphic and volcanic quartz (30%), porphyritic mafic scoria (20%), siltstone, metamorphic and other volcanic rock fragments (20%), plagioclase and K-feldspar (5%), muscovite (2%), and ferromagnesian minerals (1%). The matrix, hematite-stained clay or ash, and the cement make up 22%.

These beds are typically laminated and the laminae are often internally graded with basaltic volcanic fragments at the base.

Interpretation of volcaniclastic beds in unit D4s1

Based on the unabraded nature of the clasts, their close packing and the lack of significant amounts of nonvolcanic detritus, the massive granule conglomerate beds within unit D4s1 are inferred to be primary tuff beds modified during burial. The scoriaceous nature of the clasts and the bubble wall-controlled edges indicate that fragmentation was due to expanding volatiles. The tuff was probably erupted by Strombolian activity forming a scoria or tuff cone. The nonvolcanic grains in the matrix may have been deposited later, with submergence of the tuff beds, and may have filtered into pore spaces prior to cementation.

The fine grained laminated sandstone beds contain a significantly higher percentage of nonvolcanic clasts and have better developed bedding and lamination than the granule conglomerate beds. This suggests reworking of the mafic detritus with the addition of extraneous clastic material. The unabraded form of the mafic clasts indicates that reworking was minimal and burial rapid.

Unit D4vc1

Unit D4vc1 is a green-grey, immature, poorly sorted volcaniclastic sandstone. This unit differs from those described above in the type and abundance of mafic lapilli. The sandstone comprises wispy, irregular, black, chloritized mafic lapilli (10-20%) up to 17 mm in length, clasts of red sandstone and siltstone (0-20%) up to 3 cm, primary mica flakes, and other grains as in the nonvolcaniclastic rocks described previously (Fig. 22).

The mafic lapilli are plagioclase-phyric. They are flattened in some outcrops and define a steep foliation, but are randomly oriented in others. Lapilli range from massive, with sparse round vesicles to scoriaceous with flattened vesicles. Most of the lapilli have an even grained groundmass of chlorite, or plagioclase microcrysts in chlorite, suggesting that they were originally glassy. The edges are controlled by bubble walls indicating fragmentation by expansion of volatiles.

The preservation of unabraded lapilli indicates that they have not been transported far or reworked to any extent.

Mafic lava flows

Units D1mf1, D2mf1, D3mf1, D4mf1, and D4mf2

Basaltic lava flows D1mf1, D2mf1, and D3mf1 (from the three lower cycles) are similar in mineralogy, texture, and structure. The two flows at the top of the sequence, D4mf1 and D4mf2 (upper flows), contrast with these three lower flows and reflect a slightly different style of volcanism. The units range in maximum thickness from approximately 12 m to 460 m. The lower flow units thicken to the north and change from being relatively massive in the north to comprising pahoehoe toes in the south (unit D3mf1) (Fig. 23). These characteristics indicate a northerly source area, perhaps from a localized rift system. The basaltic flows are extensive pahoehoe sheet flows ranging in thickness from 1-12 m. Flow contacts are commonly iron-stained and have undulatory chill margins 2-3 cm thick (Fig. 24). The lower flows typically occur as a series of thin flows with interbedded peperitic breccia and less common sedimentary rock (Fig. 25).

In contrast, the upper flows, units D4mf1 and D4mf2, occur as several thick flows (typically about 12 m but as thin as 1 m) separated by sedimentary beds of units D4s1 (Fig. 26) and D4s2. Several flows have basal peperitic breccia where they are in contact with unit D4s1. Pahoehoe toes and flow lobes were not observed in D4mf1 and are rare in unit D4mf2.

All units typically contain rare plagioclase phenocrysts in a groundmass of plagioclase and clinopyroxene microlites and glass. The groundmass is now altered to chlorite, epidote,

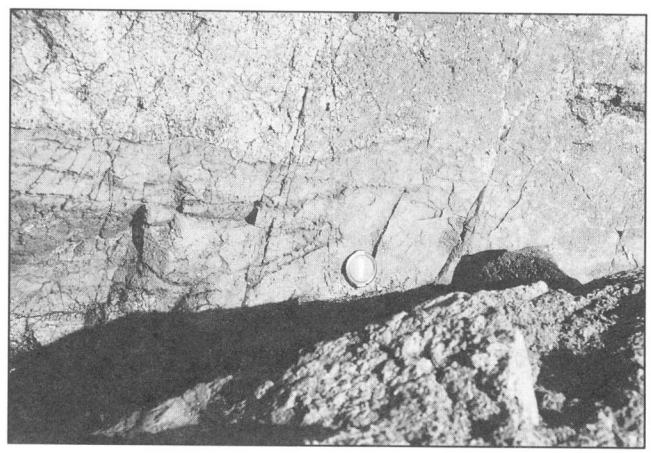

Figure 23. Pahoehoe toes with red iron-stained oxidized margins. Toes close to the south. Unit D3mf1. (GSC 1993-212E)

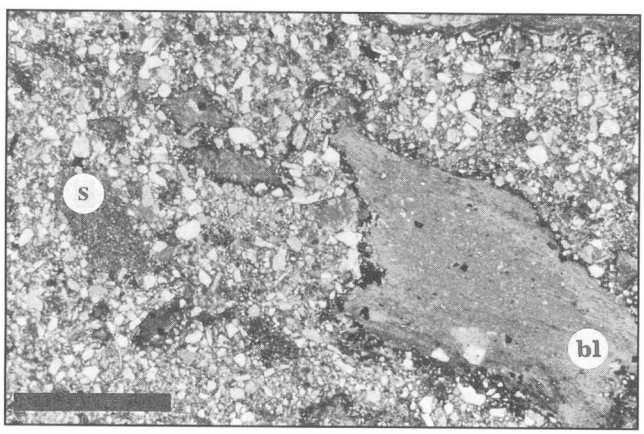

Figure 22. Photomicrograph of basaltic lapilli-bearing sandstone from unit D4vc1 showing chloritized basaltic lapilli (bl) and siltstone clasts (s) in a matrix of sand-sized particles. The basaltic lapilli have unabraded, often wispy edges. Bar scale represents 1.5 mm (plane polarized light). (GSC 1993-217H)

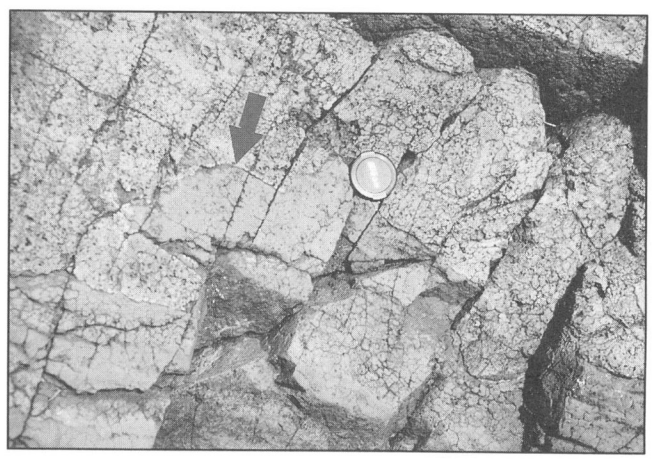

Figure 24. Basaltic pahoehoe flow showing a flow contact (arrow) in unit D3mf1. The flow contact is undulatory and iron stained. (GSC 1993-212F)

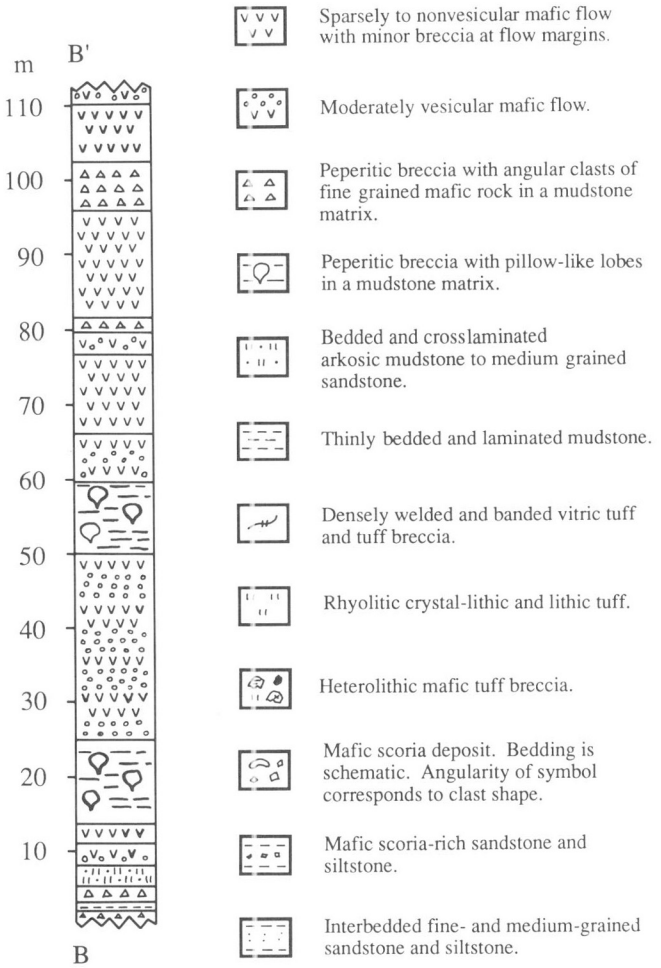

Figure 25. *Graphical log of a section of unit D2mf1. The section illustrates the relationship among mafic flows, sediment and peperitic breccia. The location of section B-B' is shown on Figure 3. The figure legend contains some symbols that correspond to Figure 34, but do not appear in this figure.*

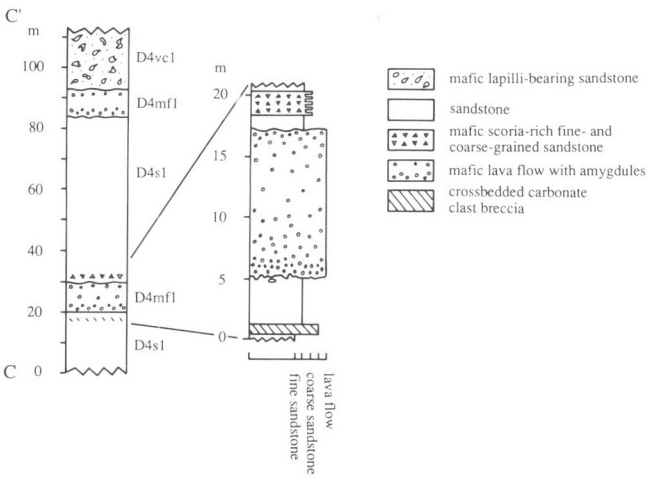

Figure 26. *Graphical log of unit D4mf1 and of over- and underlying sedimentary rocks of unit D4s1. The location of section C-C' is shown on Figure 3.*

actinolite and rare quartz. Plagioclase is commonly altered to saussurite. Several flows in units D4mf2 contain olivine phenocrysts (6-12%) and rare clinopyroxene phenocrysts. The olivine phenocrysts are altered to serpentine minerals and iddingsite. Unit D4mf1 contains rare chlorite and iron oxide pseudomorphs after olivine. A pilotaxitic groundmass texture (Fig. 27) is typical of flows of cycles 1-3, whereas an intergranular and subophitic texture (Fig. 28) is typical of cycle 4. Flows are highly to sparsely amygdaloidal with the abundance of amygdules increasing upward in most flows and up to 85% in unit D3mf1. The D4mf1 flows also have a concentration of amygdules at their base where they directly overlie sedimentary rocks (Fig. 29).

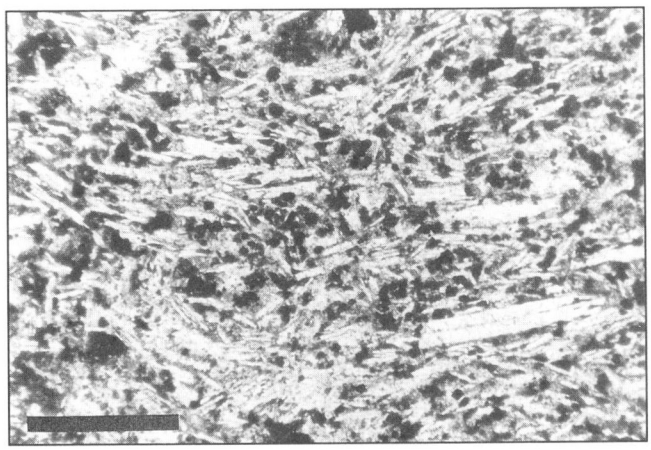

Figure 27. *Photomicrograph of porphyritic basaltic lava from unit D3mf1 showing plagioclase phenocrysts in a pilotaxitic groundmass. This texture is typical of units D1mf1, D2mf1, and D3mf1. Bar scale represents 0.3 mm (plane polarized light). (GSC 1993-217I)*

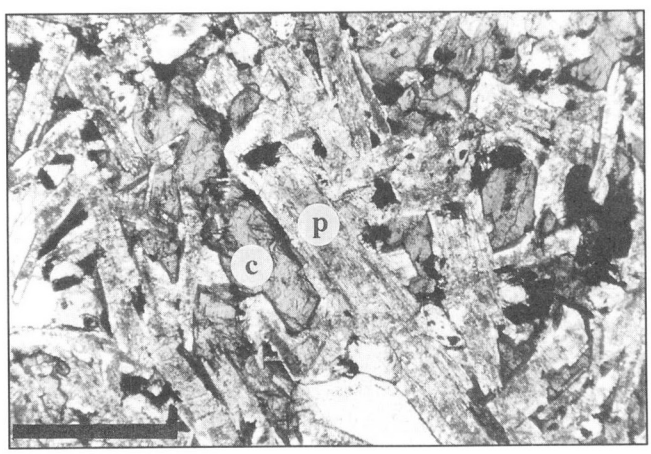

Figure 28. *Photomicrograph of basaltic lava from unit D4mf1 showing subophitic texture. This texture is typical of units D4mf1 and D4mf2. The plagioclase (p) is altered to saussurite. Clinopyroxene (c) is mid-grey and has medium to high relief. The colourless mineral is chlorite. Bar scale represents 1 mm (plane polarized light). (GSC 1993-217J)*

Peperitic breccia is interbedded with many of the mafic flows (Fig. 25; Van Wagoner et al., 1988). This breccia is a fluidized mixture of quench-fragmented volcanic debris and sediment (Honnorez and Kirst, 1975; Pichler, 1965). The fragmentation occurs either when magma penetrates (Kokelaar, 1982; Pichler, 1965) or when lava flows over (Schmincke, 1967; Waters, 1960) wet sediment. Because of the limited lateral control in this case, it is usually impossible to tell which happened. In cycles 1-3 (D1mfl, D2mfl, D3mfl), these breccia beds are 2-14 m thick and contain 30-90% mafic volcanic clasts in a very fine grained "cherty" mudstone matrix (Fig. 30). Basaltic clasts in the peperitic breccia are the same as in the flows described above, except that some vesicles contain mudstone (Fig. 31). Clasts are 2 mm-0.5 m in size, and pillow-like (Fig. 32) to angular (Fig. 30). Pillow-like fragments have fragile-looking appendages of selvage that protrude into surrounding sediment, indicating that secondary transport was minimal. Most pillow-like clasts have partial chill margins (indicating breakage after chilling), but rare clasts have complete chill margins (Fig. 32). In some cases, the margins of clasts or entire clasts are broken and juxtaposed in a jigsaw puzzle fashion (Cas and Wright, 1987) indicating little movement of clasts and quench shattering. The lack of vesicle-controlled boundaries also indicates breakage of clasts by thermal quenching rather than by expansion of volatiles.

Figure 29. *Contact of basaltic flow unit D4mfl and underlying sedimentary rocks of unit D4sl. The contact is irregular with lobes of amygdaloidal basalt extending into the underlying sedimentary rock and irregularly-shaped pods of sedimentary rock within the basalt. The base of the basalt is highly amygdaloidal. (GSC 1993-212AA)*

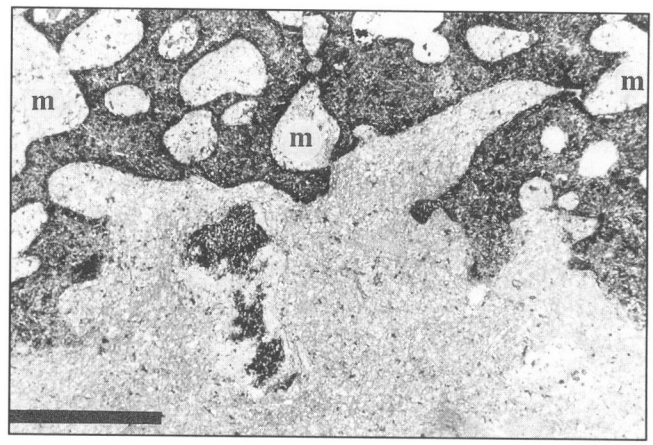

Figure 31. *Photomicrograph of peperitic breccia from unit D2mfl showing mudstone-filled (m) vesicles in basalt. Bar scale represents 1.5 mm (plane polarized light). (GSC 1993-217K)*

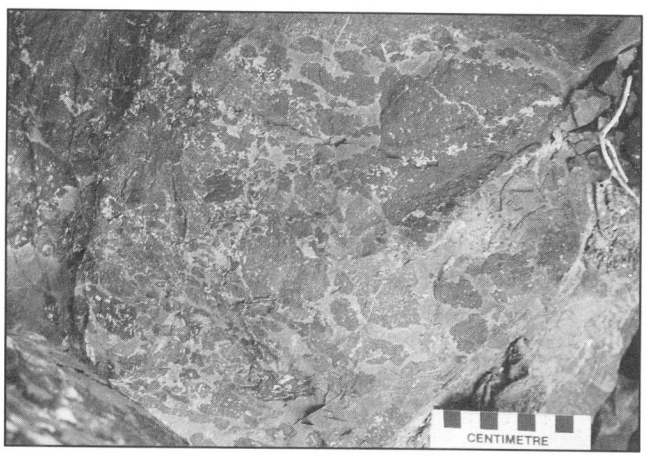

Figure 30. *Peperitic breccia from unit D1mfl showing angular to irregular clasts of amygdaloidal basalt in a cherty mudstone matrix. Some clasts are in a jigsaw puzzle arrangement indicating that little movement of clasts has occurred (Cas and Wright, 1987). (GSC 1993-212Z)*

Figure 32. *Peperitic breccia from unit D2mfl showing a pillow-like clast of basalt (arrow) in a mudstone matrix. The basalt clast has a chilled rim. Scale is 9 cm long. (GSC 1993-212Y)*

Peperitic breccia in cycle 4 (D4mf1) consists of lobes and irregular protrusions of the mafic lava into the underlying sedimentary rock, and isolated, irregular pods of sedimentary rock within the basal section of the mafic flow (Fig. 29).

The matrix of the peperitic breccia is highly fluidized mudstone to sandstone containing 15-50% silt- to fine sand-sized fragments in a clay matrix. Fragments include quartz, feldspar, and mica, and rare altered mafic minerals, chert, and basalt. Wavy extinction suggests that the quartz is vein or common quartz. Plagioclase forms tabular laths up to 0.1 mm in size that probably originated from the associated mafic flows. The sedimentary rock contains rare irregularly-shaped vesicles (Fig. 31) that formed from vaporization of interstitial fluid upon contact with magma or lava. Fluidization of the sediment is indicated by soft sediment deformational structures (Fig. 33), and by penetration of the mudstone into vesicles of the lava. Euhedral pyrite crystals are disseminated throughout the unit but concentrated in brecciated, peperitic, and vesiculated zones.

Mudstone and siltstone layers interbedded with the peperitic breccia and mafic flows are 1-5 m thick. These sedimentary layers mostly have a composition similar to the matrix of the peperitic breccia. Laminae are 1 mm-1 cm thick and massive, normally graded, internally finely laminated, or rarely crosslaminated. Soft sediment deformation structures are common and caused by a combination of density inversion and interaction of sediment with lava or magma.

A 1 m thick bed of plagioclase-arkosic mudstone to medium grained sandstone occurs near the base of unit D2mf1. Grain size ranges from 0.05-0.3 mm. The layer contains 74% rock and mineral fragments in a clay matrix. Rock and mineral fragments are 92% fresh plagioclase (0.1-0.5 mm), 3% subangular volcanic quartz (0.1-0.5 mm), 3% euhedral authigenic or secondary pyrite altered to hematite (1-3 mm), rare epidote and authigenic zircon, and 2% rock fragments of rounded to subrounded basalt, chert, and mudstone. The clay matrix is mostly altered to chlorite and sericite. Beds are 1-3 cm thick, discontinuous, and massive or graded. Coarser mineral fragments form pebble lags at the base of coarser grained beds. Lithic fragments are concentrated at the base of coarser grained and thicker beds. Authigenic pyrite occurs at boundaries between coarser- and finer-grained beds. Load structures are common along bedding planes. Basaltic volcanic material is probably the source of this sediment with other terrigenous sources contributing the quartz, chert, and mudstone (Van Wagoner et al., 1988). Rapid deposition and burial was required to preserve the feldspar grains.

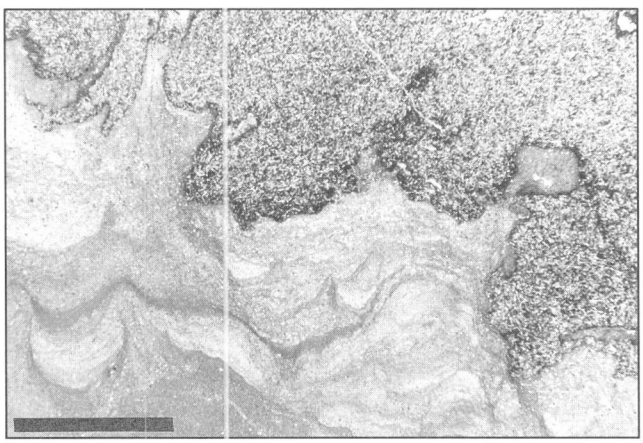

Figure 33. Photomicrograph of peperitic breccia from unit D2mf1 showing soft sediment deformation structures in the underlying sediment. Bar scale represents 3 mm (plane polarized light). (GSC 1993-217L)

Interpretation of units D1mf1, D2mf1, D3mf1, D4mf1, and D4mf2

Basaltic flows within these units are interpreted to be pahoehoe flows based on the undulatory tops, pahoehoe toes, smooth and spheroidal vesicle shapes, and the lack of any obviously fragmented upper surfaces (Cas and Wright, 1987). The flows are more similar to plains-type basaltic lava flows than flood basalts, being relatively thin (1-12 m thick) and lacking well developed columnar joints (Cas and Wright, 1987; Greeley, 1982).

The sequence of interlayered peperitic breccia and mafic flows was formed by the interaction of lava or magma with cold, wet sediment (Van Wagoner et al., 1988). Quench fragmentation occurred at the margin of the flows or shallow sills producing the peperitic breccia. Intrusion of magma or mixing of the lava with sediment resulted in the soft sediment deformation. The flow of mafic lava above unconsolidated, uncompacted, wet sediment could create a density instability that would allow the mafic flow to sink into the underlying sediment.

The flows were deposited in a tidal flat environment. Pahoehoe flows are recognized in both subaerial and subaqueous environments (Ballard et al., 1979), however, submarine pahoehoe flows should be found in association with pillow flows and hyaloclastite deposits (Cas and Wright, 1987; Furnes and Fridleifsson, 1978; Carlisle, 1963). This association is not observed in the study area. Submarine pahoehoe flow units generally have a large percentage of cylindrical tongues while these only make up a small percentage of the flow lobes in subaerial deposits (Moore et al., 1973). Pahoehoe toes and lobes recognized in the map area are ellipsoidal to irregular in shape. A littoral or transition zone environment is indicated by the association of the basalt with peperitic breccia containing tidal flat sedimentary rocks.

The flows in cycles 1-3 originated from a rift in the northern part of the map area. The source direction of flows in cycle 4 could not be determined due to limited outcrop.

Mafic pyroclastic rocks

Unit D3ms1

Unit D3ms1 is a mafic scoria. The unit is thickest in the vicinity of section E-E' and thins to the north and south (Fig. 34). Maximum thickness is about 82 m. Basaltic fragments are ash- to bomb-sized (up to 1 m in long dimension)

and commonly scoriaceous (Fig. 35). The unit contains rare accidental siltstone fragments. There is no matrix. Clasts are cemented by agglutination of fluid clasts and secondary calcite.

Interpretation of unit D3ms1

This unit is interpreted to be a mafic scoria cone, characteristic of Strombolian volcanism (Van Wagoner et al., 1988). The large size of some of the bombs suggests proximity to the vent. The occurrence of accidental siltstone fragments suggests that the volcano erupted through tidal flat deposits. Scoria cones are poorly indurated and highly susceptible to weathering and erosion (e.g., Wood, 1980), so the thickness of the unit may reflect an erosional remnant rather than the original form. Because erosion of a scoria cone tends to follow the original profile of the cone, the source of the cone was probably toward the center of the unit. The unit is not symmetrical around its thickest part, suggesting a wind direction toward the present south during eruption (Van Wagoner et al., 1988).

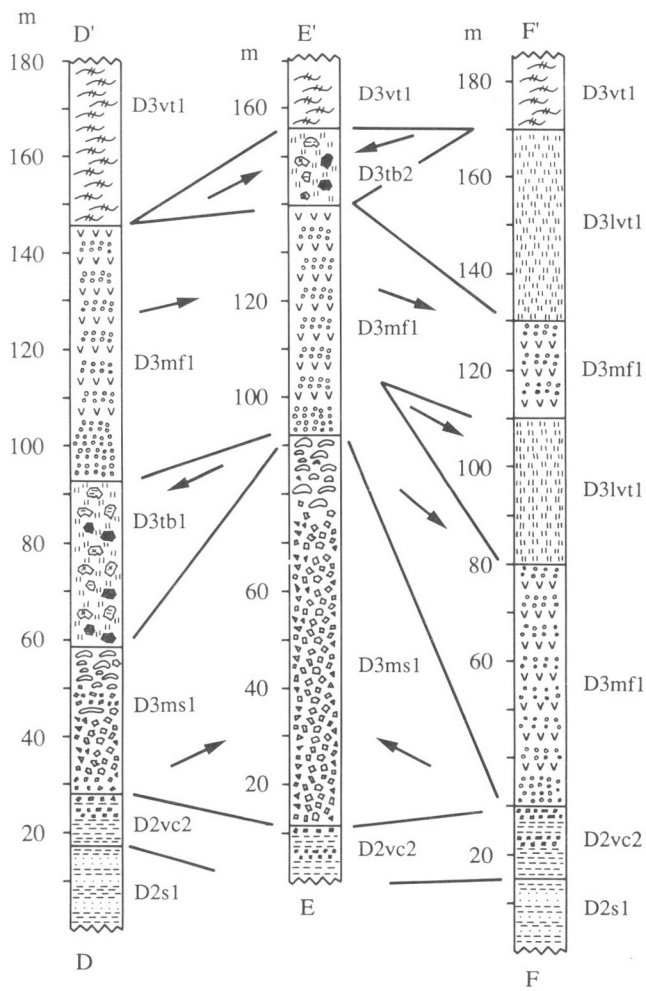

Figure 34. Correlation of measured sections through units D2sl, D2vc2, D3ms1, D3tb1, D3mf1, D3lvt1, D3lvt2, D3tb2, and D3vt1 at Holt's Point. Location of sections D-D', E-E', and F-F' is shown on Figure 3. For explanation of symbols, see legend in Figure 25.

Units D3tb1 and D3tb2

Units D3tb1 and D3tb2 are massive to vaguely-bedded heterolithic basaltic tuff breccia, with a maximum thickness of about 35 and 15 m, respectively. Both units thin away from the source over a short distance (Fig. 34).

Beds are 30 cm to 6 m thick. Clasts comprise up to 60% of these units and are up to 1 m in size, averaging 1-2 cm. They include siltstone, amygdaloidal and nonamygdaloidal basalt (Fig. 36), gabbro, and rare cored bombs of lithic clasts

Figure 35. Basaltic bomb (arrow) in basaltic scoria deposit of unit D3ms1. The bomb is approximately 2 m long. The lower margin of the bomb is irregular and protrudes downward into the underlying scoria. The upper surface is relatively planar and the contact with overlying scoria is diffuse. (GSC 1993-212G)

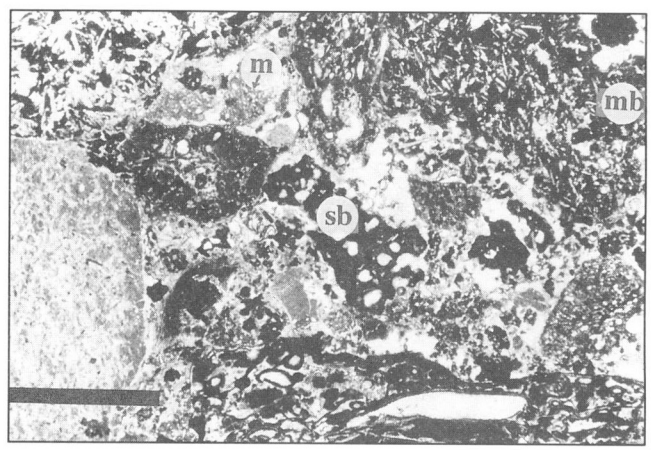

Figure 36. Photomicrograph of a mafic tuff breccia unit from unit D3tb1 showing scoriaceous (sb) and massive (mb) basalt and mudstone fragments (m), in unwelded matrix of altered mafic vitric tuff. Bar scale represents 1.5 mm (plane polarized light). (GSC 1993-217M)

rimmed by basalt (Fig. 37). Clasts are mostly angular to subangular, but some of the basaltic clasts are bomb-shaped. The matrix is nonwelded basaltic vitric tuff comprising angular and bubble-wall glass shards, altered to chlorite (Fig. 36).

Interpretation of units D3tb1 and D3tb2

The clasts of siltstone, gabbro, and angular accidental volcanic fragments represent fragmented country rock (Van Wagoner et al., 1988). Shards in the matrix and some of the basaltic clasts comprise the magmatic material. The combination of blocky nonvesicular shards and irregularly-shaped vesicular shards suggests formation by a combination of vesiculating magma and steam quenching. Lack of welding indicates that temperatures were relatively low in the eruption system. On the basis of shard type, clast type and shape, vesicularity of clasts and shards, and lack of welding, the tuff breccias are interpreted to be phreatomagmatic explosion breccias (Van Wagoner et al., 1988). The large clast size indicates a high energy eruption. Lack of primary depositional internal structures suggests origin as an air-fall deposit, probably around a tuff cone. Because this unit would be poorly indurated when deposited, the shape and size of the deposit may reflect an erosional remnant.

Unit D4lvt1

Unit D4lvt1 is a 35 m thick, dark green to green-black mafic heterolithic-vitric lapilli tuff. Exposure is limited to the side of a resistant diabase hill. Clast size in the lapilli tuff decreases upward from <50 mm to <10 mm. Sorting is poor to moderate. Crystals, small flattened or stretched vesicles, and accidental lithic clasts are crudely aligned parallel to bedding.

The lapilli tuff comprises vitric material (50-70%), lithic clasts (20-30%), and crystals (10-20%) (Fig. 38). The vitric component comprises chloritized, mafic, blocky and bubble-wall glass shards, scoria, and rare microlitic scoria. Some of the bubble-wall edges have been broken off but are found nearby, suggesting breakage of these fragile particles upon impact. Juvenile lithic clasts are basalt and vesicular basalt (25-85%). The accidental clasts are sandstone and siltstone (10-25%), and rhyolite and porphyritic rhyolite (<15%). Cored lapilli consist of vesicular basalt with a rind of altered mafic glass and ash. The crystals are plagioclase (10-20%) and minor clinopyroxene.

Interpretation of unit D4lvt1

Based on the combination of blocky and bubble-wall shards, poor to moderate sorting, and the basaltic composition, this unit was is interpreted to have been formed by a Vulcanian phreatomagmatic eruption. Impact fragmentation of mafic bubble-wall shards and crude alignment of lithic clasts and pyrogenic crystals suggests emplacement as a pyroclastic air-fall deposit.

Unit D4tb1

Unit D4tb1 comprises approximately 4 m of maroon-red, mafic, heterolithic lapilli tuff to tuff breccia and overlies 3 m of medium to light grey, felsic vitric tuff (Fig. 39). The contact between layers was not observed. Foliation in the vitric tuff is defined by alignment of light-coloured fiamme. The tuff breccia is poorly sorted. The tuff breccia and felsic tuff are discussed together, because separately they are too thin to represent mappable units.

The vitric tuff comprises recrystallized felsic shards, which have bubble-wall and blocky shapes (55-85%), fiamme (5-15%), lithic clasts (5-10%), and crystals (5-15%). Some of the fiamme contain phenocrysts of feldspar and pyroxene altered to chlorite. Shards and fiamme are deformed around lithic and crystal fragments (Fig. 40). The lithic clasts are up to 2.6 mm in size and include rounded to subangular sandstone (96-100%), rare angular to subrounded basalt, and rare rounded crystal vitric tuff. The matrix (30% of the rock) is very fine-grained ash, recrystallized to feldspar and quartz.

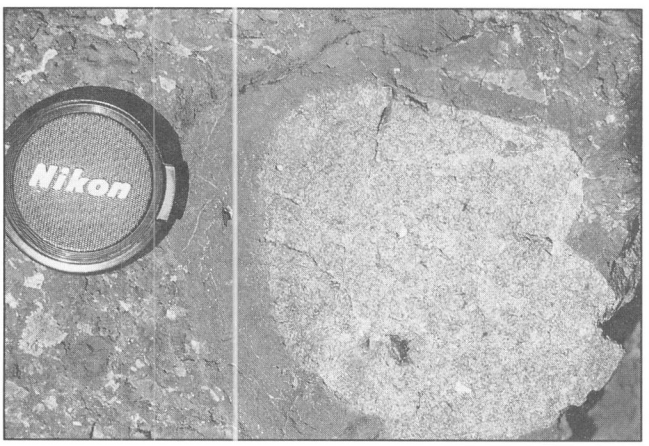

Figure 37. Gabbroic bomb with a rim of oxidized basalt in mafic tuff breccia unit D3tb1. (GSC 1993-212X)

Figure 38. Mafic heterolithic-vitric lapilli tuff from unit D4lvt1 with an angular flow-banded rhyolite clast in a matrix of foliated mafic ash. Scale is in centimetres. (GSC 1993-212W)

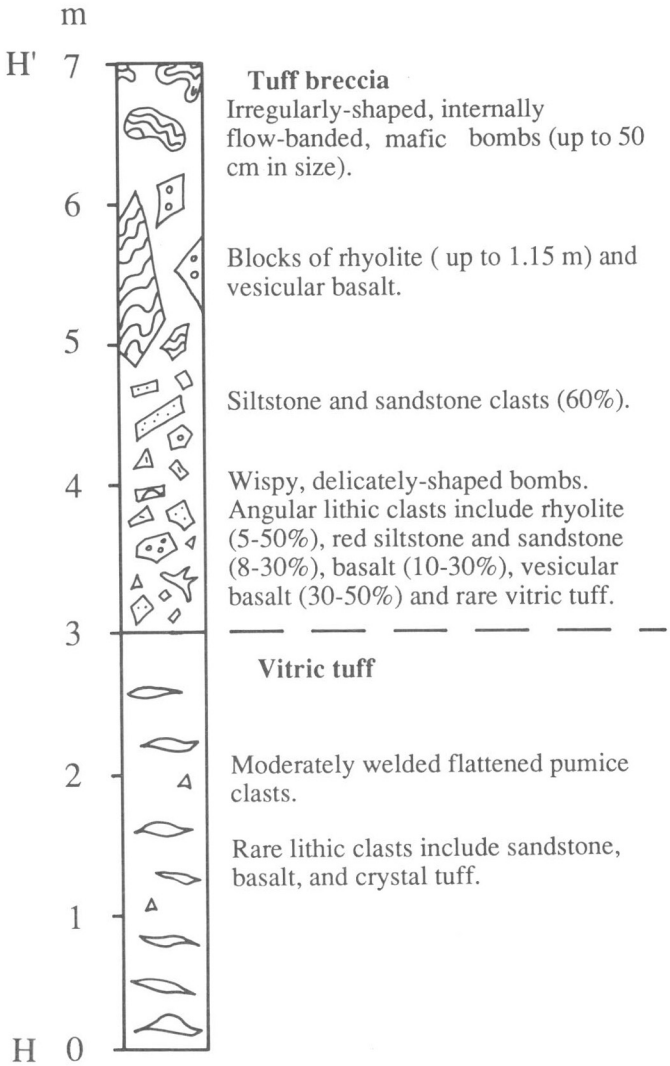

Figure 39. *Graphical log of a 7 m section through unit D4tb1 showing heterolithic tuff breccia and underlying vitric tuff. The location of section H-H' is shown on Figure 3.*

The mafic, heterolithic lapilli tuff to tuff breccia comprises ash-sized (40-80%), lapilli-sized (0-30%), and block-sized (0-20%) fragments. The vitric component of the tuff breccia (20-60%) is mafic scoria and mafic bubble-wall shards, minor flattened and recrystallized rhyolitic bubble-wall shards, and blocky and angular to rounded pumice (20-60%). The lithic clasts (30-60%) (Fig. 41, 42) include vesicular basalt (30-50%, <10 cm), nonvesicular basalt (10-30%, <7 cm), rhyolitic blocks, mafic flow-banded bombs (5-50%, <1.15 m), vitric tuff (<2%, <5 cm), and red sandstone and siltstone (8-30%, <30 cm). The mafic bombs may be essential clasts. The matrix (40-80%) is ash-sized and comprises mafic and felsic shards and crystals. Crystals (10-20% of matrix) include feldspar, metamorphic and common quartz, Fe-oxide minerals, and zircon. Many of the crystals are accidental.

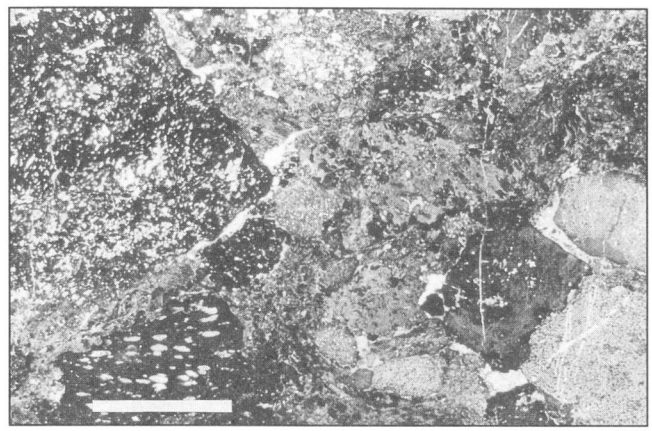

Figure 41. *Photomicrograph of heterolithic lapilli tuff to tuff breccia from unit D4tb1 showing closely-packed lithic clasts in an altered felsic ash matrix. Lithic clasts include vesicular basalt, nonvesicular basalt, rhyolite, vitric tuff, and siltstone. Bar scale represents 5 mm (plane polarized light). (GSC 1993-217O)*

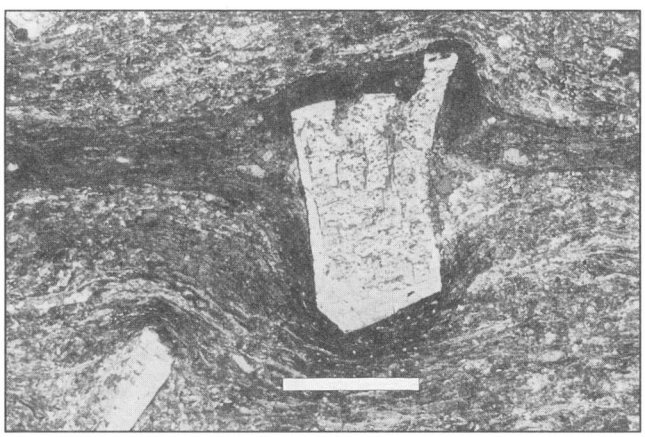

Figure 40. *Photomicrograph of vitric tuff from unit D4tb1 showing a feldspar crystal in fiamme. Shards are deformed around crystals. The matrix is devitrified and recrystallized very fine felsic ash. The rock has a eutaxitic texture and is strongly welded. Bar scale represents 3.5 mm (plane polarized light). (GSC 1993-217N)*

Figure 42. *Heterolithic lapilli tuff to tuff breccia from unit D4tb1. Lithic clasts include vesicular basalt, nonvesicular basalt, rhyolite, vitric tuff, and red sandstone and siltstone. The unit is graded with a change in both the size and abundance of lithic clasts. (GSC 1993-212H)*

In the lower 3 m of the tuff breccia, there is an upward increase in size and abundance of red siltstone and sandstone lapilli (8-60%) and angular flow-banded mafic clasts (5-50% and 0.5 cm-1.2 m). In the upper 1 m of the unit, accidental sedimentary clasts decrease in abundance upward, and mafic flow-banded, irregularly-shaped bombs (5%), 40-50 cm in length are present. The heterolithic-lapilli tuff to tuff breccia is nonwelded and highly oxidized.

Interpretation of unit D4tb1

The vitric tuff is a welded pyroclastic flow unit. The tuff is poorly sorted, massive, and comprises elongate, flattened, and aligned pumice, and shards. These features are similar to those in the massive vitric tuffs described below and are typical of pyroclastic flows. The unit is highly oxidized, consistent with subaerial emplacement.

The lapilli tuff to tuff breccia is more difficult to interpret and may be a volcanic debris flow (lahar) or a proximal air-fall deposit. Lahars and coarse grained proximal air-fall deposits are typically unsorted, include extremely large blocks (up to 1.15 m in unit D4tb1), are ungraded, and have vague internal layering (Crandell, 1971; Schmincke, 1967). Volcanic lahars however, typically have a clay matrix (Fisher, 1982) which is absent from this tuff breccia. If it is an air-fall deposit, the large magmatic bombs indicate that the unit is proximal to source.

Felsic flows and domes

Units D1ff1, 2, 3, 4; D2ff1, 2, 3, 4; D3ff1; D4ff1, 2, 3, 4; and D4td1, 2

There are three main types of felsic flows and domes: (1) pink, flow-banded, and massive sparsely porphyritic to aphyric rhyolitic flows and domes (D1ff2, D1ff3, D1ff4, D2ff2, D2ff3, D2ff4, D3ff1, D4ff1, D4ff2, D4ff3); (2) pink, porphyritic rhyolitic flows and domes (D2ff1); and (3) a grey, flow-banded rhyolitic dome with a trachytic texture (D1ff1). There are two trachydacite domes (D4td1, D4td2), and an orange, porphyritic rhyolitic dome (D4ff4) which are discussed in more detail below. Peperitic breccia is associated with D2ff1, D2ff2, D3ff1, and D4ff1 (Fig. 43). Inferred flow directions are based on variations in thickness. The units range in thickness from 60 to 435 m and have a varied lateral extent.

The pink, sparsely porphyritic to aphyric rhyolitic flows and domes (D1ff2, D1ff3, D1ff4, D2ff2, D2ff3, D2ff4, D3ff1, D4ff1, D4ff2, D4ff3) are banded to massive. Flow bands are up to 1 cm thick, planar to undulating, and defined by colour variations from dark pink to buff (Fig. 44), grain size of devitrification microstructures, and size and abundance of fine grained opaque minerals in the groundmass. The rocks commonly have a microgranophyric devitrification texture, with plagioclase microlites rarely forming a felty texture. Plagioclase, and less commonly sanidine, rarely occur as glomerophyric phenocrysts. All flows contain rare zircon. Units D4ff1 and D4ff2 contain altered ferromagnesian minerals including biotite, pyroxene, and possibly olivine. Primary structures include spherulites, concentrated along flow bands, and perlitic cracks near the tops of flows. Units D3ff1, D4ff1, and D4ff3 are discussed in more detail below.

The pink, porphyritic flows and domes (D2ff1) contain up to 20%, commonly glomerophyric, phenocrysts of plagioclase and rare sanidine. The feldspar phenocrysts are commonly zoned and altered to clay minerals. Quartz phenocrysts are rare. Mafic xenoliths are less than 3%, mostly a few centimetres, but up to 20 cm in size and rounded. The groundmass is fine grained and microgranophyric to felty or pilotaxitic. Columnar joints, perpendicular to flow margins, are poorly developed throughout unit D2ff1. Flow foliation is similar to that in the aphyric flows.

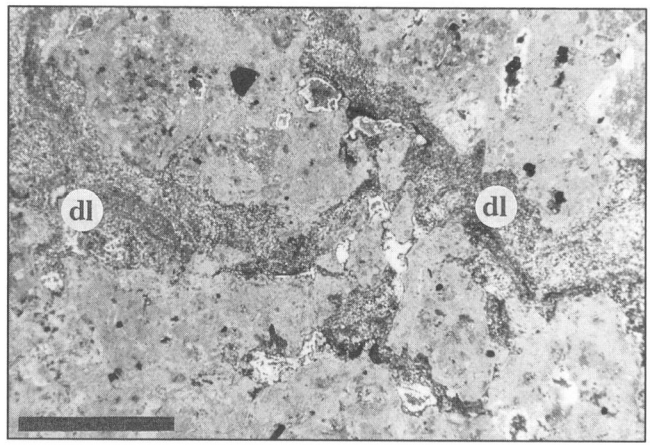

Figure 43. Photomicrograph of rhyolitic peperitic breccia from unit D2ff1. Irregular clastic dykes of siltstone to mudstone intrude a rhyolitic lava. Contacts between the dyke and rhyolite are very irregular. Vesicles form sections of the clastic dykes. Disrupted laminae (dl) are visible in the sedimentary rock. Bar scale represents 3 mm (plane polarized light). (GSC 1993-217P)

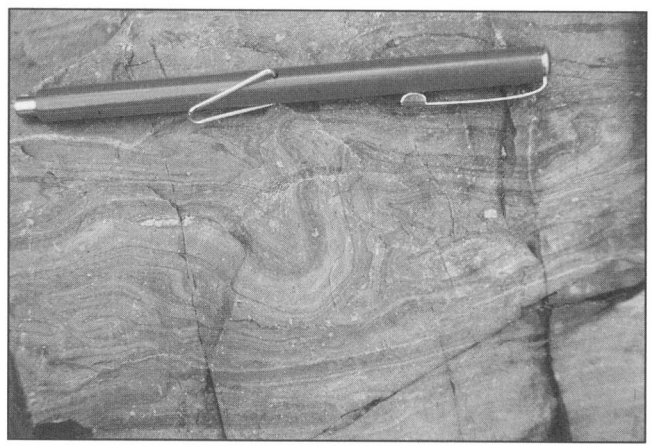

Figure 44. Contorted fluidal folds in a rhyolite lava dome of unit D4ff1. Banding in outcrop is defined by colour. (GSC 1993-212I)

The grey, flow-banded rhyolitic dome (D1ff1) is lens-shaped in outcrop, and contains up to 70% microlites of alkali feldspar in a recrystallized silicic groundmass. Bands are light grey and dark grey, 1 mm to 1 cm thick, and defined by changes in abundance of the flow-aligned microlites (Fig. 45).

Autobrecciation was observed at the margins of some of these units (Fig. 46). The autobrecciation is commonly associated with areas of tightly folded flow bands and is recognized by their progressive detachment and fragmentation (Fig. 47). Isolated fragmented flow bands (Fig. 48) occur in the more massive rhyolites. Columnar joints are well developed within unit D2ff2, on Macdougals Island (also known as Basaltic Island).

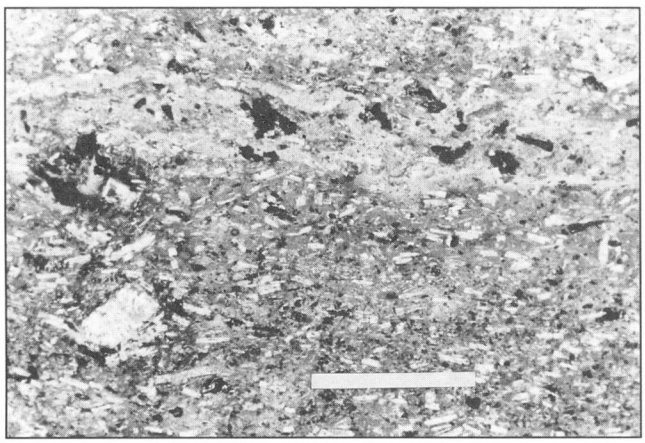

Figure 45. *Photomicrograph of flow banding in a trachytic rhyolite flow from unit D1ff1. Banding is defined by colour and by the abundance of feldspar microlites in the darker coloured bands. Bar scale represents 1.3 mm (plane polarized light). (GSC 1993-217Q)*

Figure 46. *Monolithic autobreccia at the edge of a rhyolite flow unit, D2ff4. The breccia comprises angular, massive rhyolite clasts in a similar rhyolite matrix. (GSC 1993-212V)*

Several flows also have associated peperitic breccia (Fig. 43) at the top of flow units. The rhyolitic peperite of units D2ff1 and D2ff2 is composed of fragments of porphyritic to massive rhyolite in a green-grey, massive to bedded mudstone matrix. The ratio of sediment to volcanic rock varies considerably from predominantly rhyolite with inclusions of sediment to approximately 70-80% sediment. The rhyolitic clasts are generally 1-10 cm in size and angular to subrounded.

Figure 47. *Fragmented segments of flow bands in rhyolite lava dome of unit D4ff1. The segments are similar in appearance to flattened pumice. The pencil is 16 cm long. (GSC 1993-212U)*

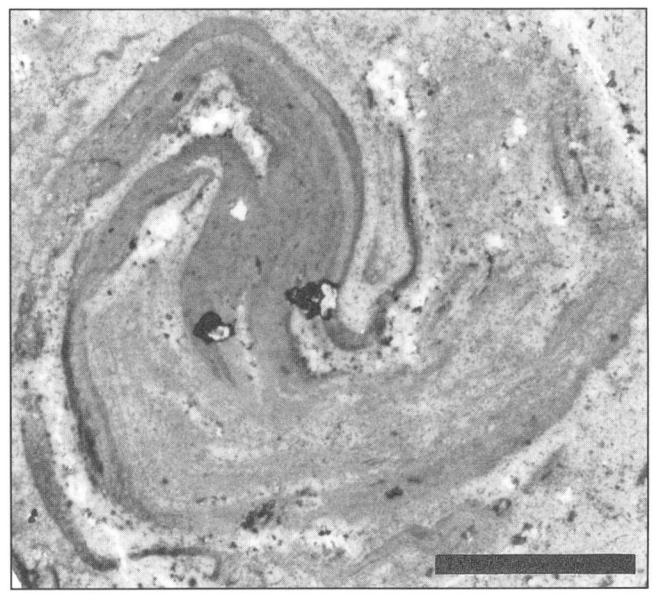

Figure 48. *Photomicrograph of an isolated segment of folded flow banding in a devitrified rhyolitic groundmass from unit D4ff1. The banding is defined by colour. The dark bands have a very high concentration of fine grained opaque minerals. Bar scale represents 2 mm (plane polarized light). (GSC 1993-217R)*

Secondary alteration phases include epidote, chlorite, quartz, and rare fluorite. Unit D2ff2 has areas of intense hydrothermal alteration that give the rock a purple-orange mottling. Pyrite, sphalerite, and fluorite are associated with the areas of hydrothermal alteration.

Interpretation of units D1ff1, 2, 3, 4; D2ff1, 2, 3, 4; D3ff1; D4ff1, 2, 3, 4; D4td1, 2

These units were emplaced as lava flows and domes. This conclusion is based on the pervasive well developed flow layering, unbroken glomerophyric phenocrysts, partially absorbed rounded mafic xenoliths and absence of abundant vitric and lithic pyroclasts (Bonnichsen and Kauffman, 1987; Cas and Wright, 1987; Fink, 1983). The in situ autobrecciation within or near the base of unit D1ff2 supports this interpretation. The intrusive domes (D4ff1, D4ff3, D4ff4, D4td1) are distinguished by their shape, and relationship with surrounding sedimentary units.

The rhyolitic lava flows and domes were emplaced in a subaerial to littoral environment, based on their spatial association with littoral sedimentary rocks and the mixture of parts of these flows with wet sediment to form peperitic breccia. Except for unit D4ff1, the flows and domes lack pillow-forms, a glassy crust, and associated rhyolitic hyaloclastite deposits, typically associated with subaqueous flows and domes (Pichler, 1965). Unit D1ff3 was probably deposited near sea level as the rhyolite flows are interbedded with thin horizons of tidal flat sedimentary rock at its base.

Unit D3ff1

Much of unit D3ff1 is extensively silicified. In the silicified zones pods of orange rhyolite are surrounded by veins, up to 10 cm wide, of grey, silicified rhyolite (Fig. 49). Fragments in this "pseudobreccia" have a jigsaw puzzle arrangement (Cas and Wright, 1987). Adjacent to this "pseudobreccia", the grey silicified rhyolite forms veins through massive orange rhyolite.

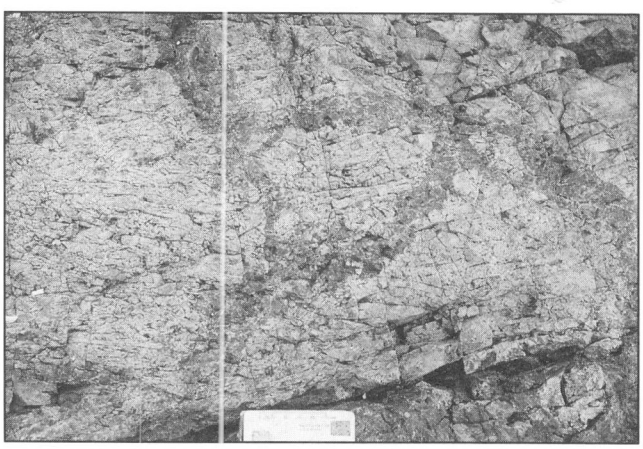

Figure 49. *Pseudobreccia in a rhyolite lava flow or dome, unit D3ff1. Pods of orange rhyolite are surrounded by altered grey rhyolite. The clasts have a jigsaw puzzle arrangement and have not rotated relative to one another. Alteration was in situ and created a breccia-like texture. Scale shown is 5 cm. (GSC 1993-212T)*

Peperitic breccia comprising angular clasts of orange rhyolite, up to 2 cm, in a matrix of siltstone to medium grained sandstone, occurs at the top of the unit. Pods of sedimentary rock occur throughout the unit.

There are two possible interpretations for the peperitic breccia at the top of unit D3ff1. The unit may have had a brecciated carapace. Subsequent to emplacement, sediment filled the spaces in the carapace. Alternately, the unit may have intruded the contact between an underlying consolidated, welded tuff (unit D3lvt3) and overlying semiconsolidated, wet sediment (unit D3s1). The top of the sill interacted with the wet sediment forming the peperitic breccia.

Unit D4ff1

Unit D4ff1 is a 435 m thick tabular dome with peperitic breccia at the upper and lower contacts (Fig. 50). The unit overlies or intrudes a sedimentary unit (D3s1). The lower contact is sharp and is not conformable with either bedding in the unit below or banding in D4ff1. Above the basal contact, clastic dykes of red, silicified sandstone cut the rhyolite in a 'net vein' arrangement up to 0.5-1 m from the contact (Fig. 51). Several larger clastic dykes up to 15 cm in width, include clasts of the rhyolite. Within the sandstone, up to about 30 cm below the contact, there are matrix-supported, angular blocks of banded rhyolite up to 20 cm in size.

There is a variation in structure upward through the central portion of the unit. Primary structures are similar to those described above for the rhyolitic flows and domes, and include flow banding and quartz-filled parting planes (Fig. 52). At approximately 315 m above the base of the unit, there is a porphyritic phase (Fig. 53) which is tightly flow folded with the phenocryst-poor rhyolite. In this phase there are approximately 20% plagioclase phenocrysts up to 5 mm in length. Also at this level in the unit, rare clastic dykes containing angular rhyolite clasts cut the rhyolite.

From 355 m to the top of the unit (435 m), the rhyolite is cut by numerous clastic dykes that range from a very fine grained "cherty" siltstone (Fig. 54) to coarse grained sandstone. Locally the outcrop is brecciated, with matrix-supported rhyolite clasts in a sedimentary matrix. Much of the rhyolite has perlitic cracks (Fig. 55), spherulites, and lithophysae. At the contact with the clastic dykes the rhyolite is vesicular with vesicles filled with quartz and chlorite, and rarely siltstone. Quartz-filled vesicles occur in the siltstone up to 5 mm away from the edge of dykes. Some clastic dykes contain angular shards of rhyolite (Fig. 56). The contact with the overlying unit (D4s1) is not exposed.

Based on the peperitic nature of both the top and bottom contacts, unit D4ff1 is interpreted to have been emplaced as an intrusive sill or dome-like body. Features that indicate that the sediment was unconsolidated and wet when the rhyolite intruded include sediment-filled vesicles in rhyolite, vesicles in siltstone, and angular, nonvesicular shards of rhyolite in the clastic dykes (Fig. 52). Perlitic cracks and spherulites in

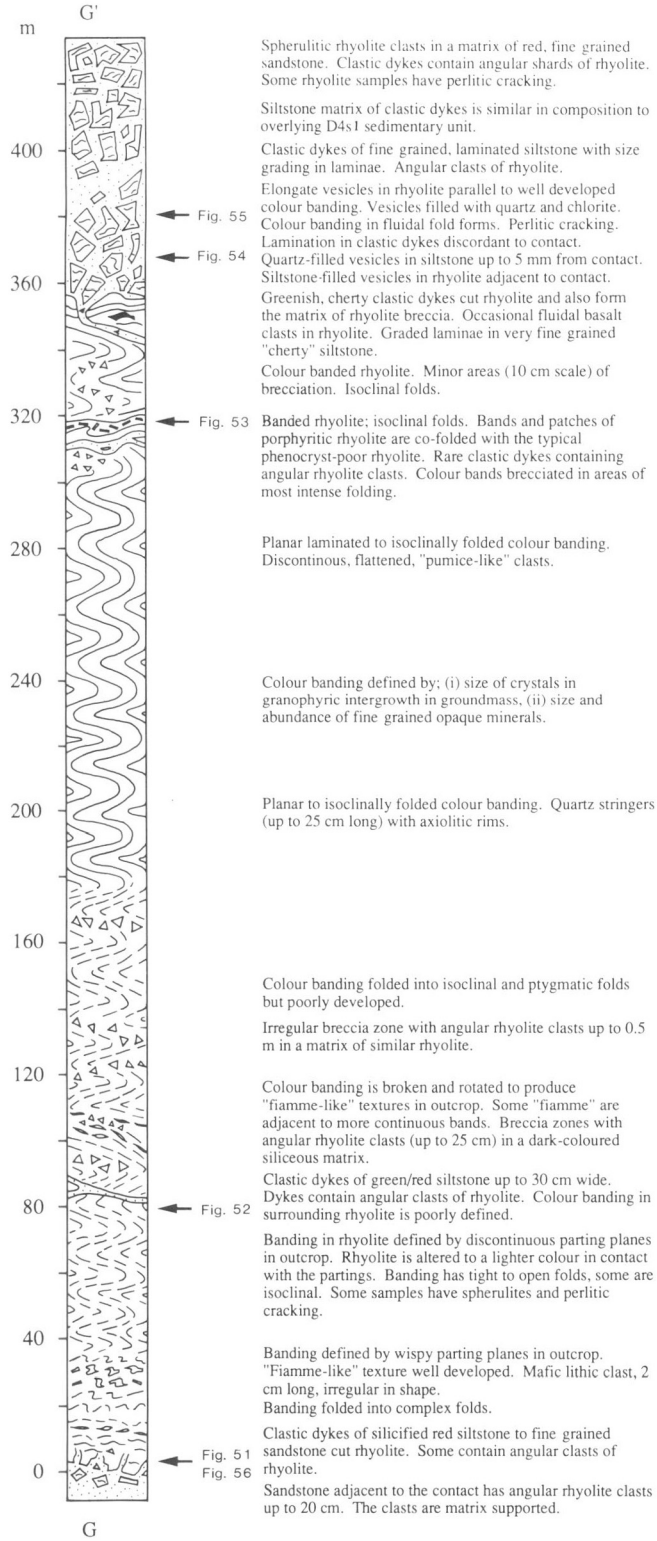

Figure 50. *Graphical log of a 435 m section through unit D4ff1. The top of the unit is at G'. The location of section G-G' is shown on Figure 3.*

the rhyolite attest to its original glassy state. The abundance of clastic dykes at the top and bottom contacts (Fig. 51), rhyolite breccia with a sedimentary matrix, and matrix-supported angular rhyolite clasts in the sandstone below the contact, all support this interpretation.

Unit D4ff3

Unit D4ff3 is pink to orange, flow-banded, vitrophyric rhyolite. The rhyolite comprises plagioclase phenocrysts (<5%, <2.2 mm) in a pilotaxitic groundmass of devitrified glass with clinopyroxene and plagioclase microlites, opaque minerals,

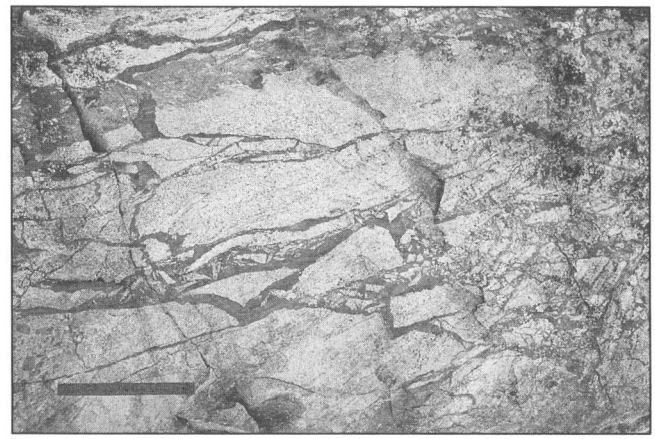

Figure 51. *Rhyolitic peperitic breccia with angular clasts of rhyolite in a grey siltstone matrix from unit D4ff1. The texture ranges from clast- to matrix-supported. Some clasts have a jigsaw puzzle arrangement. Location of this figure is shown on Figure 50. Bar scale represents 0.3 m. (GSC 1993-212J)*

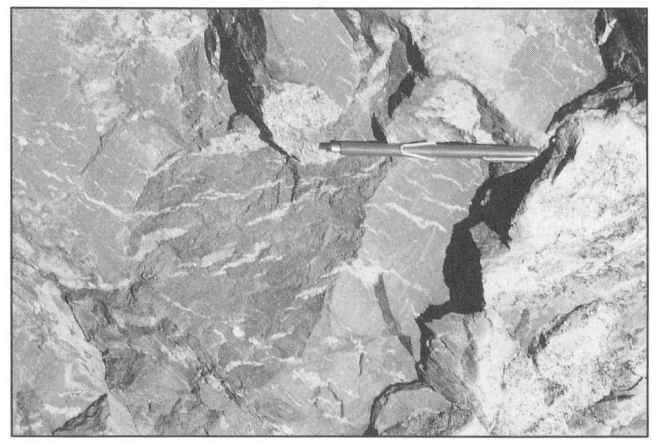

Figure 52. *Typical view of the central part of intrusive rhyolite dome, unit D4ff1. White, quartz-filled parting planes define a foliation in the rhyolite. Perpendicular to the parting planes, in this outcrop, is a foliation defined by faint colour banding. The colour banding may be an early primary structure with the parting planes formed during late movement of the rhyolite mass. Location of this outcrop is shown on Figure 50. (GSC 1993-212S)*

and rare zircon. Secondary chlorite occurs in the groundmass. Plagioclase phenocrysts are rarely broken, and generally parallel to flow bands. Spherulites up to 3 mm in diameter occur in the groundmass.

Flow banding is defined by colour and crystal content (Fig. 57), with grey bands being more crystal-rich than pink bands. Bands vary from straight to discontinuous and highly contorted. The orientation of flow banding varies from shallowly dipping inward, at the outside of the dome, to near vertical towards the centre of the dome. Banding is contorted at the contact with surrounding units.

Based on its contacts with surrounding units, unit D4ff3 is interpreted as an intrusive rhyolitic dome.

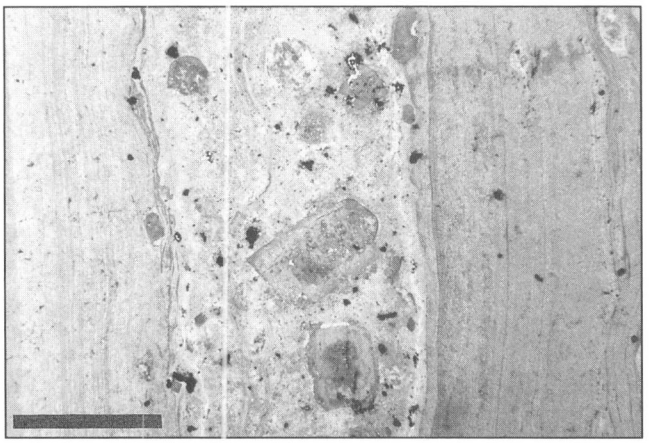

Figure 53. *Photomicrograph of flow banding in an intrusive rhyolite dome from unit D4ff1. Layers of porphyritic rhyolite with up to 20% plagioclase phenocrysts are interlayered with and flow folded with the more typical phenocryst-poor banded rhyolite. The two phases were folded during flow and intrusion of the rhyolite lava. Location of this sample is shown on Figure 50. Bar scale represents 5 mm (plane polarized light). (GSC 1993-217S)*

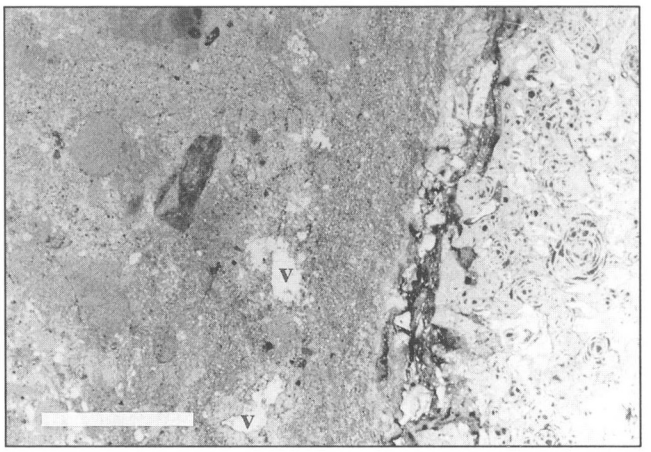

Figure 55. *Photomicrograph of felsic peperitic breccia from unit D4ff1. The rhyolite (right) has perlitic cracks and small irregular vesicles (v) at the contact with the sedimentary rock (left). The sedimentary rock has irregular vesicles (now holes) adjacent to the contact. Location of this sample is shown on Figure 50. Bar scale represents 3 mm (plane polarized light). (GSC 1993-217T)*

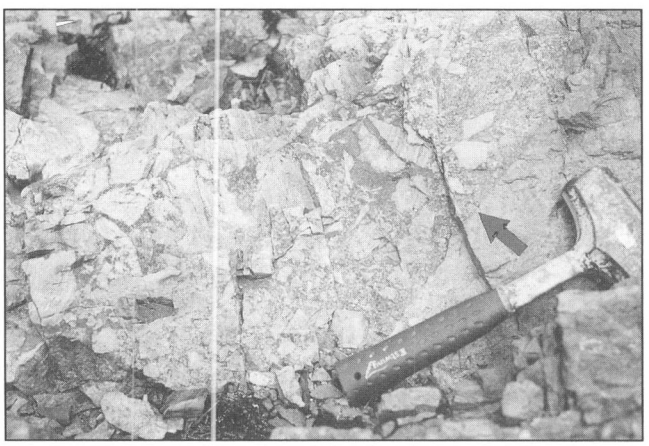

Figure 54. *Clastic dyke in an intrusive rhyolite dome, unit D4ff1. The dyke (upper left side of photo; margin indicated by arrow) is monolithic and contains angular clasts of rhyolite in a cherty siltstone matrix. Clasts have the same composition as the host rhyolite. The texture varies from clast- to matrix-supported. Location of this outcrop is shown on Figure 50. (GSC 1993-212R)*

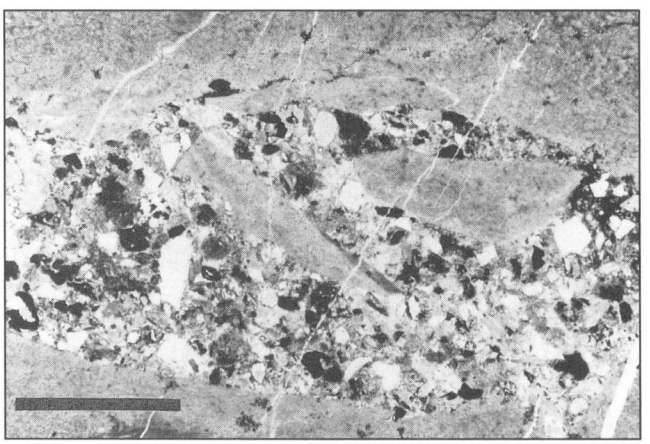

Figure 56. *Photomicrograph of felsic peperitic breccia from unit D4ff1 showing angular, matrix-supported clasts of rhyolite in a sandstone matrix. Rhyolite also occurs above and below clastic dyke. Location of this sample is shown on Figure 50. Bar scale represents 1.2 mm (plane polarized light). (GSC 1993-217U)*

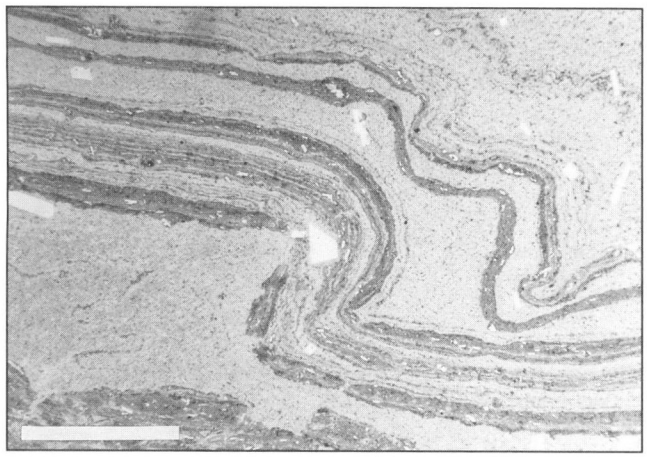

Figure 57. *Photomicrograph of a sample from an intrusive rhyolite dome, unit D4ff3, showing flow banding. The banding is defined by colour (now shades of grey) and the abundance of feldspar microlites. Banding is contorted into fluidal flow folds and is locally brecciated. Bar scale represents 5 mm (plane polarized light). (GSC 1993-217V)*

Units D4td1 and D4ff4

Unit D4td1 is an intrusive trachydacite dome that intrudes unit D4s1. The unit is approximately 1100 m by 700 m in plan view. The dome ranges in structure and composition from flow-banded to massive, sparsely porphyritic trachydacite in the south to flow-banded, more mafic trachydacite in the north. Phenocrysts include plagioclase (2-5%), altered ferromagnesian minerals, (possibly pyroxene, 1-2%), rare fresh clinopyroxene, and rare sanidine. Glomeroporphyritic aggregates of plagioclase and pyroxene are common. The groundmass is fine- and even-grained feldspar, altered ferromagnesian minerals, minor quartz, and rare apatite and zircon. Feldspar is altered to sericite. The ferromagnesian minerals are altered to chlorite and iron oxide or to calcite, chlorite, and iron oxide. There are rare lithic clasts up to 18 cm in size, of a slightly more mafic trachydacite, and rare zones with up to 20% vesicles filled with calcite and chlorite.

Flow banding is defined by colour, concentrations of fine grained opaque minerals, and quartz-filled parting planes. The banding is planar to gently folded.

Unit D4ff4 occurs as several small rhyolitic domes up to about 400 m across, that intrude unit D4s1. The domes lie along a north-trending lineament and possible fault, defined in part by the western shore of Birch Cove (Fig. 3). Unit D4td1 occurs at the southern end of this lineament and is possibly cogenetic. However, unit D4ff4 differs from unit D4td1 in phenocryst composition, and by the lack of lithic clasts and flow banding in the former. Unit D4ff4 is orange, porphyritic rhyolite. Phenocrysts include sanidine (5%) and a ferromagnesian mineral (5-10%) now altered to chlorite, actinolite, and iron oxide, which may have been an alkali amphibole such as riebeckite. The groundmass is feldspar, an altered acicular to irregularly-shaped ferromagnesian mineral (5-10%), quartz (2-10%), and rare zircon. The unit is massive in structure.

The age of these domes is not clear. They could be related to the Silurian-Devonian "Eastport" volcanism or be part of a slightly later magmatic event such as the intrusion of the Saint George Batholith.

Unit D4td2

Unit D4td2 is a dome, 4 km^2 in plan view, with a height of approximately 192 m above the surrounding area. The dome comprises grey to buff, highly porphyritic to nonporphyritic trachydacite. Phenocrysts include plagioclase (<1 mm), clinopyroxene (<3 mm), hornblende (<0.7 mm), and opaque minerals (<0.4 mm). A few clinopyroxene phenocrysts have rims of biotite. There are rare basaltic lithic fragments (<1.4 mm), and rare spherical structures with a similar composition to the groundmass of the trachydacite (<2.4 mm). Feldspar microlites define the margins of these spherical structures. The basaltic lithic fragments are probably cognate. The spherical structures are juvenile material and may represent fragmented remnants of more viscous flow layers.

The groundmass ranges from altered glass to intergrowths of feldspar, clinopyroxene, hornblende, and opaque minerals. Irregular to flattened vesicles (10%) are filled with quartz and chlorite.

Flow bands, defined by colour differences, are planar to highly contorted. Flow banding is subvertical in the central part of the dome but highly variable near the dome margins.

Unit D4td2 is inferred to be an extrusive dome based on its steep-sided domical cross-section and circular section in plan view, variation in the attitude of flow banding, and the absence of intrusive and baked contacts with the surrounding sedimentary rocks (D4s1 and the Perry Formation).

Felsic pyroclastic rocks

Massive pyroclastic rocks: units D1xvt1, 2; D1vt1, 2; D2lvt1; D2vt1; D2xvt2; D4vt1, 2

Vitric tuffs: units D1xvt1, 2; D1vt1, 2; D2vt1; D4vt1, 2

These units range in maximum thickness from 40-575 m and comprise buff, orange, and grey to purple-grey tuff (D1xvt1, D1xvt2, D4vt1, D4vt2) and ash to lapilli tuff (D1vt2, D2vt1). Most units comprise pumice, glass shards, crystals, and rare accidental lithic fragments, but are dominantly vitric material. The name, crystal-vitric tuff, is give to units with >5% crystals.

Pumice fragments, up to 60% of the vitric tuffs, are buff to orange, up to 25 cm in size, flattened, and elongate to equant. The pumice displays axiolitic devitrification texture and is aphyric to porphyritic. Crystals include plagioclase (up to 5% and 0.5-2 mm), sanidine (up to 3% and 0.5-1 mm), and rare euhedral zircon. Crystals are usually broken and more abundant in the matrix than pumice. Feldspar is altered to clay minerals or sericite. Metamorphic biotite comprises 3% of unit D4vt2. Minor accidental lithic clasts include rounded to subrounded, vesicular basalt, <2 cm in size, subangular to subrounded, and pink rhyolite, 5-10 mm in size. Unit D4vt1 comprises shards, ash (>95%), and feldspar crystals.

The matrix of the vitric tuffs is composed of granophyric, recrystallized, and devitrified ash. Relict siliceous shards (10-35%, rarely 80% of the matrix), are up to 1 mm in size, platy but rarely tricuspate, and moderately to strongly welded (Fig. 58, 59). Unit D4vt2 has recrystallized bubble-wall and pumiceous shards. The matrix of unit D2vt1 is eutaxitic (Fig. 60). Spherulites and perlitic cracks (Fig. 61) occur locally.

These units are massive and poorly sorted. Banding, where developed, is defined by parallel elongate pumice and rare lithic fragments. The units range from strongly to poorly welded, with the degree of welding defined by flattening of pumice and the sintering of shards (Fig. 58, 60). Pumice fragments and flattened shards are deflected or draped over rigid lithic clasts and crystals (D1xvt2). Unit D4vt1 is rarely brecciated. The tuff is broken into angular fragments that are <1 cm, silicified, and have perlitic cracks. The matrix of the breccia is siltstone (Fig. 61).

Unit D1xvt1 fines laterally to the southeast. The size of pumice decreases from a maximum of 10 cm in the northeast exposure to an average of 1 cm in the southeast. The degree of welding of unit D2vt1 increases laterally to the northeast.

Interpretation of units D1xvt1, 2; D1vt1, 2; D2vt1; D4vt1, 2

These pyroclastic units were emplaced primarily as pyroclastic flows. They are poorly sorted, massive, and commonly comprise elongate, flattened, and parallel aligned pumice,

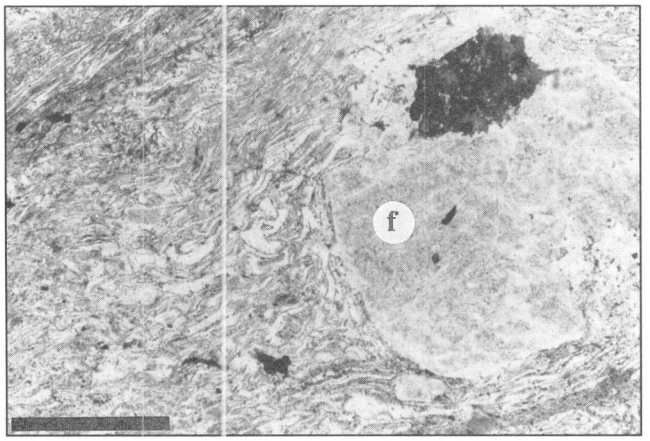

Figure 58. *Photomicrograph of massive vitric tuff from unit D1xvt1 showing deformed, platy and tricuspate, felsic shards adjacent to a feldspar crystal (f). The tuff is moderately welded. Bar scale represents 0.6 mm (plane polarized light). (GSC 1993-217W)*

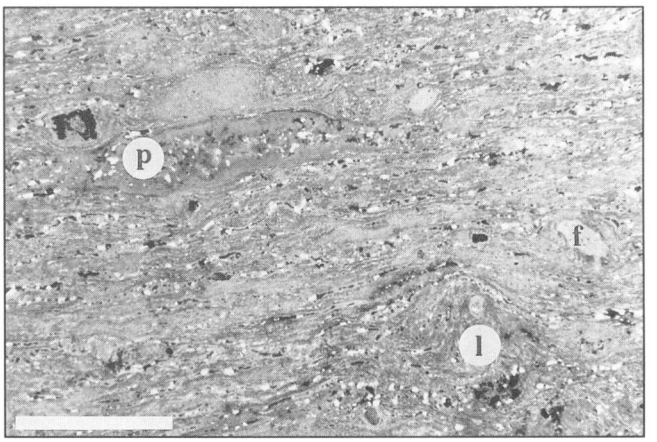

Figure 60. *Photomicrograph of massive vitric tuff from unit D2vt1 showing flattened and devitrified felsic pumice (p) and shards, feldspar crystals (f), and lithic fragments (l). The shards are deformed around the crystals and lithic clasts in a eutaxitic texture. The tuff is strongly welded. Bar scale represents 3 mm (plane polarized light). (GSC 1993-217Y)*

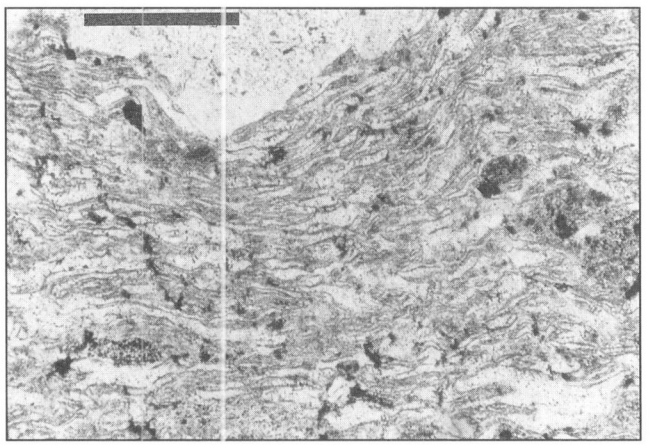

Figure 59. *Photomicrograph of massive vitric tuff from unit D1xvt1 showing flattened felsic shards and a feldspar crystal. The tuff is moderately welded. Bar scale represents 0.4 mm (plane polarized light). (GSC 1993-217X)*

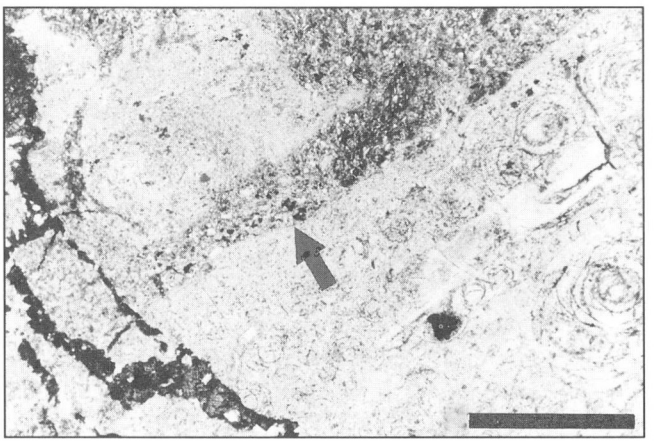

Figure 61. *Photomicrograph of massive vitric tuff from unit D4vt1 showing perlitic cracks in rhyolite, brecciation and siltstone-filled clastic dyke (arrow). Bar scale represents 1 mm (plane polarized light). (GSC 1993-217Z)*

shards, and rarely lithic fragments. These features are characteristic of pyroclastic flow deposits (Cas and Wright, 1987; Fisher and Schmincke, 1984; Self, 1982; Wright et al., 1980; Sheridan, 1979) and result from high particle concentration, laminar flow (Wright and Walker, 1981; Wilson, 1980; Wright, 1979; Sparks, 1976). The parallel alignment of pumice, shards, and lithic fragments produces a moderate to well developed flow fabric and is the result of shearing forces within a pyroclastic flow during laminar movement (Fisher and Schmincke, 1984; Wright et al., 1980). Other evidence for emplacement as pyroclastic flows includes broken crystals, crystal segregation, draping, and welding. Pyrogenic crystals are enriched in the matrix relative to pumice. The crystal content of the pumice represents the initial magmatic ratio of crystals to glass (Sheridan, 1979). Crystal segregation may occur during eruption column collapse, flow emplacement, or elutriation (Sparks and Walker, 1977). Draping textures are the result of gas escape and deflation during and immediately following flow emplacement (Sheridan, 1979). The presence of zones of welding within pyroclastic deposits, as evidenced by flattened shards and pumice, is also characteristic of pyroclastic flows. Welding may occur in air-fall and surge deposits, but is more commonly associated with pyroclastic flows (Fisher and Schmincke, 1984).

Units D1xvt1, D1xvt2, D1vt1, D1vt2, D2vt1, D4vt1, and D4vt2 are interpreted to have resulted from magmatic eruptions. That is, the energy of eruption was provided primarily by rapid and explosive exsolution and expansion of magmatic volatiles. Magmatic eruptions typically produce deposits composed dominantly of essential pyroclasts with only minor accidental or cognate lithic clasts (Fisher and Schmincke, 1984). The abundance of bubble-wall shards indicates exsolution of magmatic volatiles during eruption. The presence of these vesicular shards and pumice with the absence of significant quantities of accidental lithic clasts, nonvesicular glass, equant or blocky shards, and the relatively coarse grained nature of these deposits precludes a phreatomagmatic eruption (Fisher and Schmincke, 1984; Sheridan and Wohletz, 1983). The energy of eruption, or explosivity, which produced these deposits is considered to be sub-Plinian. Plinian eruptions are unlikely because of the absence of associated voluminous air-fall deposits and the presence of zones of welding (Self, 1982).

Lithic-vitric and crystal-vitric tuffs: units D2lvt1 and D2xvt2

Units D2lvt1 and D2xvt2 have a maximum thickness of 120 m and 700 m, respectively, and comprise reddish-purple to grey tuff, lapilli tuff, and rare tuff breccia. The tuff consists of essential vitric and crystal fragments, and accidental and cognate lithic fragments. Pumice (up to 30%, averaging 5%) is up to 4 cm in size and highly elongate to irregular and wispy. Pumice typically displays axiolitic, spherulitic, and granophyric devitrification textures. Elongate pumice fragments are commonly draped over lithic fragments. The abundance of accidental and cognate lithic material varies from 0-30%. Cognate clasts, common in unit D2xvt2, are massive to flow-banded, originally glassy rhyolite (3-5%) that are up to 10 cm, but generally 1 cm in size, and angular to subangular (Fig. 62). Accidental lithic fragments include plagioclase microphyric basalt, vesicular basalt, and siltstone. Mafic accidental clasts (10%) are up to 5 cm in size, rounded to angular, and dense or scoriaceous. Siltstone clasts (2%) are generally less than 1 cm in size, but rarely up to 1 m, and rounded. Rare subrounded fragments of rhyolitic tuff are up to 2 cm in size, and are either cognate or accidental. Crystals include plagioclase (5% and 1-5 mm) and sanidine (5% and 0.5-2.5 mm). The matrix (50-85%) is devitrified fine ash, crystal and lithic fragments, and relict siliceous shards (Fig. 63). Shards (up to 30% but generally less than 5% of the matrix) are 0.1 mm in size and have bubble-wall shapes. The matrix of D2xvt2 has perlitic cracks.

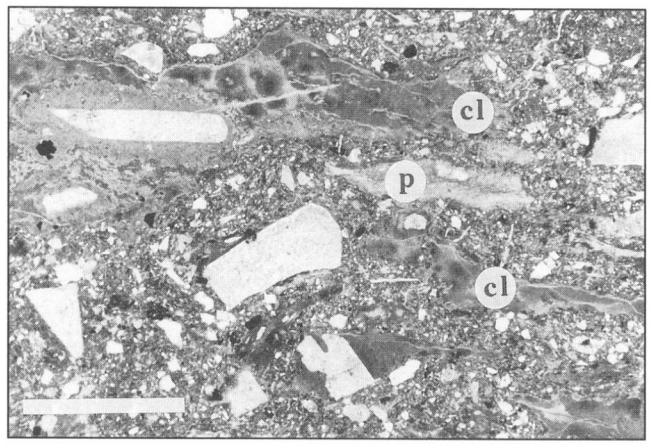

Figure 62. *Photomicrograph of massive lithic-crystal-vitric tuff from unit D2xvt2 showing angular to irregular-shaped, dense, glassy rhyolite cognate lithic fragments (cl), broken crystal fragments and light-coloured pumice (p). Bar scale represents 1.4 mm (plane polarized light). (GSC 1993-217AA)*

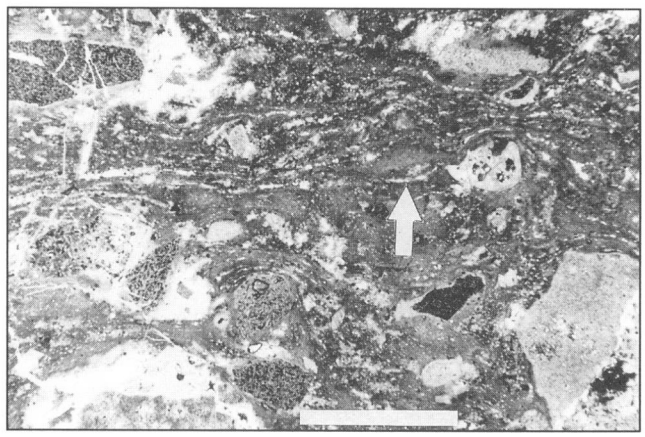

Figure 63. *Photomicrograph of massive lithic-crystal-vitric tuff from unit D2lvt1 showing relict felsic shards (arrow) now devitrified and recrystallized to quartz and feldspar. The shards are deformed around crystals and lithic fragments. Bar scale represents 3 mm (plane polarized light). GSC 1993-217BB)*

These units are massive, generally poorly sorted, and moderately to strongly welded. Near the base of unit D2xvt2 there are abundant relict glassy rhyolitic pyroclasts, which are locally block-sized and set in a flow-aligned vitrophyric matrix. The foliation, where developed, is defined by the parallel elongation of pumice, and rarely, lithic fragments. Fining of D2xvt2 to the southwest is defined by the loss of boulder-sized ejecta.

Interpretation of units D2lvt1 and D2xvt2

The lithic-vitric and crystal-vitric tuffs (D2lvt1 and D2xvt2) are interpreted to be pyroclastic flow deposits on the basis of their poor sorting, massive structure, and the flow alignment of elongate pumice and crystals. The type and combination of accidental lithic fragments are characteristic of the underlying units. The eruptive system was magmatic as indicated by the bubble-wall shards and pumice.

Welded and banded pyroclastic rocks: unit D3vt1

Unit D3vt1 is a densely welded tuff that resembles a rhyolitic lava flow. The unit comprises interlayered banded and densely welded vitric tuff and minor densely welded lithic-lapilli tuff to tuff breccia. Maximum thickness is about 500 m.

The lithic tuff to tuff breccia comprises 50-90% angular lithic clasts up to 40 cm in size. The lithic clasts are banded rhyolite (25%), spherulitic rhyolite (25%), massive rhyolite (25%), aphanitic vesicular and nonvesicular basalt (25%) (Fig. 64), diabase (<1%), and sedimentary rock (<1%). The matrix is devitrified and recrystallized purple rhyolite. Pumice forms orange spherulitic patches that are lenticular to irregular and up to 10 cm long. Crystal content is low with typically 1% altered plagioclase crystals. Many beds are normally graded from lithic tuff bases to vitric or lithic-vitric tuff with a decrease in the number of lithic clasts. Beds are 35-40 m thick.

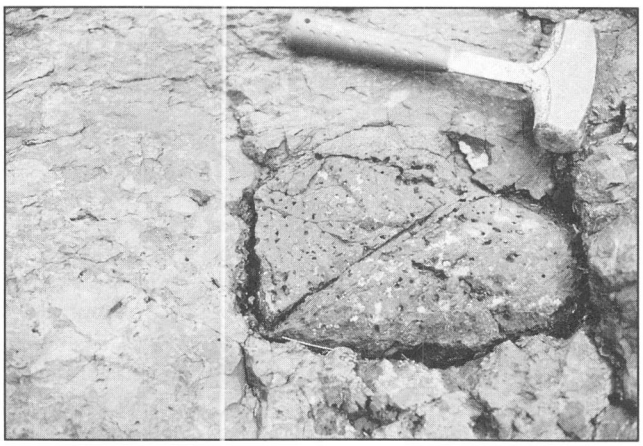

Figure 64. *Tuff breccia at the base of a graded bed in unit D3vt1. The tuff breccia comprises about 90% of angular lithic clasts up to 40 cm in length. The lithic clasts are banded rhyolite, spherulitic rhyolite, massive rhyolite, aphanitic vesicular and nonvesicular basalt, diabase, and sedimentary rock. (GSC 1993-212K)*

Interlayered with the lithic tuff and tuff breccia are beds of flow-foliated vitric tuff. The foliation is folded, often into complex folds, possibly due to rheomorphism. Flow bands are <1 mm-15 cm thick, discontinuous, and in many cases defined by extremely stretched and flattened pumice, or fiamme. Feldspar crystals are up to 5%. Other primary structures include minor flow-top breccia and local columnar joints. These beds resemble rhyolite lava flows due to the well developed flow foliation, however, the presence of fiamme distinguish them as pyroclastic flows.

Interpretation of unit D3vt1

Unit D3vt1 is interpreted to be a series of welded pyroclastic flows. The extremely stretched pumice and graded lapilli tuff and tuff breccia are typical of this depositional mechanism (Van Wagoner et al., 1988). The complexly folded flow foliation may be due to rheomorphism, or postdepositional flowage directly after deposition (Chapin and Lowell, 1979; Noble, 1968; Walker and Swanson, 1968; Schmincke and Swanson, 1967) or in the final stages of deposition (Wolff and Wright, 1981; Ragan and Sheridan, 1972; Hoover, 1964). As a result of this secondary flowage and high temperature, pyroclastic flows may develop characteristics similar to those of silicic lava flows and, in some cases, may be virtually indistinguishable. The dense welding of the vitric tuffs and coarseness of the tuff breccias suggest that these are relatively near-vent deposits (Van Wagoner et al., 1988).

Bedded pyroclastic rocks: units D1xvt3; D2xvt1; D2lvt2; D2lxt1; D2xlt1; D2tb1;, D3lvt1, 2; 3; D4lvt2, 3

Units D1xvt3 and D2xvt1

Units D1xvt3 and D2xvt1 are 200 m and 75 m thick, respectively, and comprise interbedded grey-green crystal-vitric tuff and accretionary lapilli tuff. The crystal-vitric tuff comprises vitric, crystal, and minor accidental lithic pyroclasts. The essential vitric pyroclasts (5-10%) are buff to orange pumice, 1-3 cm in size, and elongate parallel to bedding. Associated with devitrification of the pumice are zones of lithophysae. Minor plagioclase crystals are 1 mm in length and euhedral, but broken. Minor accidental lithic fragments include vesicular basalt (2 mm and subrounded) and siltstone (1-3 mm and subrounded). The matrix (90-95% of the rock) consists of devitrified glass and relict siliceous glass shards. Platy, and rarely tricuspate and bubble-wall shards (10-20%, but rarely 80%) are 0.1-1 mm in size (Fig. 65). Blocky, equant shards (5%) are 1-4 mm in size. The tuff is nonwelded (Fig. 65) to welded (Fig. 66). Beds are a few centimetres to 3 m thick, planar and internally massive with some oxidized tops.

The accretionary lapilli tuff comprises accretionary lapilli (up to 70%, but generally 5%; Fig. 67), pumice (10-20%), and crystals (5-15%) in an ash matrix. The accretionary lapilli are from 3 mm to 2.5 cm in size, rounded to slightly flattened, and concentrically zoned. Some accretionary lapilli are

deformed to conform to the shape of adjacent lapilli indicating they were either plastic when deposited or have been compacted (Fig. 68). Many accretionary lapilli are broken. Pumice is pink, wispy, and flattened along bedding planes. The pumice is 2 mm-5 cm in size, and locally displays a well developed elongation and alignment of vesicles. Plagioclase crystals (5%) are 1-3 mm in size and broken. The matrix consists of fine, devitrified ash and glass shards. The shards are 0.3-1 mm in size, and generally platy, although minor tricuspate shards are preserved. The accretionary lapilli tuff is bedded. Bedding is defined by difference in grain size, colour, and concentrations of accretionary lapilli. Beds are from 1-15 cm thick, and internally finely laminated. Internal laminations are generally planar, although locally there is large-scale crossbedding and megaripples (wave height 40 cm, wavelength 1.5 m), and normal, symmetric (fine-coarse-fine), and reverse grading. The grading is defined by change in size and concentration of accretionary lapilli.

Interpretation of units D1xvt3 and D2xvt1

Units D1xvt3 and D2xvt1 were emplaced as bedded pyroclastic surge deposits with a possible air-fall component. Surge emplacement is indicated for unit D2xvt1 by the fine grain size, planar laminations and large-scale crossbedding (Cas and Wright, 1987; Fisher and Schmincke, 1984; Sheridan and

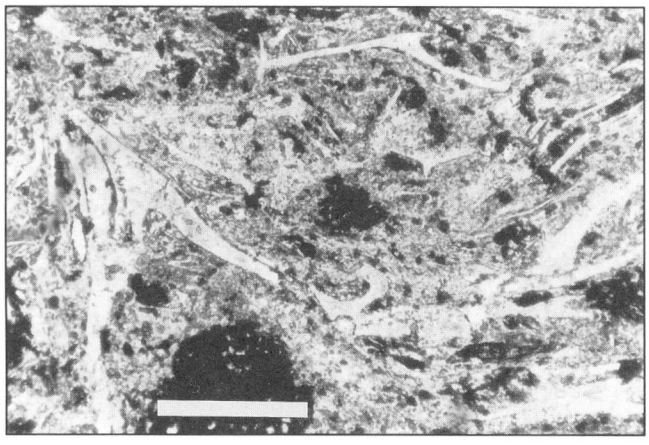

Figure 65. *Photomicrograph of bedded crystal-vitric tuff from unit D1xvt3 showing platy and bubble-wall shaped felsic shards in an altered fine ash matrix. The tuff is nonwelded. Bar scale represents 0.3 mm (plane polarized light). (GSC 1993-217CC)*

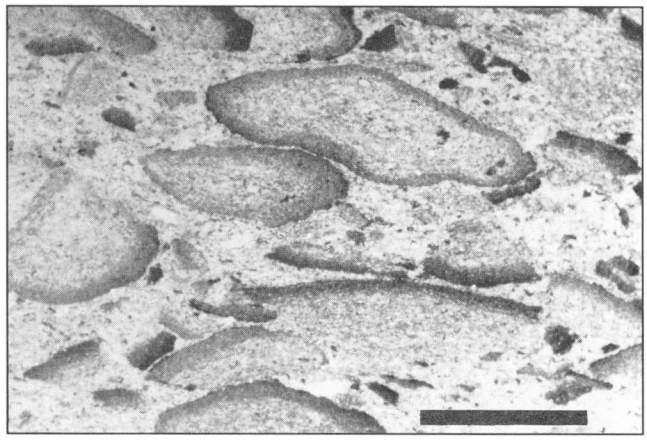

Figure 67. *Photomicrograph of bedded accretionary lapilli tuff from unit D2xvt1 showing flattened, whole, and broken accretionary lapilli in an altered and devitrified fine ash matrix. Bar scale represents 4.5 mm (plane polarized light). (GSC 1993-217EE)*

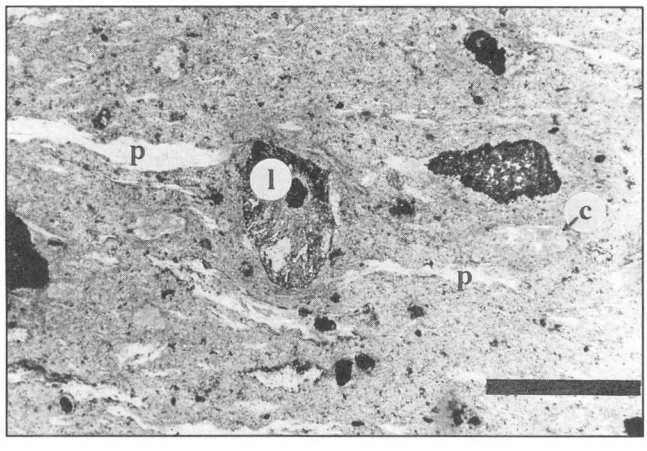

Figure 66. *Photomicrograph of bedded crystal-vitric tuff from unit D1xvt3 showing flattened pumice (p) and glass shards, angular lithic clasts (l), and crystal fragments (c) in an altered and devitrified fine ash matrix. Pumice clasts are deformed around lithic clasts. The tuff is welded. Bar scale represents 1.9 mm (plane polarized light). (GSC 1993-217DD)*

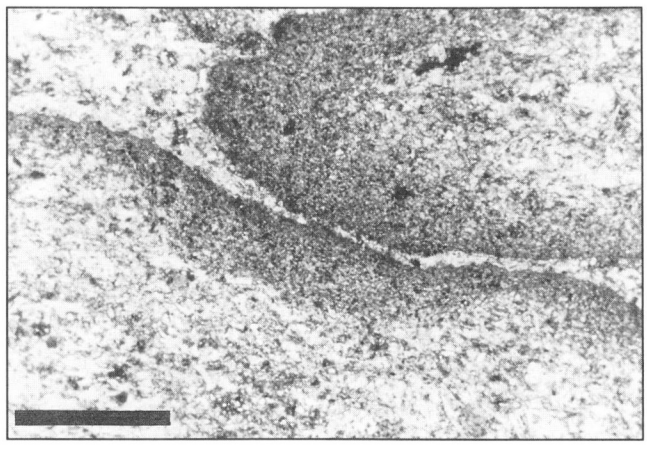

Figure 68. *Photomicrograph of bedded accretionary lapilli tuff from unit D2xvt1 showing detail of accretionary lapilli in Figure 67. The accretionary lapilli are deformed to conform to the shape of the adjacent lapilli. Bar scale represents 1 mm (plane polarized light). (GSC 1993-217FF)*

Wohletz, 1983; Self, 1982). Accretionary lapilli in the tuff were probably broken during transport. There are three types of surge deposits based on lithological associations. Ground-surges are found at the base of pyroclastic flow deposits (Self, 1982; Wright et al., 1980). Ash-cloud surges are generated in the gas-ash cloud overriding pyroclastic flows (Self, 1982). Base surges are formed by eruptive column collapse (Fisher, 1979). Unit D2xvt1 is not obviously at the base of a pyroclastic flow, and is too large in volume to represent an ash-cloud surge associated with pyroclastic flow unit D2vt1. Unit D2xvt1 was probably emplaced as a base surge as the result of column collapse. Interpretation of emplacement mechanisms for unit D1xvt3 is less obvious because the beds are internally massive, although base surge deposits may contain thick, massive beds (Sheridan and Wohletz, 1983). Alternatively, the beds may represent a succession of air-fall deposits as indicated by the excellent preservation of unabraded cuspate shards and graded bedding. Air-fall deposits are commonly associated with surges (Sheridan and Wohletz, 1983).

Units D1xvt3 and D2xvt1 were produced from phreatomagmatic eruptions. Such eruptions typically produce fine grained, thinly- to thickly-bedded deposits (Sheridan and Wohletz, 1983). The accretionary lapilli, abundant in these units, commonly form in an explosive phreatomagmatic or phreatic eruption column (Self and Sparks, 1978; Cas and Wright, 1987). The presence of magmatic pumice and bubble-wall shards in these units indicates that eruptions were phreatomagmatic rather than phreatic. Equant, blocky, poorly-vesiculated, vitric shards also indicate fragmentation of magma as the result of interaction with water (Self, 1983; Sheridan and Wohletz, 1983, 1981; Wohletz, 1983). The sequence of bedding structures of unit D2xvt1 (planar-laminated and crossbedded accretionary lapilli tuffs overlain by massive, thickly-bedded vitric tuffs) has been described for deposits resulting from Surtseyan phreatomagmatic eruptions (Sheridan and Wohletz, 1983). Surtseyan eruptions are typically basaltic, although rhyolitic examples have been described (Cas and Wright, 1987). Surtseyan phreatomagmatic eruptions are usually initiated by seawater/magma interaction (Sheridan and Wohletz, 1983). In this case, seawater/magma interaction probably occurred in a tidal flat environment.

Unit D2lvt2

Unit D2lvt2 is olive to brown, accretionary, and lithic-vitric tuff to lapilli tuff. The unit has a maximum thickness of about 50 m. Essential vitric clasts (up to 40%) are subrounded pumice up to 1 cm in size. Accretionary lapilli (up to 60% of some beds) are in layers 1-2 cm thick and are 3 mm-1 cm in diameter. The matrix is fine-ash tuff.

Beds are up to 0.5 m thick, and internally massive, cross-laminated, and normally and reversely graded from fine to medium ash. Climbing ripples occur locally.

Interpretation of unit D2lvt2

The occurrence of accretionary lapilli with juvenile pumice fragments suggests that this unit originated from a phreatomagmatic eruption (Fisher and Schmincke, 1984). Most of the bedding structures are consistent with an air-fall deposit, however the cross-stratification and climbing ripples require deposition by a current, and likely represent surge deposits (Cas and Wright, 1987).

Unit D2lxt1

Unit D2lxt1 comprises interbedded lithic-crystal lapilli tuff and lithic-crystal-vitric lapilli tuff with rare red and green siltstone and mudstone (Fig. 69). Maximum thickness is about 100 m. Individual tuff beds are 0.5 cm-15 m thick. Primary structures include parallel bedding and rare cross-bedding. Some beds are internally massive.

The lithic-crystal lapilli tuff beds comprise broken feldspar crystals (generally 5-40% but up to 80% of some beds) and lithic clasts (5-60%) in a siliceous fine-ash matrix (30-40%; Fig. 70). Lithic clasts include rhyolite (65%) up to 8 cm, and aphanitic basalt (35%) up to 4 cm. The unit has crystal-rich patches, containing up to 80% feldspar crystals, that are irregular in shape and up to 17 cm across. The matrix is altered to clay and chlorite.

The lithic-crystal-vitric lapilli tuff beds comprise broken feldspar crystals (25-30%), lithic clasts (5-20%), and pumice (55-60%; Fig. 71, 72). The lithic clasts include rhyolite (60%) up to 4 cm and basalt (40%) up to 10 cm. Pumice clasts are up to 13 cm in length, slightly flattened, and crystal-rich with up to about 20% crystals (Fig. 72). Rare visible shards have platy and bubble-wall shapes.

The beds are nonwelded to moderately welded with flattened glass shards and pumice. They are vaguely bedded and banded, normally graded, laminated, crosslaminated, and massive.

The bedded red and green siltstone and mudstone are similar to unit D2s1. The sedimentary rocks have herringbone crosslamination and worm burrows.

Interpretation of unit D2lxt1

This unit is interpreted as a sequence of flow, surge, and minor air-fall deposits. Beds with crossbedding and those with extreme crystal enrichment were probably deposited as surges. Surge deposits are commonly more crystal- and lithic-rich than their associated pyroclastic flow deposits (Fisher and Schmincke, 1984; Walker, 1971). The crystal enrichment is due to both gravitational segregation in the eruption column and elutriation of fine particles from the moving flow (Fisher and Schmincke, 1984). The massive beds with large pumice fragments and poor sorting were probably deposited as ash flows. The low degree of welding and thinness of most of tuff beds suggests that this sequence was deposited medial or distal to source.

Units D2xlt1 and D2tb1

Unit D2xlt1 is interbedded red to buff, crystal-vitric tuff, crystal-lithic tuff, and lapilli tuff, with rare interbeds of red siltstone. The unit fines to the north and tuff beds appear cherty in its northernmost outcrop. There is some evidence of welding in the south. Its maximum thickness is 534 m. In the southern part of the map area, unit D2xlt1 is interbedded with D2tb1, a heterolithic tuff breccia. This tuff breccia unit, which has a maximum thickness of about 115 m, is interpreted as a coarser grained facies of D2xlt1.

Crystals form up to 15% of unit D2xlt1 and are mostly feldspar (Fig. 73). Lithic and vitric lapilli are 1 mm-1 cm, subrounded to angular, comprise up to 90% of some layers, and include pumice, rhyolite, basalt, and rare mudstone. Welded beds contain fiamme. The pumice and fiamme are juvenile fragments, the other lithic fragments are accidental clasts, although the rhyolitic clasts may be cognate ejecta. Accretionary lapilli occur locally where they are up to 90% of reversely graded layers. They are up to 1 cm in diameter but mostly 2-3 mm. The matrix material is fine to coarse ash (Fig. 74). Felsic shards have platy and bubble-wall shapes. Devitrification textures are common and include spherulites, lithophysae, and granophyric recrystallization.

Beds are up to 2 m thick, internally massive, thinly laminated, and normally, reversely, and multiply graded. Some of the welded tuffs exhibit convolute lamination, possibly due to rheomorphism (Wolff and Wright, 1981; Chapin and Lowell, 1979; Schmincke and Swanson, 1967).

The tuff breccia (unit D2tb1) contains 30-80% clasts of pumice and rhyolitic bombs, rhyolitic blocks (Fig. 75), siltstone and basaltic lapilli, and locally fiamme. The pumice and rhyolitic bombs, and fiamme are probably juvenile fragments. The other clast types are cognate or accidental clasts. The breccia is massive or vaguely medium to thickly bedded. Beds are very rarely finely laminated and crosslaminated. Rare bomb sags occur beneath larger pumice clasts.

Interpretation of units D2xlt1 and D2tb1

Unit D2xlt1 is interpreted to be a series of mostly magmatic pyroclastic fall and flow deposits (Van Wagoner et al., 1988). The increase in the degree of welding and grain size to the south, suggests a southern source. The reversely-graded accretionary lapilli layer suggests local phreatomagmatic air-fall activity.

Unit D2tb1 is interpreted to be near-vent pyroclastic air-fall and rare surge deposits (Van Wagoner et al., 1988). The surge deposits are represented by the laminated and cross-laminated beds. The other bedding structures are more typical of air-fall deposits, probably from a magmatic Plinian or ultra-Plinian eruption (e.g., Cas and Wright, 1987). The coarser pyroclastic air-fall deposits to the south and the occurrence of welding indicate proximity to a vent area.

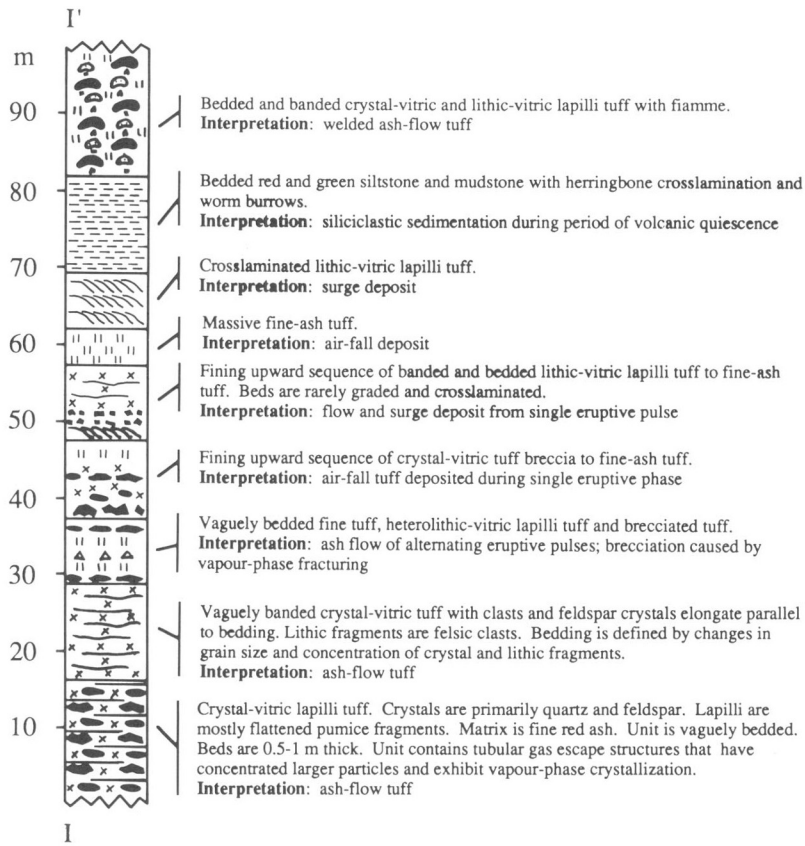

Figure 69.

Graphical log through a representative section of unit D2lxt1. Location of section I-I' is shown on Figure 3.

Figure 70. Bedded lithic-crystal lapilli tuff from unit D2lxt1. This bed has 80% feldspar crystals and 5% lithic clasts in a siliceous fine-ash matrix. Most crystals are broken. (GSC 1993-212L)

Figure 72. Lithic-crystal-vitric lapilli tuff from unit D2lxt1 comprising broken feldspar crystals, pumice and ash. The pumice clasts are slightly flattened and crystal-rich. The tuff bed is poorly to moderately welded. (GSC 1993-212Q)

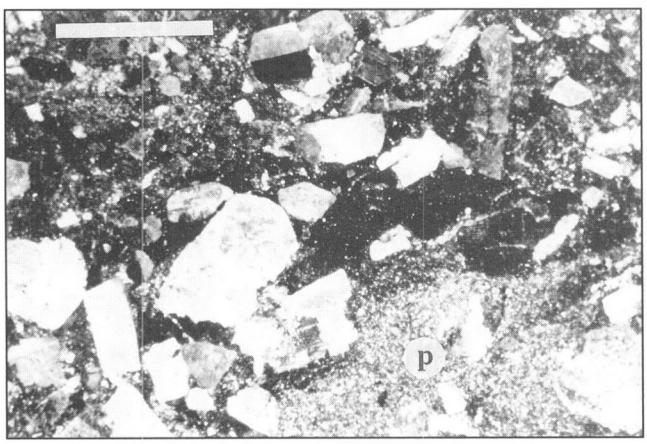

Figure 71. Photomicrograph of bedded lithic-crystal lapilli tuff from unit D2lxt1 showing broken and whole feldspar crystals and a devitrified and altered pumice clast (p; bottom right). The pumice clast has fewer crystals than the surrounding tuff. Bar scale represents 3 mm (plane polarized light). (GSC 1993-217GG)

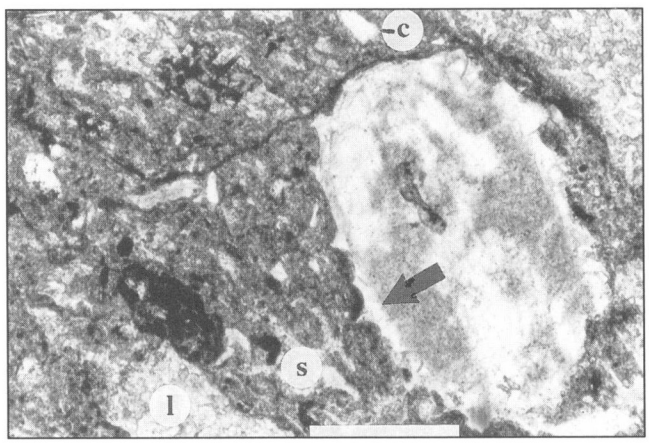

Figure 73. Photomicrograph of bedded crystal tuff unit D2xlt1 showing a feldspar crystal with a vitric rim (arrow). The rim has bubble-wall controlled edges. The tuff also comprises felsic shards (s), crystal fragments (c), and lithic clasts (l) in a devitrified and altered fine ash matrix. Bar scale represents 0.3 mm (plane polarized light). (GSC 1993-217 HH)

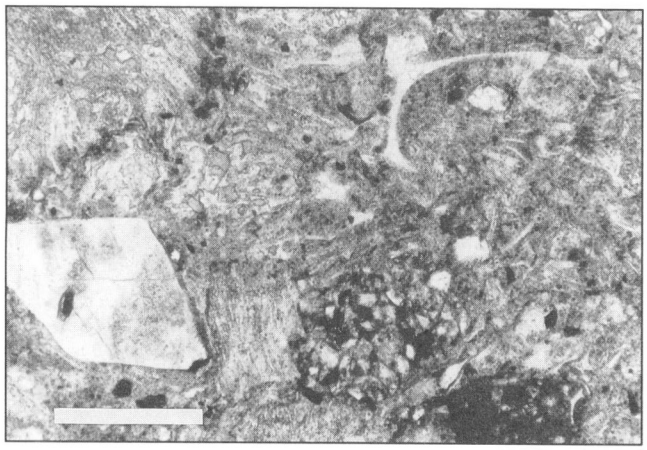

Figure 74. Photomicrograph of bedded crystal tuff from unit D2xlt1 showing the fine to coarse ash matrix. Felsic shards have platy and bubble-wall shapes. The ash is devitrified and altered. Bar scale represents 0.3 mm (plane polarized light). (GSC 1993-217II)

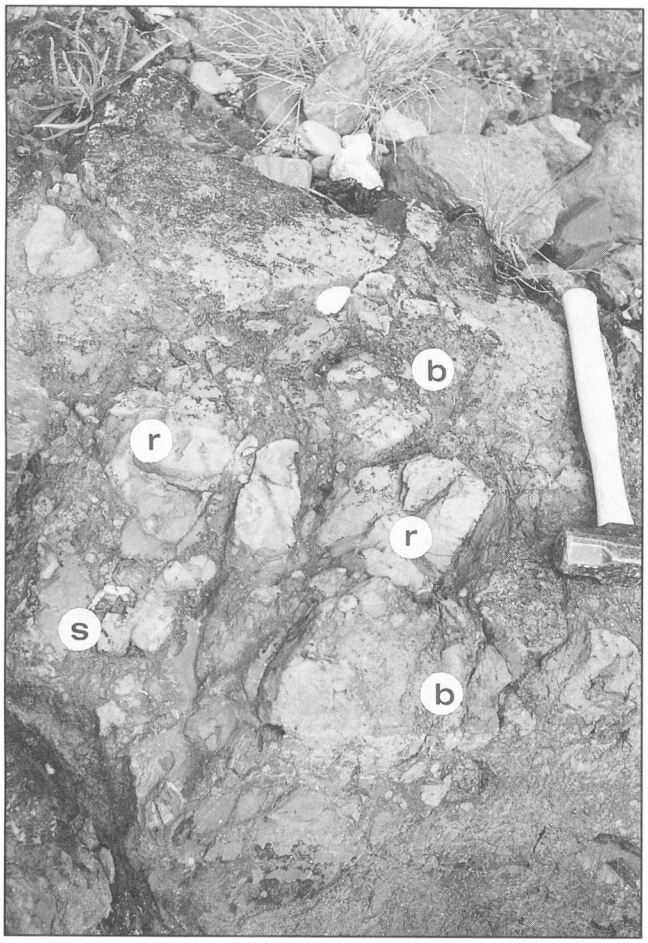

Figure 75. Outcrop of poorly sorted felsic heterolithic tuff breccia of unit D2tb1. Lithic clasts are mostly rhyolitic blocks (r). Other clasts include pumice, rhyolite bombs, siltstone (s), and basalt (b). (GSC 1993-212P)

Units D3lvt1, D3lvt2, and D3lvt3

These units are well bedded lithic-lapilli tuff, lithic-vitric lapilli tuff, vitric tuff, crystal-vitric tuff, and rare accretionary lapilli tuff. Units range in thickness from 30 to 65 m, and are thinly to thickly bedded (Fig. 76, 77). Beds are internally massive, finely laminated, normally, reversely, and symmetrically (fine-coarse-fine) graded, locally flow banded and rarely crosslaminated. Beds are discontinuous in places. Bomb sags occur locally.

The lithic-lapilli tuff layers comprise angular to rounded accidental mafic volcanic and siltstone clasts, and pyrogenic feldspar crystals (up to 90% of some beds). The matrix is vitric and largely recrystallized.

The crystal-vitric tuffs form thin beds and comprise plagioclase crystals (up to 10%) and rare pumice fragments. The lithic-vitric lapilli tuff layers comprise plagioclase (10%), and mafic and rhyolitic lithic fragments (up to 70%) that are angular to subrounded, up to 3 cm in size, and locally flattened parallel to bedding. Some beds contain pumice (up to 30%) that is up to 3 cm in size. The pumice ranges from flattened and elongate to more equant in shape. The matrix of the crystal tuff and crystal-lithic lapilli tuff comprises pumiceous, bubble-wall, platy and rare blocky shards, and recrystallized vitric material.

The vitric tuff comprises broken plagioclase crystals (1%), angular rhyolitic lithic clasts up to 5 mm in length (1%), and wispy, flattened pumice up to 7 mm (0-30%) in a felsic recrystallized vitric matrix. Some beds contain broken and whole accretionary lapilli (20-60%), that are up to 5 mm in size.

The juvenile fragments are ash, pumice (Fig. 78, 79) and plagioclase crystals. The cognate fragments are rhyolitic lithic clasts (Fig. 79), and the accidental fragments are mafic volcanic rock and siltstone. Some thicker layers are welded and contain 3-5% fiamme.

Interpretation of units D3lvt1, D3lvt2, and D3lvt3

Poor sorting, massive beds, and aligned pumice fragments indicate that the thicker beds of units D3lvt2 and D3lvt3 are welded ash-flow tuffs (Van Wagoner et al., 1988). The vesicularity of the glass shards and the pumice in unit D3lvt2 indicates magmatic eruptions. Blocky shards and/or accretionary lapilli as well as bubble-wall shards in some beds in unit D3lvt3 indicate a phreatomagmatic eruptive system. The laminated tops of some of the thicker beds in unit D3lvt3 and the crossbedded layer near the top of unit D3lvt2 are probably surge deposits. Moderate to good sorting suggests that the interbedded massive and graded, thin tuff beds are probably air-fall deposits (Van Wagoner et al., 1988).

Units D4lvt2 and D4lvt3

Unit D4lvt2 is a 10 m thick, grey lithic-vitric tuff to lapilli tuff. The vitric component (40-95%) comprises recrystallized felsic bubble-wall shards and wispy flattened pumice fragments. The lithic clasts (up to 40%) are less than 4 mm in size

and include angular rhyolite (up to 50%), subrounded to rounded basalt and diabase (up to 40%), rounded siltstone (45%), and rounded vitric tuff (35%). Crystals (up to 20%) include broken plagioclase, quartz, and opaque minerals. The matrix is devitrified and recrystallized fine ash. The unit is nonwelded and poorly sorted. Elongate shards and pumice fragments define a crude foliation.

Unit D4lvt3 is a 25 m thick, red to mottled red-green, lithic-vitric tuff to lapilli tuff. The vitric component (25-45%) of the unit comprises rhyolitic recrystallized blocky and bubble-wall shards (65-100%), wispy and slightly flattened pumice (up to 15%) and chloritized platy, blocky, and minor bubble-wall glass shards (up to 25%) (Fig. 80). The lithic clasts (20-40%) include basalt and vesicular basalt (20-40%),

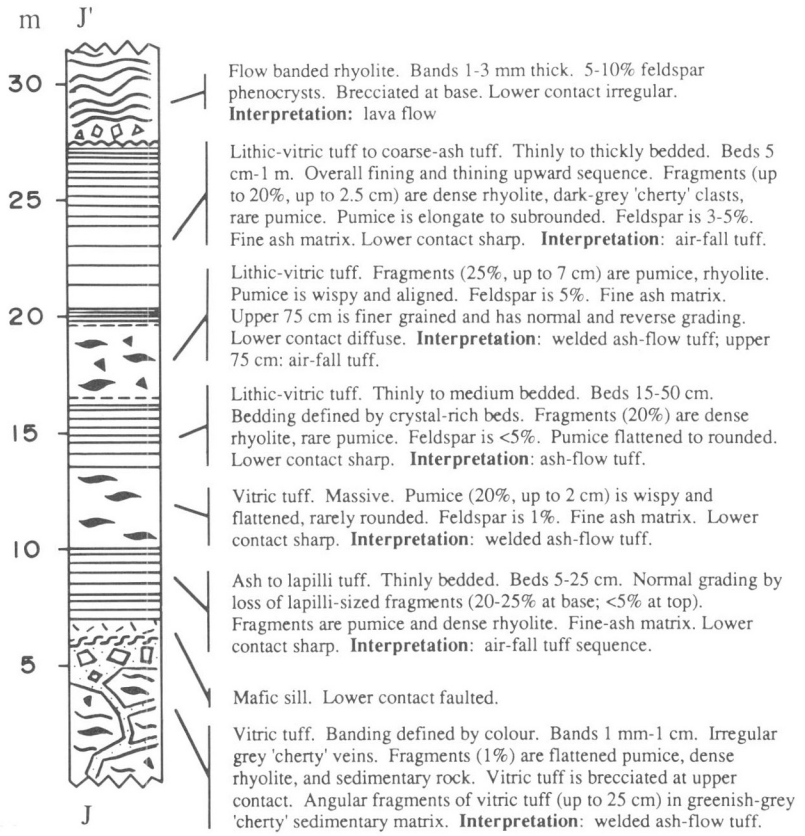

Figure 76.

Graphical log of unit D3lvt3. Location of section J-J' is shown on Figure 3.

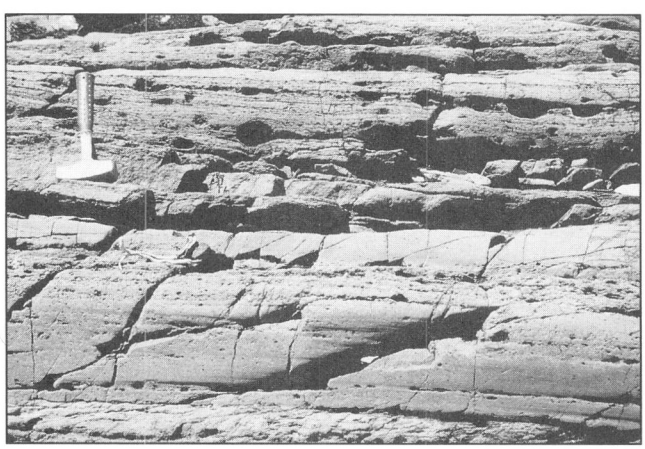

Figure 77. *Thinly- to thickly-bedded sequence of lithic-lapilli tuff, crystal-lithic tuff, and crystal tuff of unit D3lvt3. Beds are internally massive or finely laminated. Some beds are discontinuous along strike. (GSC 1993-212O)*

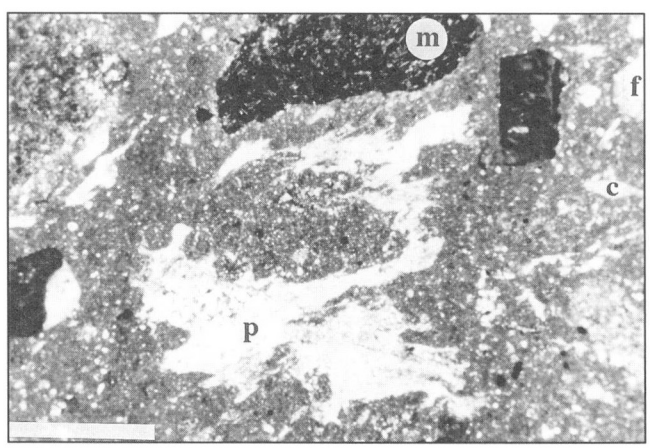

Figure 78. *Photomicrograph of bedded crystal-lithic tuff from unit D3lvt3 showing irregularly-shaped wispy pumice clasts (p), crystal fragments (c), and mafic (m) and felsic (f) lithic clasts in a devitrified and altered fine ash matrix. The tuff is poorly welded. Bar scale represents 1.5 mm (plane polarized light). (GSC 1993-217JJ)*

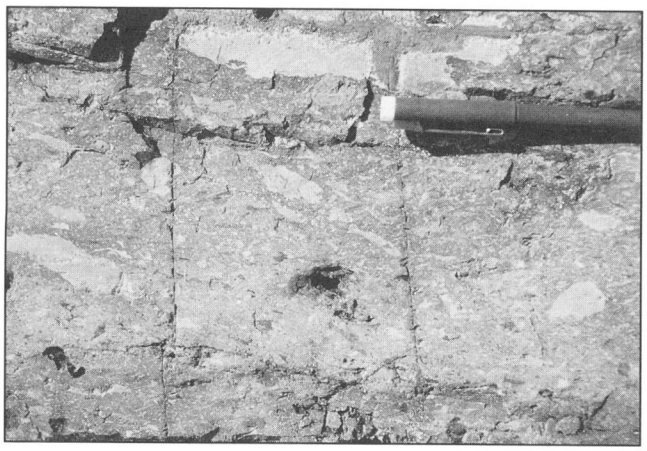

Figure 79. Bedded crystal-lithic lapilli tuff from unit D3lvt3 with light brown juvenile pumice clasts and cognate felsic lithic clasts. The matrix comprises ash and crystal fragments. The tuff bed is moderately welded. (GSC 1993-212N)

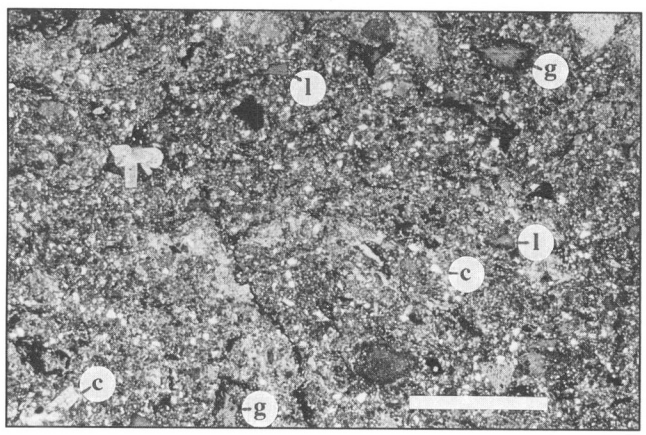

Figure 80. Photomicrograph of bedded lithic-vitric tuff from unit D4lvt2 showing chloritized shards (g), crystals (c), and lithic fragments (l) in a devitrified and recrystallized matrix. Bar scale represents 1.2 mm (plane polarized light). (GSC 1993-217KK)

sandstone and siltstone (<30%), rhyolite (<10%), and crystal tuff (<2%). The larger basaltic (up to 15 mm) and rhyolitic (up to 9 mm) clasts are predominantly angular, whereas smaller (<3 mm) clasts of all compositions are subangular to rounded. The sedimentary clasts commonly have baked rims. Crystals (25-35%) include plagioclase and rare zircon. The matrix is devitrified and recrystallized fine ash. Clast alignment defines a foliation. The unit is poorly sorted.

Interpretation of units D4lvt2 and D4lvt3

These units are interpreted as air-fall or ash-flow deposits, but resulted from different types of eruptive systems. The characteristics of these three units noted above, are found in both near vent air-fall and more distal ash-flow deposits.

Unit D4lvt2 is a deposit from a magmatic eruption. Distinguishable shards have bubble-wall shapes indicating fragmentation of the magma by vesiculation. The broken crystal fragments indicate the eruptions were explosive. Rounding of the lithic fragments may have occurred in the eruption column.

Unit D4lvt3 is interpreted to be a deposit of a phreatomagmatic eruption. The bubble-wall and blocky shards indicate fragmentation by vesiculation and quenching. Rims on the sedimentary lithic clasts indicate baking by steam in the eruption column, although lack of welding suggests relatively low emplacement temperatures, typical of phreatomagmatic deposits.

STRATIGRAPHY

The stratigraphic sequence is shown in a composite section (Fig. 81). The sequence is about 4 km thick and covers a lateral distance (east-west) of about 28 km. Correlation is based on the most laterally extensive units. Correlation becomes difficult and somewhat questionable between the eastern and central parts of the map area above unit D2mf1, and in the western part of the map area above unit D4s1. Units in the central part of the map area apparently interfinger with and lie conformably upon units in the eastern part of the map area, but it is possible that the structure is more complex. Correlation across the Bocabec River is problematic and is based on the continuity of unit D2s1 across the north-trending fault, which is exploited by the river (Van Wagoner et al., 1988). Stratigraphic interpretation of the western part of the map area, which represents the upper part of the sequence, is complicated by numerous faults, thin and laterally restricted units and the shallow dip of beds.

The eruptive sequence is bimodal and there are four cycles of mafic-felsic volcanism (Fig. 81). The Utopia Granite and the Bocabec Complex, which are phases of the Saint George Batholith, intrude units of all four cycles. Consistent with the compositional variation, several types of eruptive systems are represented (as defined for pyroclastic fall deposits, e.g., Walker, 1973; Wright et al., 1980). The mafic scoria cone (D3ms1) and mafic flow deposits (D1mf1, D2mf1, D3mf1, D4mf1, D4mf2) indicate Hawaiian and Strombolian volcanism. Some of the cycle 1, 2, and 4 massive pyroclastic flows (D1xvt1, D1xvt2, D1vt2, D2lvt1, D2vt1, D2xvt2, and D4vt1), the cycle 3 and 4 bedded tuffs (D3lvt1, D3lvt2, D3lvt3, D4lvt1), and the banded and densely welded tuff (D3vt1) indicate more explosive Plinian or sub-Plinian volcanism. The rhyolitic lapilli tuff units which contain accretionary lapilli (D2xvt1, D2lvt2, and parts of D2xlt1) and the mafic tuff breccia units (D3tb1, D3tb2, and D4tb1) suggest phreatomagmatic (Vulcanian) volcanism (Van Wagoner et al., 1988).

There are examples of most types of pyroclastic deposits including air-fall, pyroclastic flow, and surge deposits. Both welded and nonwelded varieties of these deposits occur in the area and there is some evidence for rheomorphism of the

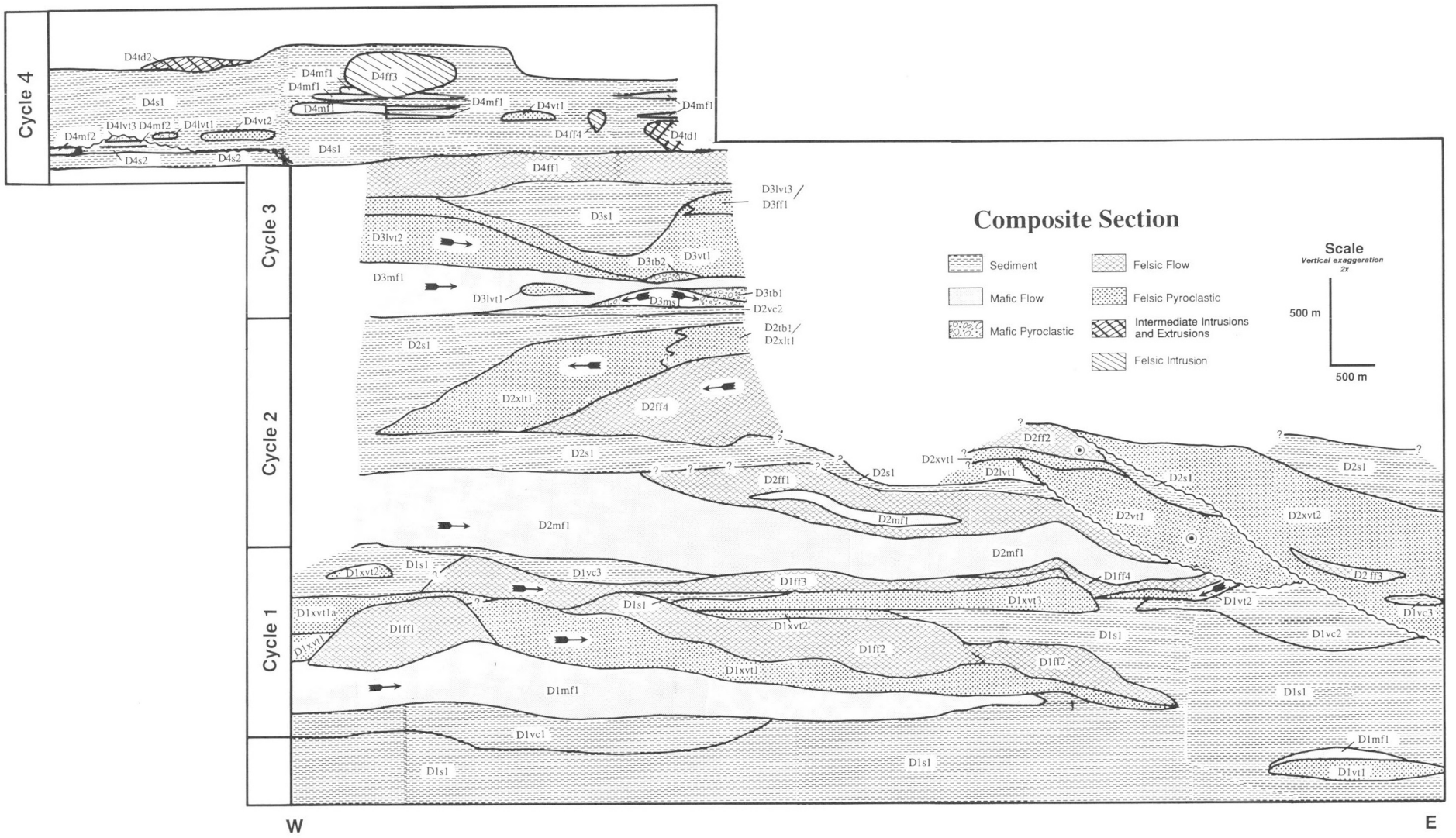

Figure 81. Composite section of the stratigraphic sequence of the map area. The four cycles of mafic-felsic volcanism are indicated on the left. Arrows indicate the major component of flow direction in the plane of the section. Circled dots indicate flow direction perpendicular to the page. Lithological codes are explained in Figure 4.

densely welded tuffs. In parts of the map area, mafic flows show evidence for interaction with wet sediment producing peperitic breccias.

There are no intervals of volcanic quiescence in cycles 1-3, which would be marked by continuous sedimentary horizons. The volcanic cycles are not separated by, but are interbedded with, sedimentary rocks. In cycle 4, sedimentary rocks predominate and separate thin mafic and felsic volcanic units. This cycle may represent the waning stages of volcanism.

The sedimentary rocks contain abundant, exceptionally well preserved shards. The excellent preservation of these shards indicates that sedimentation was rapid in a low energy environment, because any amount of reworking would destroy these fragile clasts. In addition, volcaniclastic layers such as D2vc2 and within D4s1 contain an abundance of air-fall deposits of mafic lithic fragments and shards indicating nearby mafic volcanism.

Of the volcanic rocks in the first three cycles, the rhyolitic rocks are most abundant. In the fourth cycle, rhyolitic rocks occur as thin restricted extrusive units (D4vt1, D4vt2, D4lvt2, D4lvt3, D4ff2) and as intrusive domes of uncertain age (D4ff3, D4ff4, D4td1). Sedimentary rocks predominate over volcanic rocks in the overall sequence.

Felsic lava flows and domes are common (D1ff2, D1ff3, D1ff4, D2ff1, D2ff2, D2ff3, D2ff4, D3ff1, D4ff1, D4ff2, D4ff3, D4ff4) and some are apparently quite extensive (D1ff2, D1ff3), although the nature of the exposure does not permit precise interpretation of the shapes and volumes of the flows. Within cycles 1-3, there is an association between pyroclastic deposits and rhyolite flows and domes, with the emplacement of lava flows and domes following pryoclastic volcanism. For example, a section measured at Cow Head within cycle 2 (Fig. 82), shows a sequence of pumice-rich vitric tuffs (D2vt1), overlain by thinly- to thickly-bedded accretionary lapilli tuff and vitric tuff (D2xvt1), overlain in turn by a rhyolite dome (D2ff2).

Mafic volcaniclastic units, composed dominantly of reworked scoria clasts, or primary scoria deposits (D3ms1), underlie the mafic flows in cycles 1-3 and indicate that a period of explosive mafic volcanism preceded each effusive event. The mafic volcaniclastic deposits and the mafic flows, however, have different source areas. The volcaniclastic deposits are near-vent deposits, as indicated by the preservation of unabraded clasts and shards, and the mafic flows are interpreted to have a source to the north.

Volcanic rocks are interbedded with primarily fine- and medium-grained sedimentary rocks over almost the entire thickness of the sequence. The common association of volcanic rocks with tidal flat sedimentary rocks indicates that volcanism occurred at or near sea level throughout most of the stratigraphic history. Assuming a constant sea level, the association of volcanic and sedimentary rocks indicates deposition in a rapidly subsiding basin, such that subsidence kept pace with the rate of volcanism.

Flow direction is varied and more complex than schematically illustrated on the composite section (Fig. 81), providing evidence for several small eruptive centres (Van Wagoner et al., 1988). A consistent northern source of mafic flows suggests that they were erupted from a single rift system. Other units such as D3ms1, D3tb1, D3tb2, and D4tb1, have limited areal extent and are probably near their vent area.

METAMORPHISM

The regional metamorphic grade of the study area is lower greenschist to subgreenschist facies as indicated by the presence of secondary quartz, epidote, chlorite, and albite± actinolite±pumpellyite±prehnite in the volcanic and sedimentary rocks. Greenschist facies metamorphic mineral assemblages occur in amygdules, veinlets, altered matrix material, plagioclase phenocrysts, and vitric pyroclasts.

In a contact metamorphic aureole adjacent to the Saint George Batholith the grade reaches the hornblende hornfels facies. Sedimentary rocks that are in contact with the batholith contain abundant biotite (Fig. 83) and many also have a granoblastic quartz mosaic. Volcaniclastic unit D1vc1 contains the assemblage quartz, biotite, cordierite + actinolite + garnet in outcrops adjacent to the batholith. Mafic volcanic units contain abundant actinolite. Fay (1988) and Percival and Helmstaedt (1978) noted the presence of a zoned aureole around the batholith in parts of the map area.

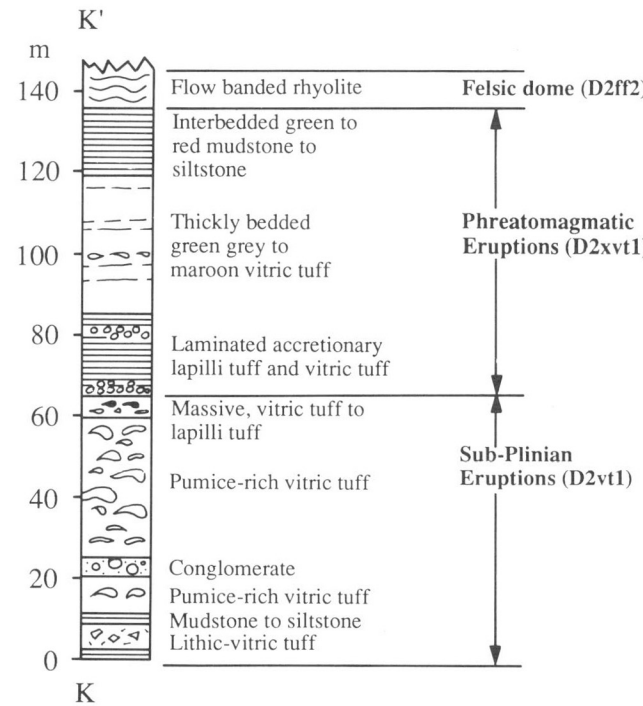

Figure 82. Graphical log and interpretation of eruptive mode of units D2ff2, D2svt1, and D2vt1 at Cow Head. Location of section K-K' is shown on Figure 3.

STRUCTURE

The map area is divided into three structural domains based on different bedding attitudes and fold style (Fig. 84). Contoured plots of poles to bedding, cleavage, and flow foliation as well as synoptic plots for domains 1 and 2 are shown in Figures 85 to 91. Bedding and cleavage attitudes were measured in sedimentary rocks and bedded pyroclastic rocks. Cleavage is poorly developed to well developed in the sedimentary rocks and rarely in the basaltic flows. There is one cleavage developed throughout the map area. Flow foliations were measured in flow-banded rhyolite and banded pyroclastic rocks. Locally, a poorly developed fracture cleavage occurs in some of the rhyolitic flows and pyroclastic rocks.

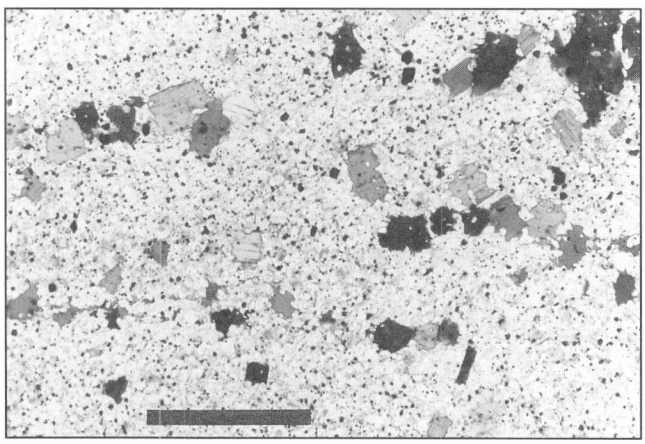

Figure 83. Photomicrograph of metamorphosed, laminated, nonvolcaniclastic siltstone from unit D1s1. Lamination in the siltstone is defined by a change in grain size and by a concentration of metamorphic biotite grains along laminae. The matrix is a mosaic of quartz and feldspar grains and opaque minerals. Bar scale represents 1.3 mm (plane polarized light). (GSC 1993-217LL)

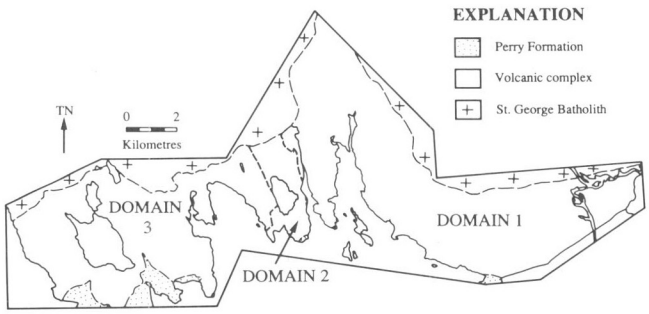

Figure 84. Structural domains in the Passamaquoddy Bay map area, southwestern New Brunswick (refer to Fig. 3, in pocket). TN = true north. Dashed lines indicate domain boundaries.

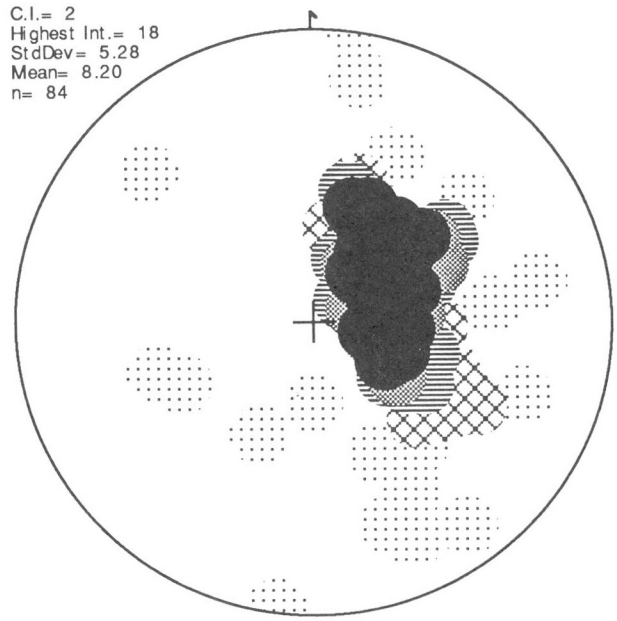

Figure 85. Contour plot of poles to bedding in Domain 1 (Fig. 84). The π-pole to the best-fit bedding plane girdle trends 20° toward 260°. In this figure and the following stereonet diagrams, C.I. = contour interval, Highest Int. = highest value of point density, StdDev = standard deviation of point densities, Mean = mean of density, n = number of points. Contours 2-4-6-8-10% per 1% area. Light stippling is the lowest contour level. Black is the highest contour level. All densities higher than 10 are included in the black.

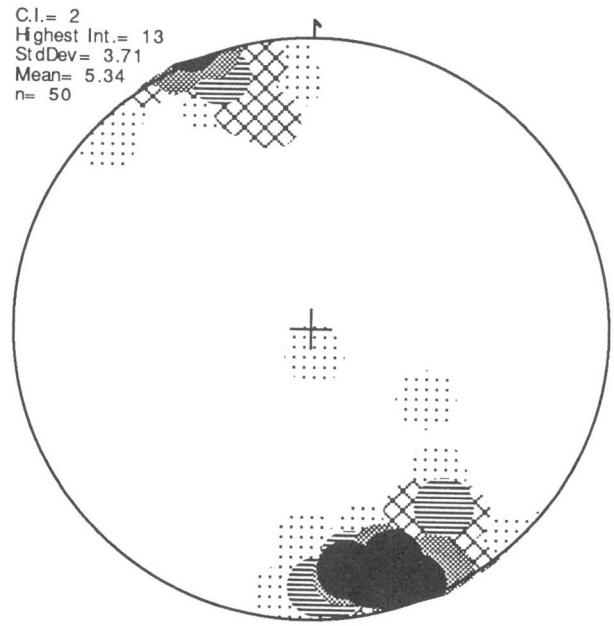

Figure 86. Contour plot of poles to cleavage in Domain 1 (Fig. 84). The cleavage strikes east-northeast and dips steeply. For explanation see Figure 85.

Domain 1

Bedding poles define a broad point maximum typical of a gently plunging, inclined broad arch (Marshak and Mitra, 1988). Bedding typically strikes northwest to east and dips and youngs moderately to the south (Fig. 85), defining a broad, open, cylindrical anticline. The fold axis plunges approximately 20° toward 260°. Cleavage strikes east-northeast to west-southwest and is steeply dipping (Fig. 86). This cleavage orientation is typical of Acadian structural trends (McLeod, 1988).

Flow foliation attitudes (Fig. 87) are generally similar to bedding attitudes with most variation explained by emplacement of the flows on an uneven surface or by measurement of attitudes in flow folded rhyolite.

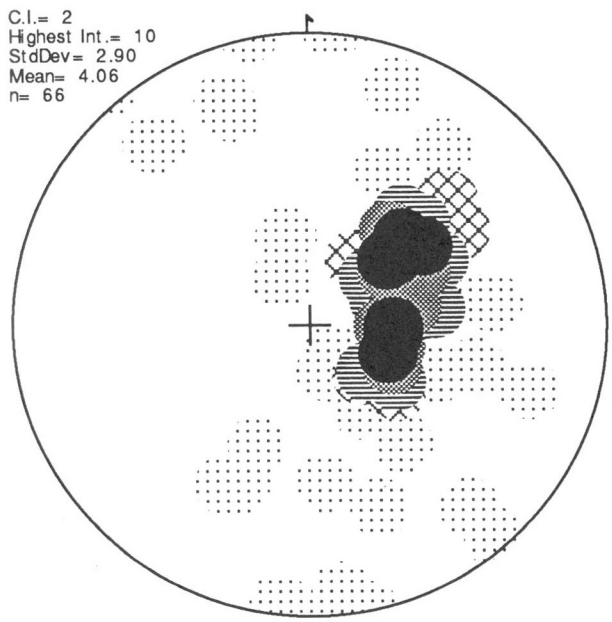

Figure 87. *Contour plot of poles to flow foliation in Domain 1 (Fig. 84). The spread of attitudes is similar to that for bedding poles (Fig. 85). For explanation see Figure 85.*

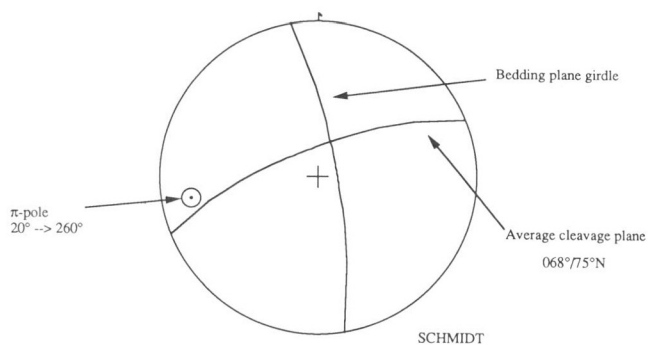

Figure 88. *Synoptic plot for Domain 1 (Fig. 84) showing the average bedding plane girdle, cleavage plane and fold axis. Net shown is a Schmidt net.*

An average cleavage plane constructed from Figure 86, bisects the bedding plane girdle (Fig. 85) and passes through the fold axis defined by the π-pole for bedding planes. This relationship (Fig. 88) suggests that cleavage parallels the axial plane of the broad anticline.

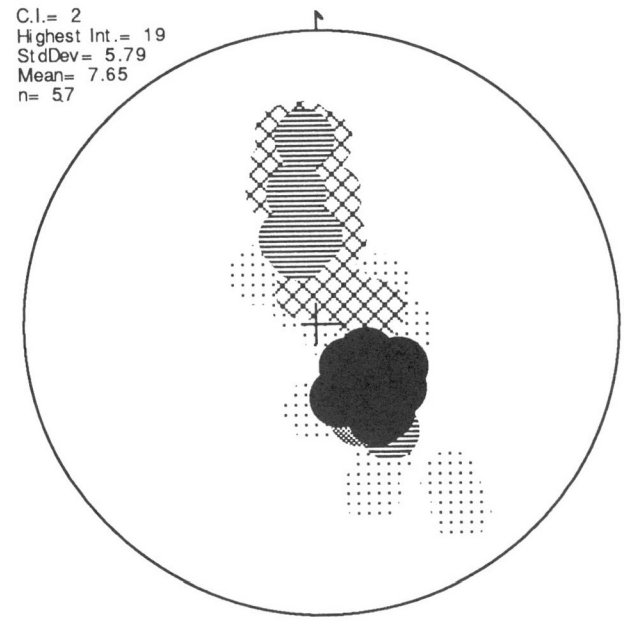

Figure 89. *Contour plot of poles to bedding in Domain 2 (Fig. 84). There are two point maxima defined by the data. The π-pole to the best-fit bedding plane girdle trends 7° toward 245°. For explanation see Figure 85.*

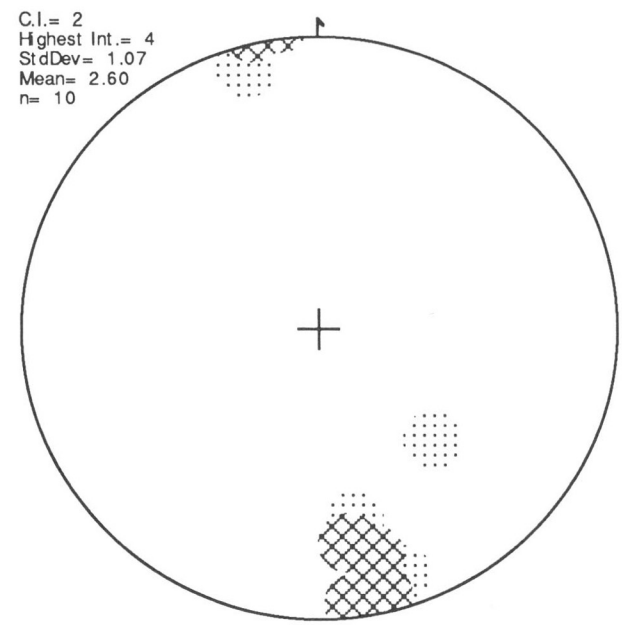

Figure 90. *Contour plot of poles to cleavage in Domain 2 (Fig. 84). The cleavage strikes nearly east-west and dips steeply north. For explanation see Figure 85.*

Faulting is minor. Trends average north to northeast and dip steeply. Faulting results in minor dextral and sinistral apparent strike-slip offset of some lithologies.

Domain 2

Bedding poles define two point maxima within a broad spread of attitudes, typical of a slightly plunging normal fold (Marshak and Mitra, 1988; Fig. 89). The maxima define two average bedding planes; one that strikes northeast and dips shallowly northwest and another that strikes roughly east and dips moderately south. The fold axis defined by these two planes plunges 7° toward 245°. Poles to cleavage define an average plane that strikes east and dips steeply north (Fig. 90). The average cleavage plane bisects the two point maxima, and although it does not pass directly through the fold axis (Fig. 91) defined by the bedding pole point maxima, it is within an acceptable range suggesting it is the axial plane cleavage to the fold.

There are two main sets of faults. A dominant set trends northwest to near north. Dip is unknown but assumed to be steep due to the straight trend of the faults over undulating topography. Apparent strike-slip offsets are both sinistral and dextral and changes in unit thickness across the faults suggests that some faults may have a dip-slip component. Several small faults trend roughly east and appear to dip steeply.

Domain 3

Bedding poles are concentrated symmetrically around the centre of the stereonet indicating the dips are shallow and strike highly variable (Fig. 92). This scatter of poles can be related to the high degree of faulting in Domain 3. Faults define blocks of varied bedding attitude. Cleavage (Fig. 93, 94) trends east-northeast and dips steeply north as in Domains 1 and 2. A fold axis cannot be determined for this domain. Poles to flow foliations are scattered and do not define a single girdle or point maximum.

The dominant fault set in Domain 3 trends northwest and dips steeply. Apparent strike-slip offset is typically sinistral and a change in unit thickness across faults suggests there is also a dip-slip component of movement. There are two major north-trending, steeply dipping faults. In the Birch Cove region, a north-striking fault coincides with a line of intrusions (D4td1, D4ff4, and Di). The north-south fault in the far west of the map area (Fig. 3) separates the outcrop range of units D4mf1 and D4mf2. Unit D4mf2 occurs only to the west of the fault, suggesting a dip-slip component of movement on the fault.

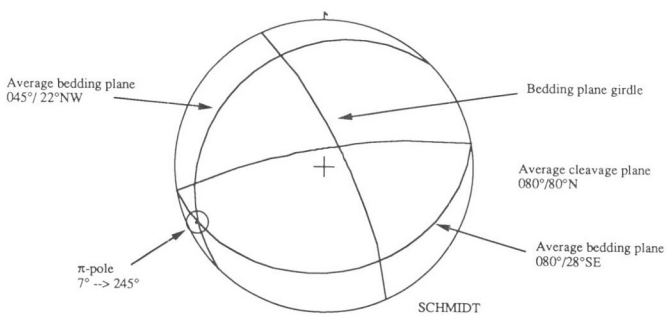

Figure 91. *Synoptic plot for Domain 2 (Fig. 84) showing the average bedding plane girdle, cleavage plane, and fold axis.*

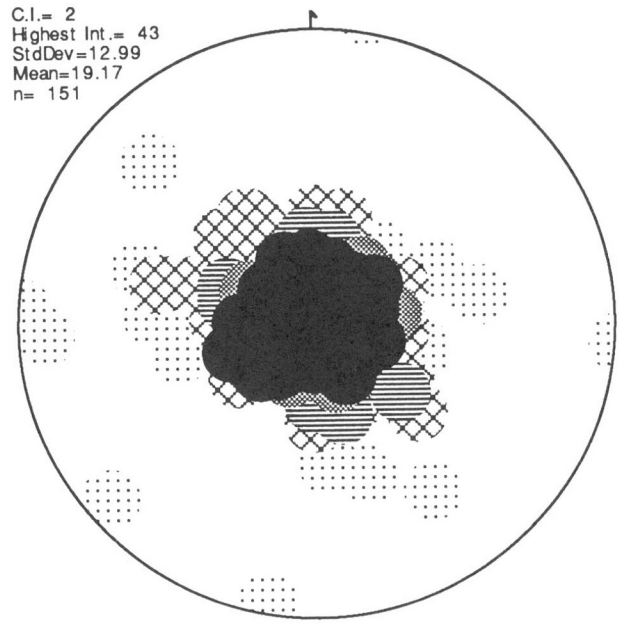

Figure 92. *Contour plot of poles to bedding in Domain 3 (Fig. 84). The data are concentrated around the centre of the stereonet. No π-pole to bedding can be determined for this domain. For explanation see Figure 85.*

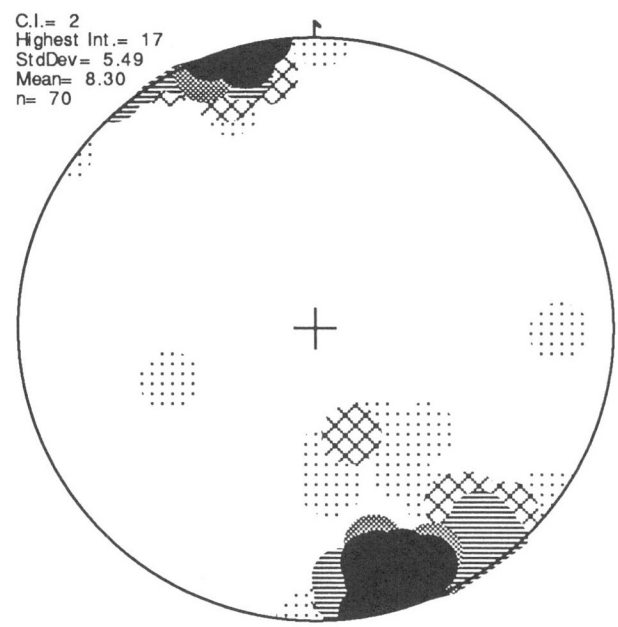

Figure 93. *Contour plot of poles to cleavage in Domain 3 (Fig. 84). The cleavage strikes east-northeast and dips steeply north. For explanation see Figure 85.*

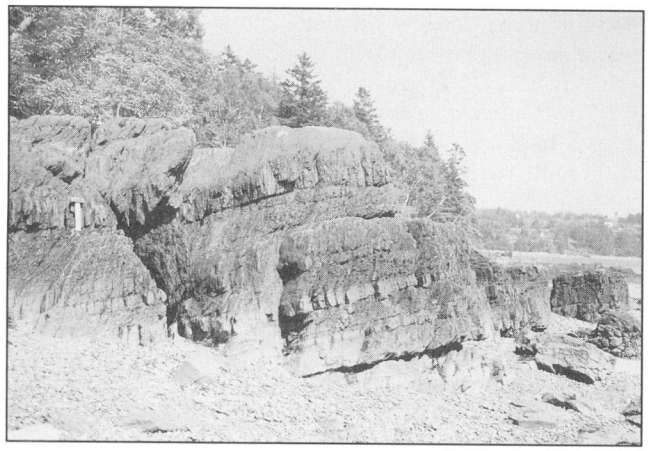

Figure 94. Interbedded, red, fine grained sandstone and siltstone of unit D4s1 in structural Domain 3 (Fig. 84). The outcrop has a well developed cleavage. The cleavage is refracted at change in grain size. (GSC 1993-212M)

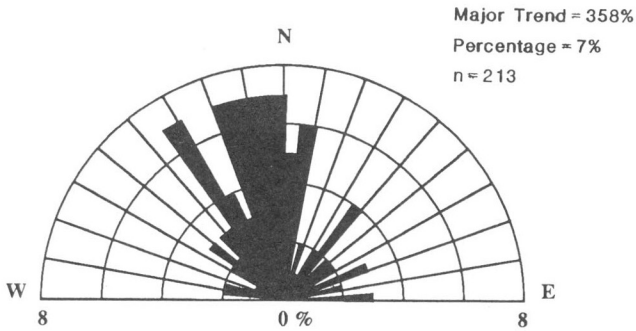

Figure 95. Rose diagram showing the trend of mafic dykes from cycles 1-4. The dykes trend approximately north to northwest and typicaly dip steeply.

MAFIC DYKES

Mafic dykes intrude rocks of all four cycles in the map area (N.A. Van Wagoner et al., unpub. data, 1990). Dykes range from highly porphyritic to aphyric and from vesicular to nonvesicular. Many dykes intrude rocks at the top of the exposed stratigraphic section and are therefore probably part of a later magmatic event. Several dykes however, may represent feeders for lava flows. The variation in petrography and the range in attitude of the dykes suggests that they may have intruded in several separate events. Dunn (1989) suggested that one of the dykes may be Late Triassic/Early Jurassic in age.

Most mafic dykes trend approximately north to northwest (Fig. 95) and are typically steeply dipping. There is a slight change in the dyke attitude upward from cycle 1 to 4. Attitudes vary from north-striking in cycle 1, to northwest-striking in cycles 3 and the lower part of cycle 4. Dyke attitudes change to approximately northeast in the upper part of cycle 4. The Late Triassic/Early Jurassic dyke, and several smaller dykes trend east and may be related to other basaltic dykes of similar age in Atlantic Canada (Dunn, 1989).

ACKNOWLEDGMENTS

This study was funded by the Canada-New Brunswick Mineral Development Agreement (MDA) 1984-1989, an NSERC operating grant to N. Van Wagoner, and contributions from the New Brunswick Department of Natural Resources and Energy, Seabright Resources, LAC Minerals, and Acadia Minerals Ventures. We wish to thank Reg Wilson and Fred Chandler for their careful review and constructive comments on the manuscript, and Ken Currie and Joe Whalen for administration of the MDA funding.

REFERENCES

Ballard, R.D., Holcomb, R.T., and Van Andel, Tj.H.
1979: Sheet flows, collapse pits, and lava lakes of the rift valley; Journal of Geophysical Research, v. 84, p. 5407-5422.

Berdan, J.M.
1971: Silurian to Early Devonian ostracodes of European aspect from the Eastport quadrangle, Maine; Geological Society of America, Abstracts with Programs, v. 3, p. 18.

Berry, W.B.N. and Boucot, A.J.
1970: Correlation of the North American Silurian rocks; Geological Society of America, Special Paper 102, 289 p.

Bevier, M.L.
1989: Preliminary U-Pb geochronologic results for igneous and metamorphic rocks, New Brunswick; in Fourteenth Annual Review of Activities, Minerals and Energy Division, Department of Natural Resources and Energy, New Brunswick, Information Circular 89-2, p. 190-194.

Bird, J.M. and Dewey, J.F.
1970: Lithosphere plate-continental margin tectonics and the evolution of the Appalachian orogen; Geological Society of America Bulletin, v. 81, no. 4, p. 1031-1060.

Bonnichsen, B. and Kauffman, D.F.
1987: Physical features of rhyolitic lava flows in the Snake River Plain volcanic province, southwestern Idaho; Geological Survey of America, Special Paper 212, p. 119-145.

Boucot, A.J.
1968: Silurian and Devonian of the northern Appalachians; in Studies of Appalachian Geology - Northern and Maritime, (ed.) E-an Zen, W.S. White, J.B. Hadley, and J.B. Thompson, Jr.; New York, Interscience, p. 83-94.

Boucot, A.J., Dewey, J.F., Dineley, D.L., Fletcher, R., Fyson, W.K., Griffin, J., Hickox, C.F., McKerrow, W.S., and Ziegler, A.M.
1974: Geology of the Arisaig area, Antigonish County, N.S.; Geological Society of America, Special Paper 139, 191 p.

Boucot, A.J., Johnson J.G., Harper, C., and Walmsley, V.G.
1966: Silurian brachiopods and gastropods of southern New Brunswick; Geological Survey of Canada, Bulletin 140, p. 1-45.

Carlisle, D.
1963: Pillow breccias and their aquagene tuffs, Quadra Island, British Columbia; Journal of Geology, v. 71, p. 48-71.

Carter, C.H.
1975: Miocene-Pliocene beach and tidal deposits, southern New Jersey; in Tidal Deposits, (ed.) R.N. Ginsburg; Springer-Verlag, New York, p. 109-116.

Cas, R.A.F. and Wright, J.V.
1987: Volcanic successions: modern and ancient; Allen and Unwin, London, 528 p.

Chapin, C.E. and Lowell, G.R.
1979: Primary and secondary flow structures in ash flow tuffs of the Gribbles Run palaeovalley, central Colorado; Geological Society of America, Special Paper 180, p. 137-154.

Cherry, M.E.
1976: The petrogenesis of granites in the St. George Batholith, southwestern New Brunswick, Canada; Ph.D. thesis, University of New Brunswick, Fredericton, New Brunswick, 242 p.

Crandell, D.R.
1971: Post-glacial lahars from Mount Rainier volcano, Washington; United States Geological Survey, Professional Paper, no. 677, 75 p.

Cumming, L.M.
1967: Geology of the Passamaquoddy Bay region, Charlotte County, New Brunswick; Geological Survey of Canada, Paper 65-29, p. 1-36.

Dewey, J.F. and Kidd, W.S.F.
1974: Continental collisions in the Appalachian-Caledonian orogenic belt: variations related to complete and incomplete suturing; Geology, v. 2, p. 29-33.

Dunham, R.J.
1962: Classification of carbonate rocks according to depositional texture; in Classification of carbonate rocks - a symposium, (ed.) W.E. Ham; American Association of Petroleum Geologists, Tulsa, p. 108-121.

Dunn, T.
1989: Petrology and geochemistry of the Minister Island Dyke, New Brunswick; Geological Association of Canada, Program with Abstracts, v. 14, p. 93.

Evans, G.
1975: Intertidal flat deposits of the Wash, western margin of the North Sea; in Tidal Deposits, (ed.) R.N. Ginsburg; Springer-Verlag, New York, p. 13-20.

Fay, V.
1988: Lower Devonian volcanic and sedimentary rocks of the Eastport Formation, southwest New Brunswick; M.Sc. thesis, University of New Brunswick, Fredericton, New Brunswick, 167 p.

Fink, J.H.
1983: Structure and emplacement of a rhyolitic obsidian flow: Little Glass Mountain, Medicine Lake Highland, northern California; Geological Society of America Bulletin, v. 94, p. 362-380.

Fisher, R.V.
1979: Models for pyroclastic surges and pyroclastic flows; Journal of Volcanology and Geothermal Research, v. 6, p. 308-318.
1982: Debris flows and lahars; in Pyroclastic volcanism and deposits of Cenozoic intermediate to felsic volcanic islands with implications for Precambrian greenstone-belt volcanoes, (ed.) L.D. Ayers; Geological Association of Canada, Short Course Notes, no. 2, p. 136-190.

Fisher, R.V. and Schmincke, H.-U.
1984: Pyroclastic rocks; Springer-Verlag, New York, 472 p.

Folk, R.L.
1980: Petrology of sedimentary rocks; Hemphills, Austin, Texas, 184 p.

Furnes, H. and Fridleifsson, I.B.
1978: Relationship between the chemistry and axial dimensions of some shallow water pillow lavas of alkaline olivine basalt and olivine tholeiitic composition; Bulletin of Volcanology, v. 41, p. 136-146.

Fyffe, L.R. and Fricker, A.
1987: Tectonostratigraphic terrane analysis of New Brunswick; Maritime Sediments and Atlantic Geology, v. 23, p. 113-122.

Gardiner, W.W.
1987: Saint George Batholith project (west); in Twelfth Annual Review of Activities, Mineral Resources Division, Department of Natural Resources, New Brunswick, Information Circular 87-2, p. 37-40.

Gates, O. and Moench, R.H.
1981: Bimodal Silurian and Lower Devonian volcanic rock assemblages in the Machias-Eastport area, Maine; United States Geological Survey, Professional Paper, no. 1184, 32 p.

Ginsburg, R.N. (ed.)
1975: Tidal Deposits; Springer-Verlag, New York, 428 p.

Greeley, R.
1982: The Snake River Plain, Idaho: representative of a new category of volcanism; Journal of Geophysical Research, v. 87, p. 2705-2712.

Hay, P.W.
1967: Sedimentary and volcanic rocks of the St. Andrews-St. George area, Charlotte County, New Brunswick; Mineral Resources Branch, Department of Natural Resources, New Brunswick, Map Series 67-1, 19 p.

Honnorez, J. and Kirst, P.
1975: Submarine basaltic volcanism: morphometric parameters for discriminating hyaloclastites from hyalotuffs; Bulletin of Volcanology, v. 39, p. 1-25.

Hoover, D.L.
1964: Flow structures in a welded tuff, Nye County, Nevada; in Abstracts for 1963, Geological Society of America, Special Paper No. 76, p. 83.

Ingram, R.L.
1954: Terminology for the thickness of stratification and parting units in sedimentary rocks; Geological Society of America Bulletin, v. 65, p. 937-938.

Kirkham, R.V. and Sinclair, W.D.
1984: Porphyry copper, molybdenum, tungsten; Chapter 17 in Canadian mineral deposit types: a geological synopsis, (ed.) O.R. Eckstrand; Geological Survey of Canada, Economic Geology Report No. 36, p. 51-52.

Kokelaar, B.P.
1982: Fluidisation of wet sediments during emplacement and cooling of various igneous bodies; Journal of the Geological Society of London, v. 139, p. 21-33.

Laporte, L.F.
1975: Carbonate tidal flat deposits of the Early Devonian Manlius Formation of New York State; in Tidal Deposits, (ed.) R.N. Ginsburg; Springer-Verlag, New York, p. 243-250.

Marshak, S. and Mitra, G.
1988: Basic methods of structural geology; Prentice Hall, New Jersey, 446 p.

McCutcheon, S.R. and Ruitenberg, A.A.
1987: Geology and mineral deposits, Annidale-Nerepis area, New Brunswick; New Brunswick Department of Natural Resources and Energy, Memoir 2, 141 p.

McLeod, M.J.
1988: Report on Saint George Batholith project; in Thirteenth Annual Review of Activities, Mineral Resources Division, Department of Natural Resources, New Brunswick, Information Circular 88-2, p. 43-46.

McLeod, M.J. and Rast, N.
1988: Correlations and fault systematics in the Passamaquoddy Bay area, southwestern New Brunswick; Maritime Sediments and Atlantic Geology, v. 24, p. 289-300.

Moore, J.G., Phillips, R.L., Grigg, R.W., Peterson, D.W., and Swanson, D.A.
1973: Flow of lava into the sea, 1969-71, Kilauea volcano, Hawaii; Geological Society of America Bulletin, v. 84, p. 537-546.

Noble, D.C.
1968: Laminar viscous flowage structures in ash flow tuff from Gran Canaria Islands: a discussion; Journal of Geology, v. 16, p. 721-723.

Percival, J.A. and Helmstaedt, H.
1978: Zoned epidote nodules from sedimentary rocks of the Eastport Formation, southwest New Brunswick; Canadian Journal of Earth Sciences, v. 15, p. 1194-1200.

Pichler, H.
1965: Acid hyaloclastites; Bulletin of Volcanology, v. 28, p. 293-310.

Pickerill, R.K. and Pajari, G.E.
1976: The Eastport Formation (Lower Devonian) in the northern Passamaquoddy Bay area, southwest New Brunswick; Canadian Journal of Earth Sciences, v. 13, p. 266-270.

Ragan, D.M. and Sheridan, M.F.
1972: Compaction of the Bishop Tuff; Geological Society of America Bulletin, v. 83, p. 95-106.

Reineck, H.-E.
1975: German North Sea tidal flats; in Tidal Deposits, (ed.) R.N. Ginsburg; Springer-Verlag, New York, p. 5-12.

Reineck, H.-E. and Singh, I.B.
1975: Depositional sedimentary environments; Springer-Verlag, New York, 439 p.

Ruitenberg, A.A.
1968: Geology and mineral deposits, Passamaquoddy Bay area; Mineral Resources Branch, Department of Natural Resources, New Brunswick, Report 7, 47 p.

Schluger, P.R.
1973: Stratigraphy and sedimentary environments of the Devonian Perry Formation, New Brunswick, Canada, and Maine, U.S.A.; Geological Society of America Bulletin, v. 84, p. 2533-2548.

Schmid, R.
1981: Descriptive classification and nomenclature of pyroclastic deposits and fragments: recommendations of the IUGS Subcommission on the Systematics of Igneous Rocks; Geology, v. 9, p. 41-43.

Schmincke, H.-U.
1967: Fused tuff and peperites in south-central Washington; Geological Society of America Bulletin, v. 78, p. 319-330.

Schmincke, H.-U. and Swanson, D.A.
1967: Laminar viscous flowage structures in ash-flow tuffs from Gran Canaria, Canary Islands; Journal of Geology, v. 75, p. 641-664.

Self, S.
1982: Terminology and classifications for pyroclastic deposits; in Pyroclastic Volcanism and Deposits of Cenozoic Intermediate to Felsic Volcanic Islands with Implications for Precambrian Greenstone-Belt Volcanoes, (ed.) L.D. Ayres; Geological Association of Canada, Short Course Notes, no. 2, p. 18-37.
1983: Large-scale phreatomagmatic silicic volcanism: a case study from New Zealand; Journal of Volcanology and Geothermal Research, v. 17, p. 433-469.

Self, S. and Sparks, R.S.J.
1978: Characteristics of widespread pyroclastic deposits formed by the interaction of silicic magma and water; Bulletin of Volcanology, v. 41, p. 196-212.

Sheridan, M.F.
1979: Emplacement of pyroclastic flows: a review; Geological Society of America, Special Paper 180, p. 125-135.

Sheridan, M.F. and Wohletz, K.H.
1981: Hydrovolcanic explosions: the systematics of water - pyroclast equilibrium; Science, v. 212, p. 1387-1389.
1983: Hydrovolcanism: basic considerations and review; in Explosive volcanism, (ed.) M.F. Sheridan and F. Barberi; Journal of Volcanology and Geothermal Research, v. 17, p. 1-29.

Sparks, R.S.J.
1976: Grain size variations in ignimbrites and implications for the transport of pyroclastic flows; Sedimentology, v. 13, p. 147-188.

Sparks, R.S.J. and Walker, G.P.L.
1977: The significance of vitric-enriched air-fall ashes associated with crystal-enriched ignimbrites; Journal of Volcanology and Geothermal Research, v. 2, p. 329-341.

Van Wagoner, N.A.
1984: Volcanic stratigraphy and physical volcanology of part of the Devonian volcanic sequence, northern Passamaquoddy Bay, southwestern New Brunswick; in Ninth Annual Review of Activities, Mineral Resources Division, Department of Natural Resources, New Brunswick, p. 37-44.
1986: Volcanic stratigraphy and physical volcanology of part of the Devonian volcanic sequence, Passamaquoddy Bay, southwest New Brunswick: a progress report; in Eleventh Annual Review of Activities, Mineral Resources Division, Department of Natural Resources, New Brunswick, p. 132-135.

Van Wagoner, N.A. and Fay, V.K.
1988: Stratigraphy and volcanology of a portion of the Lower Devonian volcanic rocks of southwestern New Brunswick; in Current Research, Part B; Geological Survey of Canada, Paper 88-1B, p. 69-78.

Van Wagoner, N.A., Dadd, K.A., Baldwin, D.K., and McNeil, W.
1989: Cyclic, bimodal volcanism in a continental volcanic zone, New Brunswick; in Fourteenth Annual Review of Activities, Minerals and Energy Division, Department of Natural Resources and Energy, New Brunswick, Information Circular 89-2, p. 215-216.

Van Wagoner, N.A., McNeil, W., and Fay, V.K.
1988: Early Devonian bimodal volcanic rocks of southwestern New Brunswick: petrography, stratigraphy, and depositional setting; Maritime Sediments and Atlantic Geology, v. 24, p. 301-319.

Van Wagoner, N.A., McNeil, W., and Thicke, M.
1987: Volcanism of the eastern portion of the Devonian volcanic belt of Passamaquoddy Bay, southwestern New Brunswick: a progress report; in Twelfth Annual Review of Activities, Mineral Resources Division, Department of Natural Resources, New Brunswick, Information Circular 87-2, p. 145-147.

Walker, G.P.L.
1971: Grain size characteristics of pyroclastic deposits; Journal of Geology, v. 79, p. 696-714.
1973: Explosive volcanic eruptions - a new classification scheme; Geologische Rundschau, v. 62, p. 431-446.

Walker, G.W. and Swanson, D.A.
1968: Laminar flowage in a Pliocene soda rhyolitic ash-flow tuff, Lake and Harney counties, Oregon; United States Geological Survey, Professional Paper No. 600-B, p. 37-47.

Walker, R.G. and Harms, J.C.
1975: Shorelines of weak tidal activity: Upper Devonian Catskill Formation, central Pennsylvania; in Tidal Deposits, (ed.) R.N. Ginsburg; Springer-Verlag, New York, p. 103-108.

Waters, A.C.
1960: Determining the direction of flow in basalts; American Journal of Science, v. 258A, p. 350-366.

Watkins, R. and Boucot, A.J.
1975: Evolution of Silurian brachiopod communities along the southeastern coast of Acadia; Geological Society of America Bulletin, v. 86, p. 243-254.

Weimer, R.J., Howard, J.D., and Lindsay, D.R.
1982: Tidal flats and associated tidal channels; in Sandstone Depositional Environments, (ed.) P.A. Scholle and D. Spearing; American Association of Petroleum Geologists, Memoir 31, p. 191-240.

Whaley, K.D.A.
1981: B.P. Minerals Ltd. Mount Blair Property Assessment Report; New Brunswick Department of Natural Resources, 26 p.

Wilson, C.J.N.
1980: The role of fluidisation in the emplacement of pyroclastic flows: an experimental approach; Journal of Volcanology and Geothermal Research, v. 16, p. 33-56.

Wilson, J.T.
1966: Did the Atlantic close and then reopen?; Nature, v. 211, p. 676-681.

Wohletz, K.H.
1983: Mechanisms of hydrovolcanic pyroclast formation: grain-size, scanning electron microscopy, and experimental studies; Journal of Volcanology and Geothermal Research, v. 17, p. 31-63.

Wolff, J.A. and Wright, J.V.
1981: Rheomorphism of welded tuffs; Journal of Volcanology and Geothermal Research, v. 10, p. 13-34.

Wood, C.A.
1980: Morphometric analysis of cinder cone degradation; Journal of Volcanology and Geothermal Research, v. 8, p. 137-160.

Wright, J.V.
1979: Formation, transport and deposition of ignimbrites and welded tuffs; Ph.D. thesis, Imperial College, University of London, U.K., 451 p.

Wright, J.V. and Walker, G.P.L.
1981: Eruption, transport and deposition of ignimbrite: a case study from Mexico; Journal of Volcanology and Geothermal Research, v. 9, p. 111-131.

Wright, J.V., Smith, A.L., and Self, S.
1980: A working terminology of pyroclastic deposits; Journal of Volcanology and Geothermal Research, v. 8, p. 315-336.